

# **FLOOD ASSESSMENT STUDIES FOR KELANI RIVER BASIN, SRI LANKA**

**A DISSERTATION**

*submitted in partial fulfilment of the  
requirements for the award of the degree*

*of*

**MASTER OF TECHNOLOGY**

*in*

**(WATER RESOURCES DEVELOPMENT)**

*by*

**Candidate: S. Rajkumar (16548029)**

**Guide: Prof. Dr. S. K. Mishra**

**Head of the Department**

**Department of WRDM**

**IITR**

**Co-Guide: Prof. Dr. R. D. Singh**

**Adjunct Professor, Dept of WRDM**

**Former Director, NIH**

**IITR**



**DEPARTMENT OF WATER RESOURCES DEVELOPMENT & MANAGEMENT**

**INDIAN INSTITUTE OF TECHNOLOGY**

**ROORKEE-247667, UTTARAKHAND, INDIA**

**May 2018**

## **Declaration by Candidate and Certification by Supervisors**

### Declaration by Candidate

I, S. Raj Kumar hereby declare that the whole work involved in this dissertation report entitled FLOOD ASSESSMENT STUDIES FOR KELANI RIVER BASIN, SRI LANKA has been solely handled by me paying due attention to the instructions given by the supervisor of Dr.S.K.MISHRA, Professor & Head, Dept of WRDM and co-supervisor of Dr.R.D.SINGH, Adjunct Professor, Dept of WRDM(Former Director, NIH) IIT Roorkee.

S. Raj Kumar

(Enrolment No. 16548029)

(Candidate)

Date:.....

### Certification by Supervisors

We certify that the original work of this dissertation report entitled FLOOD ASSESSMENT STUDIES FOR KELANI RIVER BASIN, SRI LANKA was solely carried out by the candidate during his Master degree programme in Water Resources Development in the Department of WRDM, IIT Roorkee. The work of this report was personally fabricated by the candidate under our overall supervision.

Supervisor

.....

Dr.S.K.MISHRA

Professor & Head

Dept of WRDM, IIT Roorkee

Date: .....

Co-Supervisor

.....

Dr.R.D. SINGH

Adjunct Professor

Dept of WRDM, IIT Roorkee.

Date:.....

## **Acknowledgement**

I am indebted to many people who provided assistance in the preparation of the material presented herein.

First and foremost of these, is Dr. S.K.MISHRA, Professor & Head, Dept of WRDM, who provided the original ideas, suggestions, and motivation for the work, who freely bestowed his time, guidance, encouragement, support and wisdom considerably beyond the call of duty, who was a model of professorial responsibility, professionalism, and thrift, and who has been delivered lectures on Applied Hydrology, Design of Irrigation & Drainage Works and Irrigation Structures during our Master degree programme, for which I would like to express my deepest appreciation.

I must express my sincere thanks to my co-supervisor of Dr. R.D. SINGH, Adjunct Professor, Dept of WRDM (Former Director, NIH, IIT Roorkee) who has really made me enthusiasm to take this challenge with application of relevant software and gave me assistances and supports on times to this report by sharing a profound knowledge on hydrology, with me.

I would like to offer my sincere thanks to my better-half, my kids, my parents and my siblings for their continuous support during my studies. Their financial and psychological support and encouragement is beyond repayment. Also, I must remember my better half for her support in software application included in this report.

I must remember to thank the Dept of WRDM, IIT Roorkee, for giving me an opportunity to write this report according to the academic rules. In addition, I would like to express my appreciation to my senior student, Mr. Dhananjay Singh and Ph.D. scholar, Mr. Lakhwinder Singh, in the Dept of WRDM, who really made me endeavour to learn the software being used in this study and shared me profound techniques on that. Also, I am indebted to say thank Indian Economic Technical Corporation(ITEC), Ministry of External Affairs, Govt. of India for providing financial sponsorship throughout the programme and Irrigation Department, Govt. of Sri Lanka for providing the temporal data required for my study.

S. Rajkumar

Enrolment No. 16548029

## Synopsis

Kelani River Basin in Sri Lanka experiences frequent flooding which resulted in loss of lives and properties of the people in this basin. Keeping this in view, a study was taken up for Flood Assessment in Kelani River Basin, Sri Lanka up to Hanwella gauging site using Hydrologic Modelling System tool developed by HEC, USA (HEC-HMS). In the HEC-HMS version 4.2 software, various options and methods are available under each sub models. In the study, most of the available options were considered for analysis and the values of various goodness of fit criteria, available in HEC-HMS, such as Nash-Sutcliffe Model Efficiency (NSE), Percent Error in Peak, and Percent Error in Time to Peak and Percent error in Discharge Volume (Volume Deviation ( $D_v$ )) were computed. Based on these, the performance of various methods for simulating the observed hydrographs was judged. The Basin Model was selected considering the Kelani river basin up to Hanwella gauging site as a single basin for the simulation of flood hydrographs. In the Meteorological Model, Gaged weight option, available in HEC-HMS, was considered for rainfall analysis. For the Transform Model or Direct Runoff Model in HEC-HMS, Clark UH, SCS UH & Snyder UH models were considered. The Calibration (manual and automatic) and Validation of model parameters were carried out analysing the available hourly rainfall-runoff data of the four storm events observed during the monsoon seasons of the years 2017, 2014 and 2012. The Arc Map-ArcGIS version 10.3 and HEC-GeoHMS version 10.3 were also used to process the different types of spatial data required as input for the HEC-HMS model applications. From the results of the analysis, it was found that the Snyder UH model is best suited model and the Clark UH model is the second best suited for the flood assessment of Kelani river Basin whereas SCS UH model is found to be least performing model. The calibrated & validated Snyder Model yielded 0.82 of NSE value, 2.4 % of percent error in peak, 25 % of percent error in time to peak and 15 % of percent error in discharge volume.

The representative unit hydrograph for the basin, derived from the Snyder's Model, was applied to formulate the real time flood forecast for the flood event of June 2014, considering the blocks of

hourly excess rainfall available up to the period of forecast. The forecasted and observed flood hydrographs were compared considering all the blocks of excess rainfall. It was found that both the hydrographs are in close agreement.

100-year flood was estimated convoluting the 100-year design sequence of excess hourly rainfall values for the design duration with the representative unit hydrograph. The recommended value of storm duration was considered and the 100-year rainfall value was obtained from DDF curve. The hourly rainfall values were obtained using the relationship developed between 100-year rainfall for the design duration and the storm durations. The design loss rate and base flow were considered as per the recommendations. The design loss rate was applied to compute the excess rainfall whereas the design base flow was added to the design direct surface runoff hydrograph ordinates in order to compute the flood of 100-year return period.

Standard Project Flood (SPF) was estimated using the representative unit hydrograph and hourly values of excess rainfall critically sequenced as per the recommended practices. The design duration was obtained as per recommended practices. The DAD analysis was carried out to develop the DAD curve which was used to compute the depth of desired duration for the basin. The relationship developed between the depth and duration was used to get the incremental values of hourly rainfall. Finally, the recommended values of loss rate and base flow were considered to get the estimate of SPF.

Flood frequency analysis was carried out using Gumbel and Log-Pearson type III distributions based frequency factor approach. Those flood estimates for different return periods were compared for both the distributions.

The outcome of the study would be very much beneficial for the Flood Disaster Management Authorities of Govt of Sri Lanka. It would help them for implementing various structural and non-

structural measures in Kelani river basin to minimise losses of lives and properties due to frequent occurrence of severe flood events.



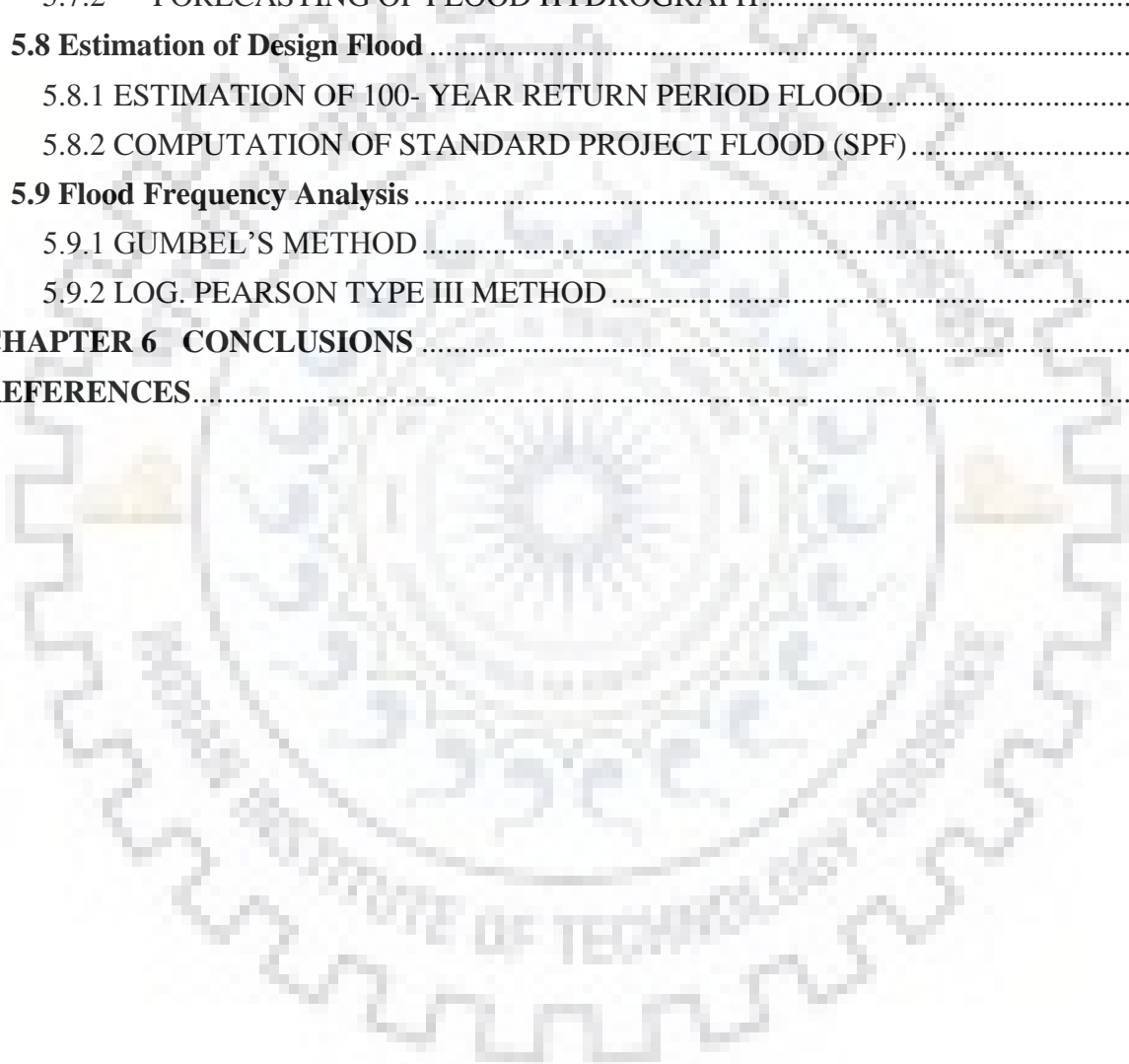
## Table of Contents

	<u>Contents</u>	<u>Page No.</u>
<b>Declaration by Candidate and Certification by Supervisors</b> .....		ii
<b>Acknowledgements</b> .....		iii
<b>Synopsis</b> .....		iv
<b>Table of Contents</b> .....		vii
<b>List of Tables</b> .....		x
<b>List of Figures</b> .....		xii
<b>List of Abbreviations</b> .....		xv
<b>CHAPTER 1 INTRODUCTION</b> .....		1
<b>1.1 General</b> .....		1
<b>1.2 Objectives of the Study</b> .....		2
<b>CHAPTER 2 REVIEW OF LITERATURE AND RESEARCH GAP</b> .....		3
<b>2.1 Review of Literature</b> .....		3
<b>2.2 Research Gap</b> .....		5
<b>CHAPTER 3 DESCRIPTION OF STUDY AREA AND DATA AVAILABILITY</b> .....		7
<b>3.1 Study Area</b> .....		7
<b>3.2 Data Availability</b> .....		8
3.2.1 METEOROLOGICAL AND HYDROLOGICAL DATA.....		8
3.2.2 SPATIAL DATA .....		9
<b>CHAPTER 4 METHODOLOGY</b> .....		10
<b>4.1 Spatial Data Processing</b> .....		10
4.1.1 PREPARATION OF BASIN MAP AND DELINEATION OF DRAINAGE NETWORK .....		10
4.1.2 PREPERATION OF DIGITAL ELEVATION MODEL .....		10
4.1.3 PREPERATION OF THIESSEN POLYGON MAP AND COMPUTATIONS of THESSEN POLYGON WIEGHTS (GAUGE WEIGHT) .....		10
4.1.4 PREPARATION OF LAND USE /LAND COVER MAP(LULC).....		10
4.1.5 PREPARATION OF SOIL MAP .....		10
4.1.6 PREPARATION OF ISOCHRONAL MAPS AND DEVELOPMENT OF TIME AREA CURVE.....		10
<b>4.2 Temporal Data Processing</b> .....		12
4.2.1 RAINFALL DATA PROCESSING .....		12
4.2.2 STREAM FLOW DATA PROCESSING .....		13
<b>4.3 Application of HEC-GeoHMS and HEC-HMS</b> .....		14
4.3.1 METROLOGICAL MODEL.....		15
4.3.2 BASE FLOW MODEL.....		16

4.3.3 LOSS MODEL.....	16
4. 3.4 TRANSFORM MODELS.....	17
<b>4.4 Sensitivity Analysis .....</b>	<b>20</b>
<b>4.5 Error Criteria for comparing the performance of Three Transform Models .....</b>	<b>20</b>
<b>4.6 Calibration and Validation of the Models .....</b>	<b>21</b>
<b>4.7 Real Time Flood Forecasting .....</b>	<b>22</b>
4.7.1 DEVELOPMENT OF UNIT HYDROGRAPH.....	22
4.7.2 FORECASTING OF FLOOD HYDROGRAPH.....	22
<b>4.8 Estimation of Design Flood .....</b>	<b>22</b>
4.8.1 ESTIMATION OF 100- YEAR RETURN PERIOD FLOOD .....	22
4.8.2 COMPUTATION OF STANDARD PROJECT FLOOD (SPF).....	23
<b>4.9 Flood Frequency Analysis .....</b>	<b>24</b>
4.9.1 GUMBEL’S METHOD .....	24
4.9.2 LOG. PEARSON TYPE III METHOD .....	25
<b>CHAPTER 5 ANALYSIS AND DISCUSSION OF RESULTS.....</b>	<b>26</b>
<b>5.1 Spatial Data Processing .....</b>	<b>26</b>
5.1.1 PREPARATION OF BASIN MAP AND DELINEATION OF DRAINAGE NETWORK .....	26
5.1.2 PREPERATION OF DIGITAL ELEVATION MODEL .....	26
5.1.3 PREPERATION OF THIESSEN POLYGON MAP AND COMPUTATIONS OF THESSEN POLYGON WIEGHTS (GAUGE WEIGHT) .....	27
5.1.4 PREPARATION OF LAND USE /LAND COVER MAP(LULC).....	28
5.1.5 PREPARATION OF SOIL MAP .....	29
5.1.6 PREPARATION OF ISOCHRONE MAPS AND DEVELOPMENT OF TIME AREARELATIONSHIP .....	30
<b>5.2 Temporal Data Processing .....</b>	<b>37</b>
5.2.1 RAINFALL DATA PROCESSING .....	37
5.2.2 STREAM FLOW DATA PROCESSING .....	37
<b>5.3 Application of HEC-GeoHMS and HEC-HMS.....</b>	<b>39</b>
5.3.1 METEOROLOGICAL MODEL .....	40
5.3.2 BASE FLOW MODEL.....	41
5.3.3 LOSS MODEL.....	42
5.3.4 TRANSFORM MODEL.....	44
<b>5.4 Sensitivity Analysis .....</b>	<b>48</b>
<b>5.5 Error Criteria for comparing the performance of Three Transform Models .....</b>	<b>51</b>
<b>5.6 Calibration and Validation .....</b>	<b>51</b>
5.6.1 CALIBRATION OF CLARK UH MODEL.....	51
5.6.2 CALIBRATION OF SCS UH MODEL .....	54



5.6.3 CALIBRATION OF SNYDER UH MODEL .....	57
5.6.4 COMPARISON OF THREE TRANSFORM MODELS DURING CALIBRATION.....	61
5.6.5 VALIDATION OF CLARK UH MODEL - EVENT JUN. 2014 .....	64
5.6.6 VALIDATION OF SCS UH MODEL - EVENT JUN. 2014.....	65
5.6.7 VALIDATION OF SNYDER UH MODEL - EVENT JUN. 2014.....	65
5.6.8 COMPARISON OF THREE TRANSFORM MODELS DURING VALAIDATION ...	66
<b>5.7 Real Time Flood Forecasting .....</b>	<b>67</b>
5.7.1 DEVELOPMENT OF UNIT HYDROGRAPH.....	67
5.7.2 FORECASTING OF FLOOD HYDROGRAPH.....	68
<b>5.8 Estimation of Design Flood .....</b>	<b>70</b>
5.8.1 ESTIMATION OF 100- YEAR RETURN PERIOD FLOOD.....	70
5.8.2 COMPUTATION OF STANDARD PROJECT FLOOD (SPF) .....	76
<b>5.9 Flood Frequency Analysis .....</b>	<b>88</b>
5.9.1 GUMBEL'S METHOD .....	88
5.9.2 LOG. PEARSON TYPE III METHOD .....	88
<b>CHAPTER 6 CONCLUSIONS .....</b>	<b>91</b>
<b>REFERENCES.....</b>	<b>94</b>



## List of Tables

<u>Description of Tables</u>	<u>Page No.</u>
<i>Table 3.1 Meteorological and Hydrological Data</i> .....	8
<i>Table 5.1 Gauge weights from Thiessen polygon</i> .....	28
<i>Table 5.2 Description of Land Use Land Cover</i> .....	29
<i>Table 5.3 Description of Soil data</i> .....	30
<i>Table 5.4 Physical Characteristics of River Reaches</i> .....	30
<i>Table 5.5 Details of Points located on the river and its tributaries and Time of Travels up to the gauging site</i> .....	31
<i>Table 5.6 Time - Area table of IDW interpolation method</i> .....	33
<i>Table 5.7 Time - Area table of Kriging interpolation method</i> .....	35
<i>Table 5.8 Time - area table of synthetic method</i> .....	36
<i>Table 5.9 Storm Events considered for Rainfall-Runoff Modelling</i> .....	37
<i>Table 5.10 Calculations for Stage-Discharge Relationship-Analytical Method</i> .....	38
<i>Table 5.11 Parameters Tc and R on sensitivity analysis</i> .....	48
<i>Table 5.12 Parameter Lag time and NSE on sensitivity analysis</i> .....	49
<i>Table 5.13 Parameters Standard Lag and Cp on sensitivity analysis</i> .....	50
<i>Table 5.14 Average of optimized Parameters – Clark UH Transform Model</i> .....	52
<i>Table 5.15 Optimized Parameters and Representative Parameters – SCS UH Transform Model</i> .....	55
<i>Table 5.16 Optimized Parameters and Representative Parameters – Snyder UH Transform Model</i> .....	58
<i>Table 5.17 Time-Area relations to develop Snyder UH from Clark IUH</i> .....	67
<i>Table 5.18 Risk Assessment at Hanwella maintained by Dept. of Irrigation, Sri Lanka</i> .....	69
<i>Table 5.19 Forecasted flood hydrograph peak and corresponding water levels, time to peak and lead time along with limits of risks for Jun.2014 event</i> .....	69
<i>Table 5.20 Max.Rainfall Depth for various Duration and various Frequency</i> .....	71
<i>Table 5.21 Design storm from DDF curve (100 yrs. Return Period)</i> .....	71
<i>Table 5.22 Rainfall excess of design storm from DDF curve</i> .....	73
<i>Table 5.23 Ordinates of 100- years Return Period Design flood hydrograph</i> .....	75
<i>Table 5.24 Max. Rainfall Depth (mm) of six (6) Stations for different Durations</i> .....	77
<i>Table 5.25 Computation of Max.average Rainfall Depth, from Isohyet Map of 1 hr. duration</i> .....	77
<i>Table 5.26 Computation of Max.average Rainfall Depth, from Isohyet Map of 2 hr. duration</i> .....	78
<i>Table 5.27 Computation of Max.average Rainfall Depth, from Isohyet Map of 3 hr. duration</i> .....	79
<i>Table 5.28 Computation of Max.average Rainfall Depth, from Isohyet Map of 1-day duration</i> .....	80
<i>Table 5.29 Computation of Max.average Rainfall Depth, from Isohyet Map of 2-day duration</i> .....	81
<i>Table 5.30 Computation of Max.average Rainfall Depth, from Isohyet Map of 3-day duration</i> .....	82
<i>Table 5.31 Design storm from DAD curve(SPS)</i> .....	83
<i>Table 5.32 Rainfall excess of design storm from DAD curve</i> .....	84

<i>Table 5.33 Ordinates of Design Flood Hydrograph(SPF) .....</i>	<i>86</i>
<i>Table 5.34 Statistical Parameters derived from Annual maximum peak flood series .....</i>	<i>88</i>
<i>Table 5.35 Flood Estimates for different return periods using Gumble distribution .....</i>	<i>88</i>
<i>Table 5.36 Statistical Parameters of Log-Pearson Type III distribution.....</i>	<i>89</i>
<i>Table 5.37 Floods estimated using Log Pearson Type 3 Distribution for different return periods.....</i>	<i>89</i>
<i>Table 5.38 Comparison of Floods of different Return Periods using Gumbel and Log Pearson Type 3 Distribution.....</i>	<i>89</i>



## List of Figures

	<u>Description of Figures</u>	<u>Page No.</u>
Figure 3.1	Gross Basin – Kelani River.....	7
Figure 3.2	Digital Elevation Model – Layer Properties.....	9
Figure 3.3	Satellite Image – Layer Properties .....	9
Figure 4.1	Flow Diagram of HEC-HMS Process.....	15
Figure 5.1	Delineated Watershed & Drainage Network of Kelani River Basin up to Hanwella Gauging Site .....	26
Figure 5.2	Digital Elevation Map of Kelani River Basin up to Hanwella Gauging Site.....	26
Figure 5.3	Thiessen Polygon Map of Kelani River Basin up to Hanwella Gauging Site .....	27
Figure 5.4	Land use land cover map of Kelani River Basin up to Hanwella Gauging Site .....	28
Figure 5.5	Soil Map of Kelani River Basin up to Hanwella Gauging Site .....	29
Figure 5.6	Longest Flow Path and River Reaches .....	30
Figure 5.7	Points and Time of travel.....	32
Figure 5.8	Isochrones of Kelani River Basin (IDW) .....	33
Figure 5.9	Time-Area histogram & Cumulative Time-Area percent curves-IDW.....	34
Figure 5.10	Isochrones of Kelani river Basin (Kriging Method).....	34
Figure 5.11	Time-Area histogram & Time-Area percent curves-Kriging.....	35
Figure 5.12	Time-Area histogram & Time-Area percent curves-Synthetic.....	36
Figure 5.13	Comparison of Time-Area percent curves .....	37
Figure 5.14	Logarithmic Plot.....	38
Figure 5.15	Basin Model processed in HEC-GeoHMS.....	39
Figure 5.16	Models used in HEC-HMS for Event May 2017 .....	40
Figure 5.17	Meteorological Model used in HEC-HMS.....	41
Figure 5.18	Output of Rainfall in HEC-HMS for the Event May 2017 .....	41
Figure 5.19	Base flow Model used in HEC-HMS.....	42
Figure 5.20	Output as Base flow in HEC-HMS for the Event May 2017.....	42
Figure 5.21	Loss Model used in HEC-HMS.....	43
Figure 5.22	Output as Soil Infiltration in HEC-HMS for the Event May 2017.....	43
Figure 5.23	Output of Excess Rainfall in HEC-HMS for the Event May 2017.....	44
Figure 5.24	Clark UH Model used in HEC-HMS.....	44
Figure 5.25	Time Area Percent Curve used in Clark UH Model of HEC-HMS.....	45
Figure 5.26	Output as Direct Runoff (Clark UH) in HEC-HMS for the Event May 2017.....	45
Figure 5.27	Summary Results of HEC-HMS for the Event May 2017.....	46
Figure 5.28	SCS UH Model used in HEC-HMS.....	46
Figure 5.29	Output as Direct Runoff (SCS UH) in HEC-HMS for the Event May 2017.....	47
Figure 5.30	Snyder UH Model used in HEC-HMS.....	47

<i>Figure 5.31 Output as Direct Runoff (SCS UH) in HEC-HMS for the Event May 2017.....</i>	<i>48</i>
<i>Figure 5.32 Contour of NSE model efficiency with Sensitive Parameters Tc &amp; R.....</i>	<i>49</i>
<i>Figure 5.33 Variation of NSE with model Parameter Lag Time .....</i>	<i>50</i>
<i>Figure 5.34 Variation of NSE with Parameters C<sub>p</sub> &amp; Standard Lag (t<sub>p</sub>).....</i>	<i>51</i>
<i>Figure 5.35 Comparison of observed and Simulated Flood Hydrographs using optimised parameters of Clark Model for all the three events considered for Calibration.....</i>	<i>52</i>
<i>Figure 5.36 Comparison of observed and Simulated Flood Hydrographs using optimised as well as representative parameters of Clark Model for May 2017 event .....</i>	<i>53</i>
<i>Figure 5.37 Comparison of observed and Simulated Flood Hydrographs using optimised as well as representative parameters of Clark Model for Dec 2014 event.....</i>	<i>54</i>
<i>Figure 5.38 Comparison of observed and Simulated Flood Hydrographs using optimised as well as representative parameters of Clark Model for Nov 2012 event.....</i>	<i>54</i>
<i>Figure 5.39 Comparison of observed and Simulated Flood Hydrographs using optimised parameters of SCS Model for all the three events considered for Calibration.....</i>	<i>56</i>
<i>Figure 5.40 Comparison of observed and Simulated Flood Hydrographs using optimised as well as representative parameters of SCS Model for May 2017 event .....</i>	<i>56</i>
<i>Figure 5.41 Comparison of observed and Simulated Flood Hydrographs using optimised as well as representative parameters of SCS Model for Dec 2014 event .....</i>	<i>57</i>
<i>Figure 5.42 Comparison of observed and Simulated Flood Hydrographs using optimised as well as representative parameters of SCS Model for Nov 2012 event .....</i>	<i>57</i>
<i>Figure 5.43 Comparison of observed and Simulated Flood Hydrographs using optimised parameters of Snyder Model for all the three events considered for Calibration.....</i>	<i>59</i>
<i>Figure 5.44 Comparison of observed and Simulated Flood Hydrographs using optimised as well as representative parameters of Snyder Model for May 2017 event .....</i>	<i>59</i>
<i>Figure 5.45 Comparison of observed and Simulated Flood Hydrographs using optimised as well as representative parameters of Snyder Model for Dec 2014 event.....</i>	<i>60</i>
<i>Figure 5.46 Comparison of observed and Simulated Flood Hydrographs using optimised as well as representative parameters of Snyder Model for Nov 2012 event.....</i>	<i>60</i>
<i>Figure 5.47 Comparison of observed and Simulated Flood Hydrographs using Representative Parameters of three transform models for May 2017 event .....</i>	<i>61</i>
<i>Figure 5.48 Comparison of Percent Errors of Three Transform Models during Calibration using Representative Parameters -May 2017.....</i>	<i>62</i>
<i>Figure 5.49 Comparison of Observed and Simulated Flood Hydrographs using Representative Parameters of three transform models for Dec 2014 event.....</i>	<i>62</i>
<i>Figure 5.50 Comparison of Percent Errors of Three Transform Models during Calibration using Representative Parameters -Dec 2014 .....</i>	<i>63</i>

<i>Figure 5.51 Comparison of Observed and Simulated Flood Hydrographs using Representative Parameters of three transform models for Nov 2012 event.....</i>	<i>63</i>
<i>Figure 5.52 Percent Errors of Three Transform Models during Calibration using Representative Parameters -Nov 2012 .....</i>	<i>64</i>
<i>Figure 5.53 Comparison of observed and Simulated flood hydrograph at Hanwella gauging site using representative parameters of Clark model for Jun.2014 event considered for validation.....</i>	<i>64</i>
<i>Figure 5.54 Comparison of Observed and Simulated Hydrograph at Hanwella gauging site using representative parameters of SCS model for Jun.2014 event considered for validation.....</i>	<i>65</i>
<i>Figure 5.55 Comparison of Observed and Simulated Hydrograph at Hanwella gauging site using representative parameters of Snyder model for Jun.2014 event considered for validation.....</i>	<i>65</i>
<i>Figure 5.56 Comparison of observed and Simulated Flood Hydrographs of Three Transform Models during Validation considering Jun.2014 event.....</i>	<i>66</i>
<i>Figure 5.57 Comparison of Percent Errors of Three Transform Models during Validation using Representative parameters considering Jun 2014 event.....</i>	<i>66</i>
<i>Figure 5.58 Snyder Unit Hydrograph.....</i>	<i>68</i>
<i>Figure 5.59 Forecasted Flood Hydrograph in real time for different lead times for Jun.2014 event.....</i>	<i>68</i>
<i>Figure 5.60 Comparison of Observed &amp; Forecasted Flood Hydrographs (considering 16 hrs of excess rainfall) using Snyder UH model for Jun 2014 event .....</i>	<i>70</i>
<i>Figure 5.61 Depth – Duration - Frequency Curve .....</i>	<i>71</i>
<i>Figure 5.62 Design Flood Hydrograph corresponding to 100 yrs. Return Period Storm (DDF Curve) .....</i>	<i>76</i>
<i>Figure 5.63 Isohyet Map of 1 hr Duration.....</i>	<i>77</i>
<i>Figure 5.64 Isohyet Map of 2 hr Duration.....</i>	<i>78</i>
<i>Figure 5.65 Isohyet Map of 3 hr Duration.....</i>	<i>79</i>
<i>Figure 5.66 Isohyet Map of 1-day Duration .....</i>	<i>79</i>
<i>Figure 5.67 Isohyet Map of 2-day Duration .....</i>	<i>80</i>
<i>Figure 5.68 Isohyet Map of 3-day Duration .....</i>	<i>81</i>
<i>Figure 5.69 Depth – Area – Duration Curve.....</i>	<i>82</i>
<i>Figure 5.70 Depth – Area Relation plot for the basin for 72-hour duration.....</i>	<i>83</i>
<i>Figure 5.71 Design Flood Hydrograph (SPF).....</i>	<i>87</i>
<i>Figure 5.72 Comparison of Floods of different Return Periods using Gumbel and Log Pearson Type 3 Distribution.....</i>	<i>90</i>

## List of Abbreviations

ArcGIS	-	Aeronautical Reconnaissance Coverage Geographic Information System
CWC	-	Central Water Commission
DAD	-	Depth - Area - Duration
DDF	-	Depth - Duration- Frequency
DEM	-	Digital Elevation Model
DSRH	-	Direct Surface Runoff Hydrograph
FAO	-	Food & Agriculture Organization
GIUH	-	Geomorphologic Instantaneous Unit Hydrograph
HEC-GeoHMS	-	Hydrologic Energy Center - Geospatial Hydrologic Modelling System
HEC-HMS	-	Hydrologic Energy Center - Hydrologic Modelling System
HFL	-	High Flood Level
IDW	-	Inverse Weighted Distance
ILWIS	-	Integrated Land & Water Information System
IUH	-	Instantaneous Unit Hydrograph
MSL	-	Mean Sea Level
NAM	-	Nedbor Afstromnings Model
NSE	-	Nash - Sutcliffe Efficiency
SCS-CN	-	Soil Conservation Service - Curve Number
SMA	-	Soil Accounting Moisture
SPF	-	Standard Project Flood
SPS	-	Standard Project Storm
SRTM	-	Shuttle Radar Topographic Mission
SUH	-	Synthetic Unit Hydrograph
UH	-	Unit Hydrograph
USACE	-	United States Army Corps of Engineers

## CHAPTER 1 INTRODUCTION

### 1.1 General

Hydrology defines that it is a scientific study of water. It is the science that associates with the occurrence, circulation and distribution of water of the earth and earth's atmosphere. One of the most crucial water sources of earth is rainfall, extreme of which causes flood disaster. The rainfall characteristics are the temporal and spatial distribution of the rainfall quantity (*S.K. Jain et al. 2000*). The runoff estimation is a crucial aspect of watershed planning (*C. Rakesh Kumar et al. 2004*). Hence study of transformation from rainfall to runoff also referred to as rainfall- runoff modelling or watershed modelling or hydrological modelling is highly necessary in the academic background of water resources engineering for the mitigation measure against flood disaster and the future development of water resource structure.

There are numerous sources currently available for the application of rainfall- runoff modelling. However, the modern rapid developed technology and software tools assist water resource professionals to model the natural phenomena. The software tools such as (HEC-HMS) and (ArcGIS) are simultaneously employed in such modelling task nowadays (*H.K. Nandalal et al, 2010*). The software tool however requires data for its input to run the model systematically.

The system of hydrological modelling requires a set of meteorological data (rainfall etc.), hydrological data (stream flow), and spatial data (topography, land use land cover & soil type) of the relevant watershed. Mostly it is obvious that precise temporal data and high quality of spatial data are not affordable. It is therefore huge challenge in application of those data with rainfall – runoff modelling. However, the lumped conceptual models which are not much expecting higher accuracy of data can be applied in this scenario. The modelling HEC-HMS used herein is also one of the lumped conceptual model categories. (*H.K. Nandalal et al, 2010*)

In order to manage the frequent occurrence of floods, the Govt. of Sri Lanka are planning to take immediate steps to safe guard the capital of the country from this frequent flood menace by adopting suitable structural and non-structural flood mitigation measures such as (i) Diverting the flood water through a constructed channel at Hanwella gauging station minimising the floods in the downstream , (ii) Providing embankments and levees along the both riverbanks for flood protection and (iii) Real



time flood forecasting for the evacuation of the people from the areas likely to be affected during the floods.

For adopting above measures, the flood assessments are required analysing the rainfall-runoff data of some severe events occurred in the Kelani river basin. For this purpose, it is required to understand the rainfall-runoff mechanism considering the historical rainfall-runoff events observed in the Kelani river basin. (M.M.G.T. De Silva et al. 2014). Thus, the flood assessment in the Kelani River basin is very much imperative for the water managers and decision makers since the Kelani river is frequently hit by flood due to South-west monsoon storm.

## 1.2 Objectives of the Study

The objectives of the study are:

- (i) Application of Hydrologic Modeling System (HEC-HMS) for event base modeling to simulate the Flood Hydrograph of different events in Kelani river basin.
- (ii) Calibration and Validation of Various Flood Simulation Models of HEC-HMS.
- (iii) Comparison of the simulation results based on different objective functions to select a suitable model for Flood Simulation.
- (iv) Formulate the Real Time flood forecast at the Hanwella gauging site to provide the Advance information about the Flood for its Management.
- (v) Estimation of Design Flood Hydrograph for Diverting the Flood at Hanwella gauging site.
- (vi) Estimation of Floods for Different Return period using flood frequency Analysis for the Hydrological Design of Levees and Embankments.

## CHAPTER 2 REVIEW OF LITERATURE AND RESEARCH GAP

### 2.1 Review of Literature

A flood estimation study was carried out using HEC-HMS by the professionals of University of Tun Hussein Onn Malaysia. The watershed area taken for this study only of 272 sq.km. The SCS UH model was preferred as Transform model. The initial and constant loss rate method was chosen as loss model. The model was calibrated using 10 years data hence it was a continuous based model HEC-HMS also was used to find the missing data and compute the flood from the rainfall data. Further the HEC-HMS was applied for prediction of future flood level. (*M. A. M Razi et al – 2010*)

The study for design flood estimation using GIS supported GIUH approach was undertaken by the professionals of National Institute of Hydrology, Roorkee, India the particular approach was applied over an ungauged catchment. The GIS is applied to support to produce GIUH in order to compute the design flood. An own mathematical was developed by those professionals. This model enabled the study by evaluation of Clark UH model parameters using geomorphological characteristics of the catchment. The peak flood and time to peak of the earlier estimates were quite more than the peak flood and the time to peak of the GIUH approached, considering the same design storm with the critical sequencing. (*S. K. Jain. et. al.- 2000*)

A study for estimation of Clark's instantaneous unit hydrograph parameters and development of direct surface runoff hydrograph was conducted by the university professionals of Pakistan and USA. The study was carried using multiple sub basins as the basin area was more than 5000 sq.km The UH parameters time of concentration ( $T_c$ ) was derived from time-area diagram whereas storage coefficient  $R$  was found from the optimization approach based on Downhill Simplex Technique Code developed in FOR-TRAN. Ten (10) numbers of randomly selected events were considered for calibration process and another five (5) number of events were considered validation process. The impact of  $T_c$  and  $R$  were investigated and found that DSRH was more sensitive to  $R$  than  $T_c$ . Approximately equal values of  $T_c$  and  $R$  showed that the shape of DSRH for a larger catchment was dominated by runoff diffusion and translation flow effects (*M. M. Ahmad et. al – 2009*)

A runoff estimation study for an ungauged catchment using GIUH models was undertaken by professionals of National Institute of Hydrology, Roorkee, India. Clark IUH and Nash IUH models used in this study were related to GIUH computed from the geomorphological characteristics of a

catchment. The software ArcGIS and ILWIS were used for this study. The DSRO of the GIUH based Clark and Nash models were compared with the Clark IUH model available under HEC-1 package and Nash IUH model respectively, based on certain generally used objective functions. The inter comparison of both the models of GIUH based revealed that DSRHH were estimated with comparable accuracy with the both models. (*Rakesh Kumar et. al. – 2004*)

A review study of the synthetic unit hydrograph from the empirical UH to advanced geomorphological methods was carried out by the academicians from Anand Agricultural University, Gujarat and IIT Roorkee, India. This review analysed the latest improvements in the approach of conventional SUH for ungauged catchment. The SUH models were classified into four (4) main categories such as (i) Traditional or Empirical model, (ii) Conceptual model, (iii) Probabilistic models (iv) Geomorphological models. The review study articulated the water resource professionals on looking for models to analyse the flood hydrograph and its related mechanism for ungauged basin. (*P. K. Singh. et al. – 2014*)

A study on flood estimation in a river basin downstream of a major reservoir in coastal region was undertaken by academicians of IIT, Roorkee. The flood estimation was carried out by using conventional UH based hydro-meteorological approach as well as by using HEC-HMS model. The results of each approach have been compared. The river basin was divided into two sub basins as per the stream flow data availability. In conventional approach, Nash model UH was developed. Since the regional formula developed by CWC was much lesser, a fresh regional formula was developed for the basins for the determination of time to peak  $t_p$  by using the  $L/\sqrt{S}$  &  $t_p$  relationship. PMF hydrograph was developed using 2-bell method in conventional approach. In HEC-HMS model approach, initial & constant for loss model, Clark UH for transform model, monthly constant for base flow model, Muskingum method for routing and specified hydrograph precipitation analysis for meteorological model were employed to run the model. NSE and  $D_v$  were used as goodness of fit criteria of the model. (*Jaya Ram Prajapati. et al. – 2017*)

A study was carried out on flood zone mapping for Kelani river basin, Sri Lanka by the IIT, Roorkee professionals. The study aimed to develop the methodology for flood plain zoning and to establish its use for the Kelani river basin. The software GIS and MIKE 11 were used to execute the objectives of the study. Flood frequency analysis was carried out to estimate flood quantiles for six different gauging stations. MIKE11 NAM model was calibrated and validated based on the performance

criteria NSE. Flood inundation area in each land use land cover class for various return periods were determined from the flood plain mapping ( *A. D. S. Iresh et. al – 2017* )

A case study has been carried out by professionals from university Peradeniya, Sri Lanka, for the Kaluganga River basin which is the adjacent basin to the Kelani River Basin. This study presents a rainfall-runoff model developed for this basin using HEC-HMS lumped conceptual hydrologic model. Two different models, one having four sub basins and the other having ten sub basins were formulated. They were calibrated and verified using four historical flood events. Stream flow data at three gauging stations along the river were used in the calibration and verification. The above study has mainly focused on the effect of sub basin analysis with HEC-HMS model. The inter-comparison of simulated and observed flood hydrographs based on the goodness of fit criteria such as NSE, Peak flood and Time to peak revealed that there was no significant effect on number of sub basins considered. (*H. K Nandalal et al.-2010*)

Another case study has been carried out by professionals from university of Peradeniya, Sri Lanka, for modelling of event and continuous flow hydrographs. Here, event and continuous hydrologic modelling is used in the Kelani River basin in Sri Lanka using the HEC–HMS. The calibrated, direct runoff and base flow parameters were then used in the continuous hydrologic model. Extremely high rainfall events with hourly based data were employed for the calibration and validation of event base modelling. The calibrated model parameters were employed in the continuous base modelling with daily based data. The Green and Ampt infiltration loss method was used to account for infiltration loss in event-based modelling and five-layer soil moisture accounting loss method was employed in continuous modelling. The Clark unit hydrograph method and the recession base flow method were used to simulate direct runoff and base flow, respectively. (*M. M. G. T De Silva et al.-2014*)

## **2.2 Research Gap**

Irrigation department, Sri Lanka plays a significant role in mitigation of flood which hits the almost all over the island since it experiences two seasonal storms which are from North –East monsoon and South –West monsoon. Even though number of flood studies were carried out in the Kelani river basin over the decades, those application of studies have not been implemented in practical manner so far. These have been done for the academic purposes only. Further, none of the professionals in the Irrigation Department have used the Hydrologic Engineering Centre–Hydrologic Modelling System (HEC–HMS) model tool so far.

In this HEC-HMS model, the available options as far as possible have been used according to the available hydrological data of the Kelani river basin. Since the study area which is the Kelani River basin area falls lesser than 5000 sq.km, single basin approach is well enough to carry out the study. However, at least two sub basin approaches also could be taken into consideration for the better outcome since the observed flow data of the additional gauging station within the study area is available. Further the outcome results from the different options of models and computational managers could be analysed systematically. In the development of hydrographs, the time of concentration  $T_c$  which is one of most crucial hydrograph properties is derived by various methods for obtaining the regional formula. And different methods are used to develop isochrones of the study area in case of plotting of time area histograms. However, three different type of transform models have been used for simulation process and evaluated based on the chosen objective functions of the study.

In addition, the estimation of designed flood for the Kelani river basin was obtained from the unit hydrograph developed in the HEC-HMS model. In this study, design storm is derived from two methods namely depth – area - duration curve and depth – duration – frequency curve in order to estimate the design flood. This value of designed flood was compared with the value of flood peak found from the various distribution of flood frequency analysis.

## CHAPTER 3 DESCRIPTION OF STUDY AREA AND DATA AVAILABILITY

### 3.1 Study Area

Kelani river is the second largest river of Sri Lanka. Its catchment area up to Hanwella gauging site is 1836 sq.km which covers five districts namely Colombo, Gampaha, Kegalle, Ratnapura and Nuwara-Eliya. In the catchment, the topographical elevations vary between 16 m and 2320 m above mean sea level. The contributions of the flow to the river come from the rainfall mostly occur during the two distinct monsoon seasons i.e. North-East and South-West monsoon. The Administrative Capital ‘Sri Jayewardenepura ‘and the Commercial Capital ‘Colombo’ are located in the downstream of the Hanwella gauging site. The district Colombo in Western Province with the current population of 300 head per day has an area of 699 sq.km with population of 2.3 Million and has population density likely to be 60 times of the average population density which is 340 heads per sq.km.

Figure 3.1 shows the gross basin of Kelani river and the locations of gauging station over the basin. The calibration and validation process are setup with the observed stream flow data of Hanwella gauging station. Therefore, all the data processing was carried out in the upper catchment of Hanwella gauging station. It is referred to as Kelani river basin in this study.

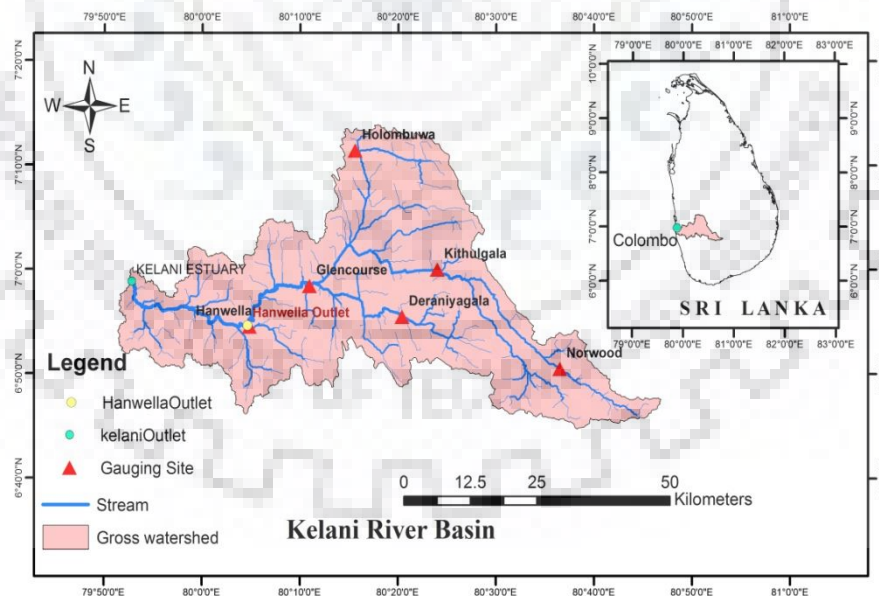


**Figure 3.1 Gross Basin – Kelani River**

Kelani River in Sri Lanka is being contributed with runoff from both monsoon seasons rainfall, but the major share of its flow contribution is due to the rainfall during South-West monsoon season. The district Colombo frequently experiences flood menace almost every year. It causes loss to the lives and severe damages to infrastructures, properties and ultimately livelihood of the communities

residing in district Colombo. Thus, the economic growth of Sri Lanka dramatically reduces due to the extensive damages caused by frequent flooding.

### 3.2 Data Availability

#### 3.2.1 METEOROLOGICAL AND HYDROLOGICAL DATA

Meteorological data (rainfall) on daily basis and hourly basis for selected extreme flood events and Hydrological data (discharge only on daily basis & water level on daily basis & on hourly basis for selected extreme flood events) at six (06) gauging stations (shown in Figure 3.1) namely Hanwella, Norwood, Deraniyagala, Kithulgala, Holombuwa and Glencourse located in the upper basin were obtained. These data were obtained from the Department of Irrigation, Colombo, Sri Lanka for model calibration and validation. The event-based model calibration and validation is carried out by considering the extremely heavy rainfall events and other events occurred in the recent past years. (Table 3.1).

*Table 3.1 Meteorological and Hydrological Data.*

Gauging Station	Daily Rainfall, Water Level & Discharge		Hourly Rainfall & Discharge for Selected Flood Events	
	Period	No of Years	No of Events	Year of Event & No of Consecutive Days
Norwood	1974-2016	43	4	2017(14), 2014Dec (8), 2014Jun (16) & 2012(9)
Kithulgala	1974-2016	43	4	2017(14), 2014Dec (8), 2014Jun (16) & 2012(9)
Holombuwa	1974-2016	43	4	2017(14), 2014Dec (8), 2014Jun (16) & 2012(9)
Deraniyagala	1974-2016	43	4	2017(14), 2014Dec (8), 2014Jun (16) & 2012(9)
Glencourse	1974-2016	43	4	2017(14), 2014Dec (8), 2014Jun (16) & 2012(9)
Hanwella	1974-2016	43	4	2017(14), 2014Dec (8), 2014Jun (16) & 2012(9)

In addition to this, the annual HFL reported at the gauging station Hanwella also were obtained from the same department for the purpose of frequency analysis

### 3.2.2 SPATIAL DATA

The Digital Elevation Model (DEM) and Satellite Image of 30m resolution which is freely available were downloaded from United States Geological Survey (USGS) website. The DEM is the fundamental need of the HEC-Geo HMS tool to create the basin model this study area. And the source of soil data map was downloaded from FAO website and the soil data of this study area was developed. The satellite image was employed to develop land use land cover map. The layer properties of the DEM and satellite image are shown in the Figure 2. and Figure 3. respectively.

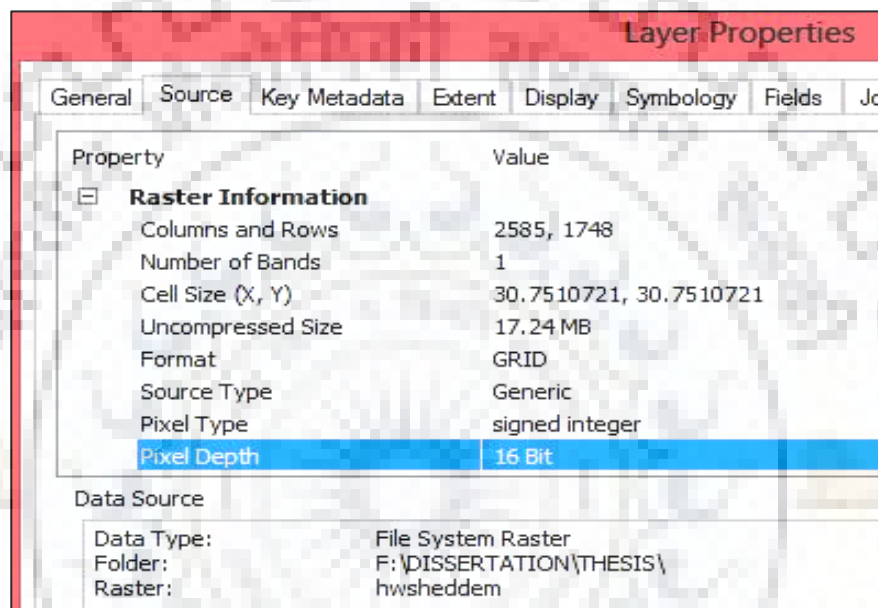


*Figure 3.2 Digital Elevation Model – Layer Properties*

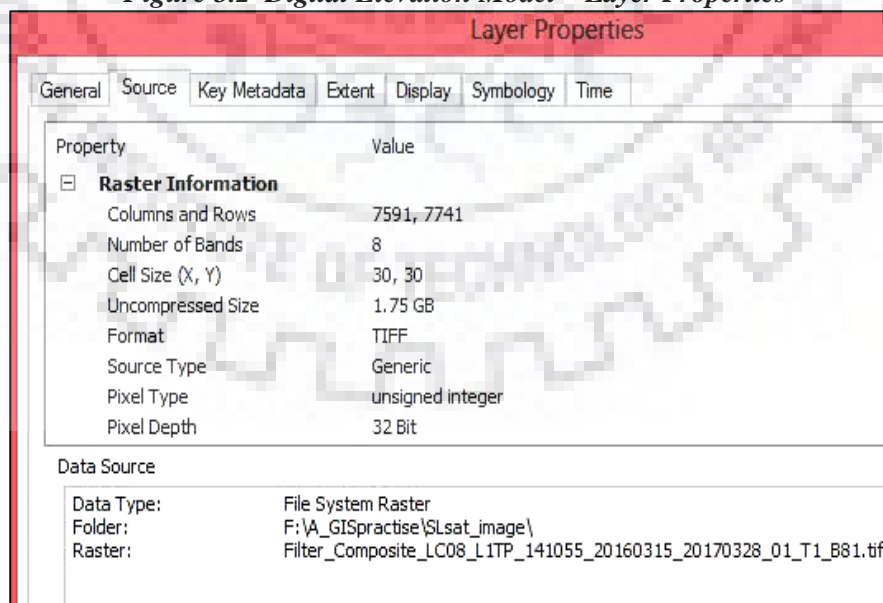


*Figure 3.3 Satellite Image – Layer Properties*



## **CHAPTER 4 METHODOLOGY**

### **4.1 Spatial Data Processing**

#### **4.1.1 PREPARATION OF BASIN MAP AND DELINEATION OF DRAINAGE NETWORK**

The basin map for river Kelani up to Hanwella gauging site was prepared using the SRTM raw DEM data downloaded from USGS website as described in section.3.2.2 using ArcGIS software. Also, the drainage network of the river basin was delineated using the same software. The tool namely “hydrology”, available in ArcGIS toolbox, was used to define the river basin.

#### **4.1.2 PREPERATION OF DIGITAL ELEVATION MODEL**

The raw DEM and shape file of the delineated basin were used to prepare final DEM considering the different elevation classes and the terrain surface of the basin was identified.

#### **4.1.3 PREPERATION OF THIessen POLYGON MAP AND COMPUTATIONS of THESSEN POLYGON WIEGHTS (GAUGE WEIGHT)**

The Thiessen polygon map was prepared using the tool “Thiessen polygon”, available in ArcGIS software. The geographical coordinates of each rain gauge were supplied as input to the software. The gauge weights were computed using the ArcGIS software. The computed gauge weights were considered as input to the HEC-HMS under its Meteorological Model.

#### **4.1.4 PREPARATION OF LAND USE /LAND COVER MAP(LULC)**

The LULC map was prepared from the “Landsat 8” satellite imagery of year 2014 containing eight different colour band combinations. The combination of “supervised” and “unsupervised” options in ArcGIS were used to classify the LULC of the basin.

#### **4.1.5 PREPARATION OF SOIL MAP**

The soil map was prepared using the “clip” tool of ArcGIS for extracting the soil map for the basin from FAO website (<http://www.fao.org/soils-portal/soil-survey/soil-maps-and-databases/en/>) where such maps are available in digital form for entire world.

#### **4.1.6 PREPARATION OF ISOCHRONAL MAPS AND DEVELOPMENT OF TIME AREA CURVE**

For preparing the isochronal map of the basin, some points, located on the Kelani river and its tributaries in the basin were identified using HEC-GeoHMS. The time of travels from all these points

up to Hanwella Gauging site were required to be estimated. In this regard, the time of travels of all the segments, obtained from considering the two consecutive points on the streams, were taken to be directly proportional to  $L/\sqrt{S}$ . This can be demonstrated from the Manning's equation as follows

$$V = \frac{R^{\frac{2}{3}} \times S^{1/2}}{n} \quad (4.1)$$

Where  $V$  is average velocity of the stream in m/s at the end of the segment.

$R$  is hydraulic radius in m for the stream cross section at the end of the segment,

$S$  is average longitudinal slope of the channel segment and

$n$  is Manning's Roughness Coefficient of the Channel segment at its end.

However, the Manning's equation can be rearranged in terms of stream length  $L$  and time of travel  $t_c$  considering the end channel as a wide rectangular channel and  $V = L/t_c$ . The equation may be written as:

$$t_c = C \cdot L/\sqrt{S} \quad (4.2)$$

where  $C = R^{2/3}/n$ . It is considered to be constant.

The time of travel from the farthest point of the catchment to the outlet of the basin along the longest stream was considered as time of concentration of the catchment ( $T_c$ ). The time of travel for  $i^{th}$  segment was computed as  $t_{ci} = C L_i/\sqrt{S_i}$ . Subsequently, the time of travel for each river was computed as the  $C$  times sum of the  $L/\sqrt{S}$  for each individual segments of the river and the tributaries i.e.  $[C(L_1/\sqrt{S_1} + L_2/\sqrt{S_2} + L_3/\sqrt{S_3} + \dots + L_n/\sqrt{S_n})]$ , where  $n$  is number of segments for any river reach. The max value of  $C \sum (L/\sqrt{S})$  was found from all the river reaches. It was equal to time of concentration ( $T_c$ ). Thus

$$T_c = C \sum (L/\sqrt{S}) \quad (4.3)$$

An initial estimate of  $T_c$  was obtained from the excess rainfall hyetograph and direct surface runoff hydrograph for a storm event. The  $T_c$  is the time from the end of excess rainfall to point of inflection

on the recession limb of the direct surface runoff. Now Eqn. (4.3) was used to get the value of Constant  $C$  knowing the value  $T_c$  and  $\sum \left( \frac{L}{\sqrt{S}} \right)$  for the longest flow path.

For preparing the isochronal maps, the following interpolation methods, available in the ArcGIS, were used:

- a. Inverse Distance Weighted (IDW) Interpolation
- b. Kriging Interpolation

The Time-Area curve was developed using the above methods. It was presented in the form of Time-Area Histogram as well as cumulative Time-Area Percent curves. In addition to this, a synthetic Time-Area curve is developed within the HEC-HMS programme, considering the diamond shape of the basin. It provides an option for using the inbuilt time area curve in place of user defined time area curve. The HEC-HMS software has a predefined typical time-area relationship which has been built inside the programme as shown in Eq (5.1) by considering the shape of the basin as diamond shape in order to make the time – area relationship smooth.

$$\frac{A_t}{A} = \begin{cases} 1.414 \left( \frac{t}{T_c} \right) & \text{for } t \leq \frac{T_c}{2} \\ 1 - 1.414 \left( \frac{t}{T_c} \right) & \text{for } t \geq \frac{T_c}{2} \end{cases} \quad (4.4)$$

Where  $A_t$  = Cumulative watershed area contributing at time  $t$ ;  $A$  = total watershed area; and  $T_c$  = time of concentration of the watershed. The table below shows the synthetic method time and area. Table 5.8 was performed using the time area relationship shown in Eq (5.1) to develop time-area diagram and time area percent curve.

## 4.2 Temporal Data Processing

### 4.2.1 RAINFALL DATA PROCESSING

There were the rain gauge stations at different locations in the river basin reporting the hourly rainfall values. For each storm events, the average hourly rainfall values for the basin were computed using the gauge weights obtained from the Thiessen polygon method.

#### 4.2.2 STREAM FLOW DATA PROCESSING

There was no hourly stream flow data at the gauging site of outlet considered. From the observed daily gauge and discharge data, stage – discharge relationship, which is also known as Rating Curve, for the gauging site of the outlet was developed. The standard form of the rating curve for any gauging station may be expressed as follows:

$$Q = a.(S)^b \quad (4.5)$$

Where,  $Q$  is daily stream flow in cumec,

$S$  is daily stage values in metre given as  $S=H-H_0$ ,

$H$  is daily gauge values in metre

$H_0$  is the zero of the gauge which corresponds to the zero discharge, and

$a$  and  $b$  are rating curve constants to be derived from analysing the daily gauge & discharge data.

For developing the rating curve, following methods were used:

- (i) Graphical Method
- (ii) Analytical Method

**(i) Graphical Method**

In graphical method the daily stage and corresponding discharge values were plotted on log-log graph paper considering the discharge ( $Q$ ) values on  $x$ -axis and the stage ( $S$ ) values on  $y$ -axis and a best fit line was drawn through the plotted points. The equation of the best fit line provides the rating curve using graphical method. The form of the rating curve equation is given as:

$$\text{Log } Q = b. \text{log } S + \text{log } a \quad (4.6)$$

Where  $b$  and  $\text{log } (a)$  represents the slope and intercept of the best fit line, if it is expressed in the form of  $Y=m X +C$  considering  $Y$  as  $\text{log } Q$ ,  $X$  as  $\text{log } S$  and  $C$  as  $\text{Log } (a)$ .

**(ii) Analytical Method:**

In the analytical method, least square approach (or alternatively known as simple linear regression approach) is used for finding the constants  $a$  and  $b$  of the rating curve. The following steps are involved for developing the rating curve using analytical method:

- (a) Consider the linear form of the daily gauge and discharge relationship in the form of  $Y = b X + c$  where  $Y$  is equal to  $\log (S_{comp})$ ,  $X$  is equal to  $\log Q$  and  $C$  is equal to  $\log (a)$ .
- (b) Compute sum of error squares as  $\epsilon = \sum(Y_i - \hat{Y}_i)^2$ , where  $Y_i$  is the value  $\log (Q_{obs})$  and  $\hat{Y}_i$  is the value of  $\log (Q_{comp})$
- (c) Estimate the value of  $b$  and  $C$  using method of least square. The values of  $b$  and  $C$  are given as:

$$b = \frac{(N(\sum XY) - \sum X \cdot \sum Y)}{N(\sum X^2) - (\sum X)^2} \quad (4.7)$$

$$\log(a) = C = \frac{\sum Y - b \cdot \sum X}{N} \quad (4.8)$$

The coefficient of correlation  $r$  can be computed for least square method is given as

$$r = \frac{N(\sum XY) - (\sum X) \cdot (\sum Y)}{\sqrt{\{N \cdot (\sum X^2) - (\sum X)^2\} \{N \cdot (\sum Y^2) - (\sum Y)^2\}}} \quad (4.9)$$

For best fit rating curve, the value of  $r$  should be closer to 1. The lower values of  $r$  indicate more scattered points of daily stage and discharge values even in the log domain. For all practical purposes, the acceptable range of  $r$  values are between 0.6 and 1.0. If the value of  $r$  is exactly equal to one, it indicates that there is perfect linear correlation between daily stage and discharge values in log domain. However, it is unlikely to get such scenario with the field data due to many issues involved with the river flow hydraulics.

The hourly discharge values were calculated at the gauging site of the outlet using the developed rating curve corresponding to hourly observed stages. The developed rating curve was also used for determining annual maximum stream flow series corresponding to the observed annual maximum stage series. The annual maximum flow series was utilised for carrying out flood frequency analysis.

### 4.3 Application of HEC-GeoHMS and HEC-HMS

HEC-GeoHMS is Geospatial Hydrological Modelling System, the extended supplementary application tool of ArcGIS and used to develop basin model and its characteristics from the raw digital

elevation model (DEM) in the convenient manner. Basin Model is created by HEC-GeoHMS with a single basin and used for the calibration and verification process. The required basin characteristics such as longest flow path, river lengths, upstream & downstream elevations and slopes of each river segments are obtained via this HEC-GeoHMS application process. The element network of the basin which was represented in HEC-HMS desktop was also performed by HEC-GeoHMS. Then the developed basin model representing element network in HEC-GeoHMS is imported to HEC-HMS for its further application. HEC-HMS is the simulation software developed to simulate all type hydrological process of watershed (D.S. Sampath et al, 2015) It is available as online resource software designed by USACE with updated versions and treats user friendly manner. The entire modelling process mainly is executed by the software namely HEC-GeoHMS and HEC-HMS. The Figure 4.1. illustrates the calibration and validation process of the modelling of this study.

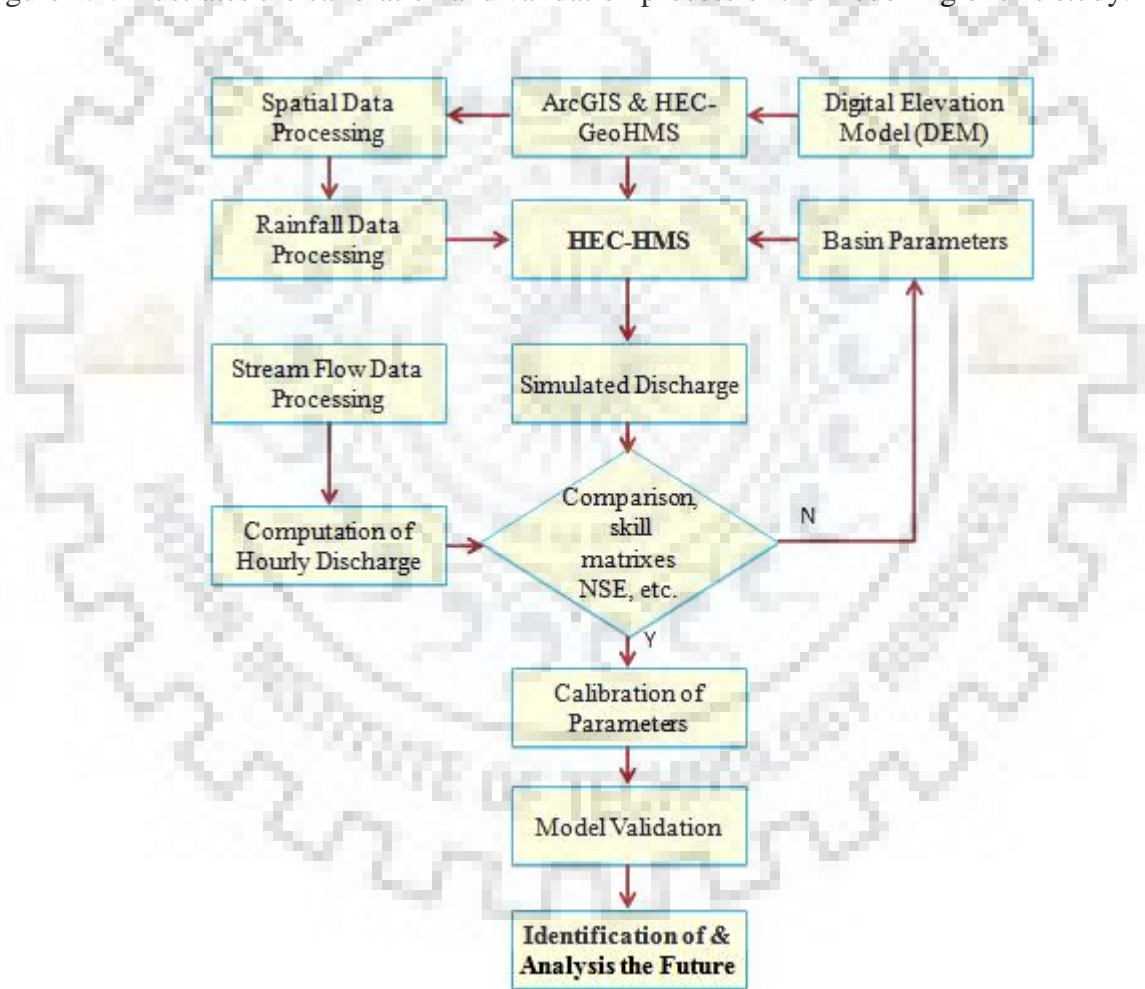


*Figure 4.1 Flow Diagram of HEC-HMS Process*

#### 4.3.1 METROLOGICAL MODEL

Meteorological Model is created by selecting gage weight option available in this HEC-HMS model. Gage weights, which have been estimated from Thiessen polygon method, are used for this option.

#### 4.3.2 BASE FLOW MODEL

There are three options available in the HEC-HMS program for the computation of baseflow. Those are:

- a. Constant, Monthly - varying value
- b. Exponential recession model
- c. Linear-reservoir accounting model

In this study, the exponential-recession model was used for separating the baseflow from the flood hydrographs resulting due to different storm events in order to estimate the direct surface runoff hydrographs. This base flow model, which defines the exponential form of relationship, is described below:

$$Q_t = Q_o.k^t \quad (4.10)$$

Where  $Q_t$  is the base flow in  $m^3/s$  (at any time  $t$ ),  $Q_o$  is the initial base flow in  $m^3/s$  (at time zero) and  $k$  is an exponential decay constant or recession constant.

In this base flow model, the contribution of base flow decays exponentially from the initial flow. As per the HEC-HMS program,  $k$  is defined as the ratio of the base flow at time  $t$  to the base flow one day earlier. The base flow model includes the parameters such as initial base flow, the recession constant and the threshold flow. The threshold flow in stream flow hydrograph may be defined as the flow at which, base flow is defined by the initial base flow recession.

#### 4.3.3 LOSS MODEL

There are numerous runoff volume models also known as loss models are applicable in HEC-HMS modelling.

- i. Initial and Constant Rate Loss Model
- ii. Deficit and Constant Rate Loss Model
- iii. SCS - CN Loss Model
- iv. Green and Ampt Loss Model
- v. SMA Loss Model

In the application of loss model, the method Initial loss & constant rate is used in this work. This method includes two parameter such as initial loss ( $I_a$ ) and constant loss rate. These parameters are highly depending on the physical properties of the river basin soil, land use and the antecedent moisture condition.

#### 4. 3.4 TRANSFORM MODELS

The HEC-HMS program consists of various transform models as given below

- i. Clark UH Model
- ii. SCS UH Model
- iii. Snyder UH Model
- iv. Mod. Clark Model
- v. Kinematic Wave Model.

In this study, the Clark UH, SCS UH and Snyder UH transform models were used for the event-based rainfall-runoff modelling.

##### 4.3.4.1 CLARK UH MODEL

The basic concept of this model defines that the temporary storage of water over the basin (in the soil and channels) plays important role in the transformation of rainfall excess to direct runoff. The linear reservoir relationship is generally used to show the effects of this temporary storage. The linear reservoir relationship may be represented with the following continuity equation.

$$\frac{dS}{dt} = I_t - O_t \quad (4.11)$$

Where  $dS/dt$  is the time rate of change of water in storage at time  $t$ ;  $I_t$  is the average inflow to the storage at time  $t$ ; and  $O_t$  is the outflow from storage at time  $t$ .

Storage and outflow at time  $t$  have the relationship with the linear reservoir model as follows.

$$S_t = R.O_t \quad (4.12)$$



Where  $R$  is constant linear reservoir parameter (storage coefficient). From the above equations (4.11) and (4.12), the following relationships are yielded.

$$O_t = C_A I_t + C_B O_{t-1} \quad (4.13)$$

Where  $C_A$  and  $C_B$  are routing coefficients. The computation of these coefficients is given below:

$$C_A = \frac{\Delta t}{R + 0.5\Delta t} \quad (4.14)$$

$$C_B = 1 - C_A \quad (4.15)$$

The average outflow is given by

$$\bar{O}_t = \frac{O_t + O_{t-1}}{2} \quad (4.16)$$

Since the cumulated effects of all basin storage is represented in this Clark UH model, the reservoir may be considered to be located conceptually at the outlet considered. In addition to this lumped model of storage, the Clark UH model computes the time required for water to move outlet from basin. It carries out with linear channel model, in which water is routed from remote points to the outlet with delay (translation) but without attenuation. This delay is implicitly related with time and area so called time-area histogram. This specifies the basin area contributing flow at the outlet as a function of time. If the area is multiplied by the unit depth of excess rainfall and divided by the time step  $\Delta t$ , the result is inflow,  $I_b$  to the outlet (linear reservoir)

However, application of Clark UH model in HEC-HMS requires the parameters described below.

- a) Time of concentration  $T_c$
- b) The Storage Coefficient,  $R$
- c) The properties of Time-area histogram or Time-Area Percent Curve of the basin

The time of concentration  $T_c$  and the storage coefficient  $R$  were estimated from sensitive analysis to employ as initial parameter values. The time – area percent curves are developed using various methods as described under section 4.1.6.

#### 4.3.4.2 SCS UH MODEL

This model is applicable for single -peaked UH. The SCS suggests the following relationship.

$$U_p = C \cdot \frac{A}{T_p} \quad (4.17)$$

Where  $A$  is basin area;  $C$  is conversion constant (2.08 for SI unit);  $T_p$  is the time to peak. The  $T_p$  is related as:

$$T_p = \frac{\Delta t}{2} + t_{lag} \quad (4.18)$$

Where  $\Delta t$  is excess rainfall duration;  $t_{lag}$  is the basin lag which defines as the time difference between the center of mass of rainfall excess to and the UH peak. For this model only one parameter, known as basin lag, is available transform model of HEC-HMS. The initial value of this parameter was found from the sensitive analysis. When the basin lag is fed as input to this model in HEC -HMS program, the equations (4.17) and (4.18) are solved to compute peak discharge and time to peak.

#### 4.3.4.3 SNYDER UH MODEL

In the Snyder UH model, the critical characteristics of the UH are the lag, peak flow and total time base. Snyder (1938) stated the following relationship for a standard UH.

$$t_p = 5.5 t_r \quad (4.19)$$

Where  $t_r$  is the rainfall duration;  $t_p$  is basin lag which means the difference time of UH peak and the time of centroid of the excess rainfall of hyetograph. If the desired UH for a specific basin is significantly varied from standard UH, the following relationship may be defined to compute the lag of desired UH.

$$t_{pR} = t_p - \frac{t_r - t_R}{4} \quad (4.20)$$

Where  $t_R$  is duration desired UH; and  $t_{pR}$  is lag of desired UH. Snyder further found that the following relationship in the case of standard UH.

$$\frac{U_p}{A} = C \frac{C_p}{t_p} \quad (4.21)$$

Where  $U_p$  is peak of standard UH;  $A$  is basin drainage area;  $C_p$  is UH peaking coefficient; and  $C$  is conversion constant (2.75 for SI unit). For other desired UH, the UH peak  $Q_{pR}$  is defined as:

$$\frac{U_{pR}}{A} = C \frac{C_p}{t_{pR}} \quad (4.22)$$

Snyder UH model in HEC-HMS requires two parameters such as standard lag,  $t_p$ , and peaking coefficient  $C_p$ . The HEC-HMS program uses the computed UH peak and time to peak, to find an equivalent Clark's model UH. From this approach, it computes the time base and all ordinates except the peak of UH. However, the initial parameter values for the Snyder UH model were obtained from the result of sensitivity analysis.

#### 4.4 Sensitivity Analysis

The sensitivity analysis was carried out for the three transform models in order to define the range of initial parameters to be considered during the optimisation. In this regard, NSE values were computed for different sets of parameters values for different transform models. As the Clark UH and Snyder UH models are two parameters models, NSE contours were drawn considering different values of one parameter on x-axis and correspondingly the other parameter values on y-axis. Such contours were helpful for identifying the band of the maximum NSE value. Finally, the initial parameters values of those transform models were decided considering them within this band. SCS transform model is one parameter model. For this model, different values of the parameters were considered on x-axis and corresponding computed NSE values were considered on y-axis. The initial parameter value was chosen corresponding to the maximum NSE value.

#### 4.5 Error Criteria for comparing the performance of Three Transform Models

For comparing the performance of the three transform models during calibration and validation, the error criteria such as Nash-Sutcliffe Efficiency, Percentage Error Peak, Percent Error Time to Peak

and Percent Error Discharge volume (Volume Deviation  $D_v$ ) were obtained through HEC-HMS software based on the observed and computed direct surface runoff hydrographs. These error criteria are described below:

- (i) Nash-Sutcliffe Model Efficiency Coefficient(NSE)

$$NSE = 1 - \left[ \frac{\sum_{i=0}^n (Q_{obs}(i) - Q_{com}(i))^2}{\sum_{i=0}^n (Q_{obs}(i) - \bar{Q})^2} \right] \quad (4.23)$$

Where  $Q_{obs}$ ,  $Q_{com}$  and  $\bar{Q}$  are the observed, simulated and observed mean discharge over the  $n$  hours respectively. The most optimal value of  $NSE$  is 1.

- (ii) Volume deviation ( $D_v$ )

$$D_v = \left| \frac{(V_{obs} - V_{com})}{V_{obs}} \right| \times 100\% \quad (4.24)$$

Where  $V_{obs}$  and  $V_{com}$  are the observed and simulated volume of runoff over the  $n$  hours respectively. The most optimal value of  $D_v$  is 0.

- (iii) Percent error in peak ( $Z$ )

$$Z = \left| \frac{Q_{obs}(peak) - Q_{com}(peak)}{Q_{obs}(peak)} \right| \times 100\% \quad (4.25)$$

Where  $Q_{obs}(peak)$  and  $Q_{com}(peak)$  are the observed and simulated peak discharge of runoff over the  $n$  hours respectively. The most optimal value of  $Z$  is 0.

The  $NSE$  was reported as best performance criteria of simulation (Mc Cuen et al.2006). However, in addition to the  $NSE$ , percent error in peak, percent error in time to peak, percent error in discharge volume of each direct runoff model were compared individually for each of the flood events considered for calibration and validation.

#### 4.6 Calibration and Validation of the Models

Calibration of transform models was carried out using the automatic calibration (optimization) option available in HEC-HMS. However, for taking the optimisation runs, the initial parameter values of the

models were required to be estimated. In this regard, sensitive analysis was carried out for estimating the parameters. The calibrations of the model were carried based on the various goodness of fit measures derived from the observed and simulated hydrographs in HEC-HMS programme. Based on these measures, the optimised parameters of the transform models were selected. Calibration was carried out for selected number of events and the representative parameters were derived taking the average of the optimised parameters obtained for each event considered for calibration. The representative parameters of all the transform models were used in HEC-HMS for their validation over the selected storm events not considered for calibration.

## **4.7 Real Time Flood Forecasting**

### **4.7.1 DEVELOPMENT OF UNIT HYDROGRAPH**

The UH was developed using the validated parameters of the best transform model using HEC-HMS.

### **4.7.2 FORECASTING OF FLOOD HYDROGRAPH**

The direct surface runoff hydrograph was forecasted at hourly time step considering the information available for excess rainfall till that time step using the principle of proportionality and principle of superimposition inherent with the unit hydrograph.

## **4.8 Estimation of Design Flood**

Depending on the size of hydraulic structure, the following are the design criteria adopted for small and intermediate storage structures (*Manual on Estimation of Design Flood-2001, Hydrologic Studies Organization, CWC, New Delhi*)

- I. For Small structures, 100 yrs. return period flood is adopted
- II. For intermediate structures, Standard Project Flood (SPF) is adopted

In this study, the different methodologies were used for the above two cases. Those are described below: are, and depth-area-duration curve were developed to estimate the design flood for the small and intermediate size of hydraulic structure respectively.

### **4.8.1 ESTIMATION OF 100- YEAR RETURN PERIOD FLOOD**

To compute the floods of 100-year return period, a rainfall for 100- year return period is estimated developing depth-duration-frequency (DDF) curve. For this, the available long period rainfall records

of the different rain gauge stations in the basin for the various durations are considered for the preparation of this curve. Initially, the maximum rainfalls for a desired duration was sorted as per their probability of occurrence or return period. Likewise, the other durations of rainfall occurrence were considered to get the relationship with its probability of occurrence or return period. Then the number of DDF curves were drawn for different durations. The design duration of the rainfall was considered as per the recommendations of the publications (*Publication on Rationalization of Design Storm Parameters for Design Flood Estimation. (Dec.1993) Hydrology Studies Organization, Central Water Commission, New Delhi*). Subsequently, the DDF curve for 100-year return period for that design duration was adopted for 100-year rainfall as design storm. Hourly rainfall values of design storm were obtained fitting the polynomial equation between the 100-year rainfall values at hourly time interval considering it as dependent variables and time duration incrementing at hourly interval as well as its polynomials as independent variables. The recommended design loss rate (*Manual on Estimation of Design Flood-2001, Hydrologic Studies Organization, CWC, New Delhi*) was considered and excess rainfall hyetographs were computed at hourly interval for the design duration. Now the design sequence of the excess rainfall hyetograph was found arranging them against the unit hydrograph ordinates such that the highest rainfall corresponds to the UH peak, second highest rainfall block corresponds to the second highest ordinate of the UH and so on. The sequence of the hourly excess rainfall, thus obtained, is reversed to get the design sequence of the excess rainfall hyetograph. The design rainfall hyetograph was convoluted with the ordinates of Unit Hydrograph to compute the design direct surface runoff hydrograph. The recommended design base flow (*Manual on Estimation of Design Flood-2001, Hydrologic Studies Organization, CWC, New Delhi*) was added with the ordinates of direct surface runoff to get the design flood hydrograph. The peak of the design flood hydrograph corresponds to the flood of 100-year return period.

#### 4.8.2 COMPUTATION OF STANDARD PROJECT FLOOD (SPF)

For the estimation of SPF, the standard project storm (SPS) is required to be determined. For SPS, the depth-area-duration(DAD) curve was developed analysing the maximum amount of rainfall, derived from the observed rainfall data at the existing rain gauge stations in the region for different durations; no transposition was carried out due to lack of sufficient data. For developing DAD curve, the interpolation technique of ArcGIS was used to prepare the isohyet maps for various durations of storms over the basin. The mean depth of consecutive isohyet value and the corresponding enclosed area by the isohyet line were used to develop the DAD curves for various durations. The design duration of the storm is obtained as mentioned under section 4.12.1. The depth corresponding to design duration for given basin area was obtained from DAD curve. This provides the design depth

of the rainfall. Now the procedure described under section 4.12.1 were repeated to get the design flood hydrograph from the estimated design storm of the design duration. The design flood hydrograph, thus obtained, represents the estimate of Standard Project Flood (SPF).

#### 4.9 Flood Frequency Analysis

In Sri Lanka, Gumbel Distribution has been frequently used for estimating the floods of specific return period. In some parts of the country, Log Pearson Type 3 has also been used. Thus, in this study, these two distributions were considered for flood frequency analysis to estimate the floods of Specific return period.

The annual HFL data, as available at the gauging site, were used in the rating curve to determine the annual peak flood series. The flood frequency analysis was carried out utilising the annual peak flood series fitting those two distributions following the frequency factor approach:

##### 4.9.1 GUMBEL'S METHOD

Gumbel (1941) introduced this method for flood frequency analysis. Following relationships were applied in this analysis to estimate the floods of T-year period.

$$X_T = \bar{X} + K_T S_x \quad (4.26)$$

Where

$X_T$  = variate  $X$  with return period  $T$ ,

$\bar{X}$  = mean variate, (mean of the annual maximum peak of flood series) in  $m^3/s$

$S_x$  = standard deviation of the sample size  $N = \sqrt{\frac{\sum(X-\bar{X})^2}{(N-1)}}$ , in  $m^3/s$

$K_T$  = frequency factor expressed as

$$K_T = - \left[ 0.45 + 0.7797 \cdot \ln \cdot \ln \left( \frac{T}{T-1} \right) \right] \quad (4.27)$$

Eqn.(4.26) and Eqn (4.27) were used to find out the flood magnitude relevant to the specified return period based on the annual peak flood series. The series was assembled and the sample size was noted down. Here, the annual peak flood value was the variate  $X$ . Then  $\bar{X}$  and  $S_x$  were computed. Then  $K$  was found. Ultimately  $X_T$  was determined as per the Eqn. (4.26) for required return period  $T$ .

#### 4.9.2 LOG. PEARSON TYPE III METHOD

The variate  $X$  is transformed logarithmic form (base 10) for frequency analysis. Then the logarithmic variate  $Z$  is given by

$$Z = \log X \quad (4.28)$$

$$Z_T = \bar{Z} + K_Z \cdot \sigma_Z \quad (4.29)$$

Where  $K_Z$  = a frequency factor which is a function of return period  $T$  and skewness  $C_s$

$\sigma_Z$  = standard deviation of the  $Z$  variate sample

$$= \sqrt{\frac{\sum (Z - \bar{Z})^2}{(N - 1)}} \quad (4.30)$$

$C_s$  = Skewness of variate  $Z$

$$= \frac{N \cdot \sum (Z - \bar{Z})^3}{(N - 1) \cdot (N - 2) \cdot \sigma_Z^3} \quad (4.31)$$

$\bar{Z}$  = mean  $Z$

$N$  = sample size (number of years of record)

$$X_T = 10^{Z_T} \quad (4.32)$$

The frequency factor  $K_z$  was picked up from the Table 7.6 of Ref. xiv. for different return periods considered. Then  $Z_T$  was computed using the Eqn. (4.29) and  $X_T$  was computed using the Eqn. (4.32) for desired return period  $T$ .



## CHAPTER 5 ANALYSIS AND DISCUSSION OF RESULTS

### 5.1 Spatial Data Processing

#### 5.1.1 PREPARATION OF BASIN MAP AND DELINEATION OF DRAINAGE NETWORK

For Kelani river basin, the watershed was delineated and drainage networks were drawn using ArcGIS software. Figure 5.1 shows the delineated watershed and the drainage network of Kelani river up to Hanwella gauging site. The shape of the river basin seems to be significantly irregular shape. The drainage density over the river basin is also almost equally distributed.

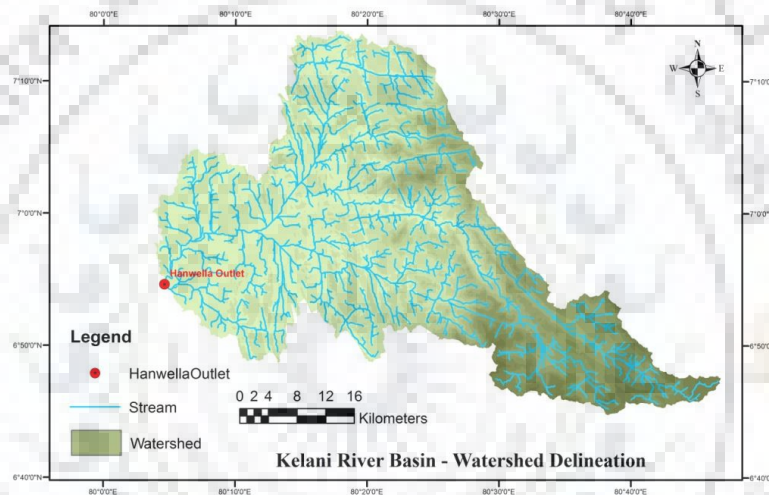


*Figure 5.1 Delineated Watershed & Drainage Network of Kelani River Basin up to Hanwella Gauging Site*

#### 5.1.2 PREPARATION OF DIGITAL ELEVATION MODEL

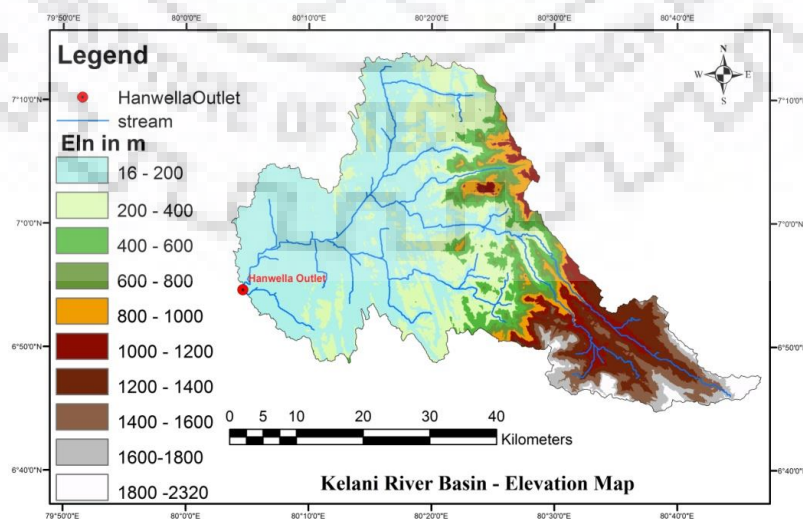


*Figure 5.2 Digital Elevation Map of Kelani River Basin up to Hanwella Gauging Site*

The digital elevation model was used to prepare digital elevation map of Kelani river Basin up to Hanwella gauging site. Figure 5.2 shows the digital elevation map of the Kelani river basin. In this figure various elevation classes of the Kelani river basin are illustrated. From the figure, it is observed that the elevation varies from 16 m to 2320 m above MSL. The major portion of the river basin is flat having elevation range varying between 16 m to 200 m above MSL whereas upper portion of the river basin is hilly having the elevation range varying between 200m to 2320m above MSL.

### 5.1.3 PREPERATION OF THIESSEN POLYGON MAP AND COMPUTATIONS OF THESSEN POLYGON WIEGHTS (GAUGE WEIGHT)

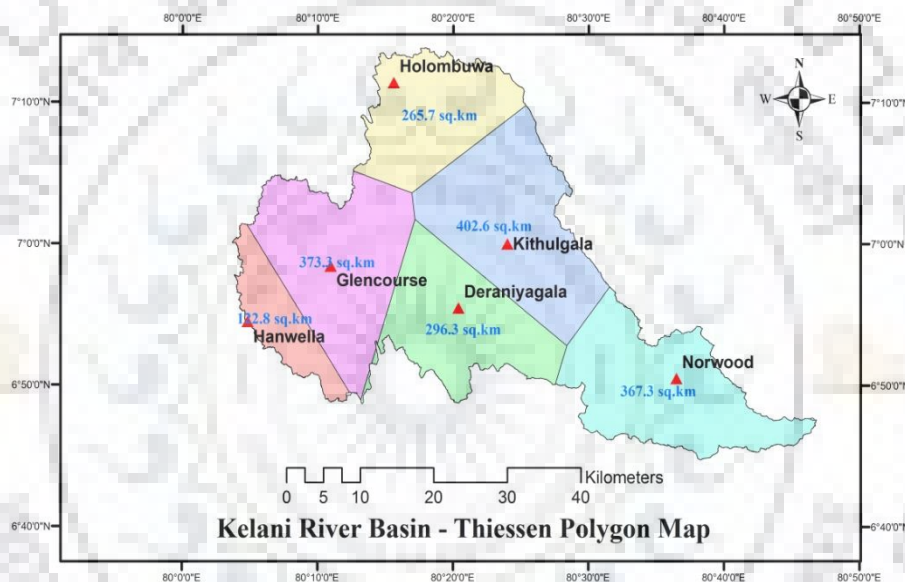


**Figure 5.3 Thiessen Polygon Map of Kelani River Basin up to Hanwella Gauging Site**

Thiessen polygon map was developed using ArcGIS as shown in the Figure 5.3. Hourly rainfall values were available four storm events at 6 rain-gauge stations located within the basin. The locations of those six rain gauge stations were considered for preparing this map. Table 5.1 provides gauge weights computed using Thiessen polygon method. From the table it is observed that the Hanwella rain-gauge station is having least Thiessen Gauge Weight as compare to the other rain gauge stations. The Thiessen Gauge Weights for other five rain gauge stations vary between 0.15 to 0.22. The Thiessen Gauge weights of all the six rain gauge stations were considered as input in the Meteorological Model for HEC-HMS programme to compute the average hourly rainfall over the basin for all four storm events using Thiessen Polygon Method.

**Table 5.1 Gauge weights from Thiessen polygon.**

Station Name	Coordinates		Thiessen Gauge Weight	
	Northing	Easting	Area(sq.km)	Wt. factor
Norwood	06-50-30N	80-36-30E	367.3	0.20
Kithulgala	07-00-00N	80-24-00E	402.6	0.22
Holombuwa	07-11-24N	80-15-36E	265.7	0.15
Deraniyagala	06-55-28N	80-20-24E	296.3	0.16
Glencourse	06-58-25N	80-10-57E	373.3	0.20
Hanwella	06-54-30N	80-04-50E	122.8	0.07
			<b>1828.0</b>	<b>1.00</b>

**5.1.4 PREPARATION OF LAND USE /LAND COVER MAP(LULC)**

The land use-land cover map was prepared using ArcGIS software. This map is shown in Figure 5.4 having the accuracy of 81 %. From the figure, it is observed that the river basin is predominantly covered by the dense forest with 67 % of the basin area whereas the basin is covered with building (urban) and water body by 4 % and 1 % of the basin area respectively. However, while preparing the land use and land cover map, seven (7) land use-land cover classes were considered and processed. The percentage areas covered by different land use land cover classes are given in Table 5.2. The percent area of the building (urban) represents the imperviousness in the basin. Accordingly, it was considered as one of the input for the loss model during HEC-HMS application.

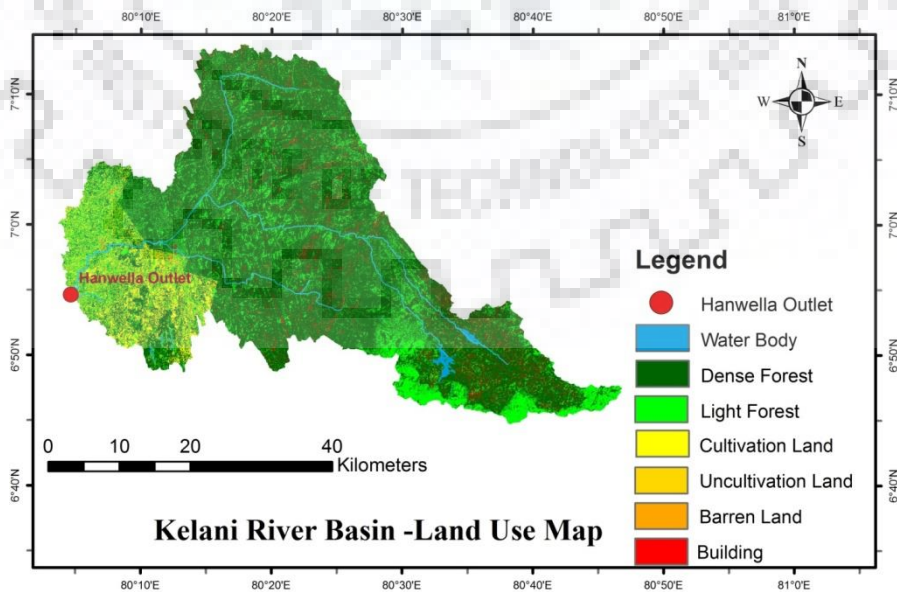


**Figure 5.4 Land use land cover map of Kelani River Basin up to Hanwella Gauging Site**

**Table 5.2 Description of Land Use Land Cover.**

No	Class of Land use	Area SQKM	Area in Percent
1	Water Body	11.32	1%
2	Dense Forest	1,226.51	67%
3	Light forest	390.63	21%
4	Cultivated Land	77.16	4%
5	Uncultivated land	44.99	2%
6	Barren land	4.07	0.2%
7	Urban	78.27	4%
	<b>Total</b>	<b>1,832.95</b>	<b>100%</b>

### 5.1.5 PREPARATION OF SOIL MAP

The constant rate may be estimated if the soil type existing over the basin is known. The constant loss rate is the function of soil type of the basin. The soil data map was prepared using ArcGIS by downloading the soil base data from on-line resource of FAO. The soil map is shown in Figure 5.5. The basin is predominantly covered by sandy loam with 93 % of basin area whereas the other soil classes such as loam and clay loam cover only 6 % and 1 % of the basin area respectively as given in Table 5.3. The range of loss rates for different soil class is described in the Technical Manual of HEC –HMS (Skaggs and Khaleel, 1982). However, a suitable value from this applicable range was adapted to setup in the model as initial parameter for the constant loss rate.

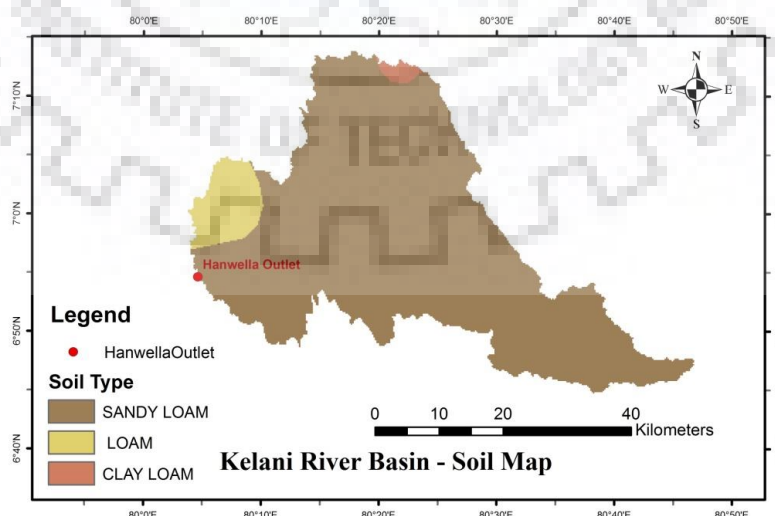


**Figure 5.5 Soil Map of Kelani River Basin up to Hanwella Gauging Site**

**Table 5.3 Description of Soil data**

Soil Class	Area SQKM	Percent Area
Sandy Loam	1702.4	93%
Loam	114.6	6%
Clay Loam	16.2	1%

**5.1.6 PREPARATION OF ISOCHRONE MAPS AND DEVELOPMENT OF TIME AREARELATIONSHIP**

The isochrone map was prepared following the methodology under section 4.1.6. The longest flow path and river reaches were identified using HEC-GeoHMS software. Figure 5.6 shows the longest Flow Path and river reaches. The physical characteristics of the known river segments are given in the Table 5.4.

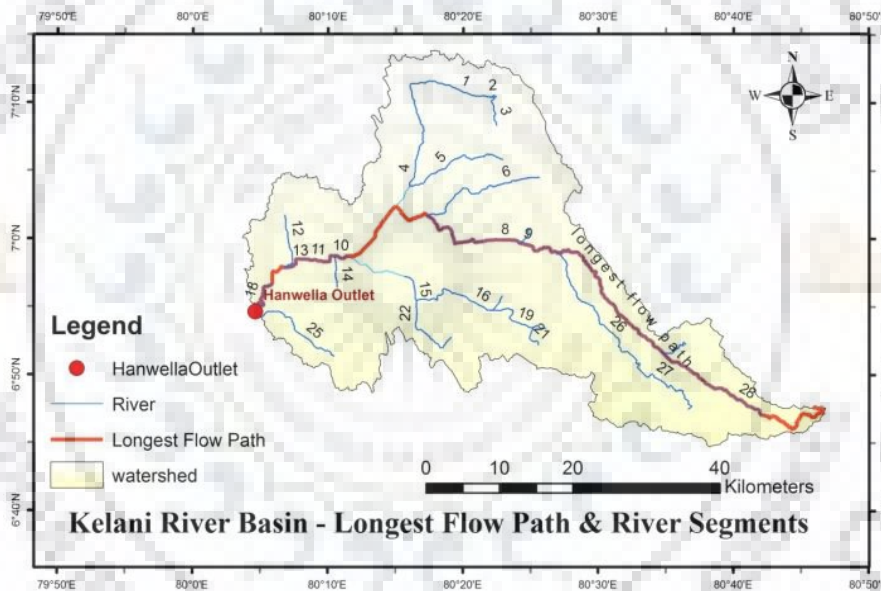


**Figure 5.6 Longest Flow Path and River Reaches**

**Table 5.4 Physical Characteristics of River Reaches**

River Reaches	Length of the River Reaches (L) in m	Slope (S)	$L/\sqrt{S}$
1	12,587.05	0.006276	158,884.91
2	881.87	0.001134	26,187.71
3	5,111.16	0.012913	44,978.57
4	15,369.95	0.001431	406,305.42
5	15,836.79	0.002841	297,119.74
6	19,474.87	0.023209	127,834.02

7	3,201.31	0.003748	52,291.15
8	16,264.82	0.002152	350,613.12
9	6,759.80	0.005178	93,940.55
10	2,051.05	0.006826	24,825.22
11	4,874.87	0.000615	196,573.83
12	8,468.30	0.000118	779,570.17
13	3,934.33	0.000254	246,861.63
14	4,600.75	0.001087	139,544.89
15	4,153.96	0.000481	189,404.05
16	12,958.63	0.004553	192,048.19
17	2,881.06	0.002083	63,125.99
18	6,429.00	0.000622	257,779.58
19	8,439.66	0.010308	83,126.13
20	2,369.75	0.018567	17,391.30
21	3,538.48	0.034195	19,135.31
22	10,924.05	0.00595	141,620.16
23	24,312.39	0.040926	120,178.86
24	4,321.09	0.023837	27,987.71
25	15,015.97	0.003596	250,405.30
26	23,984.68	0.044028	114,306.13
27	11,594.76	0.014403	96,612.97
28	17,696.25	0.017009	135,688.10

Max value of  $\sum \left( \frac{L}{\sqrt{S}} \right)$  is found from the Table 5.5. Thus, the  $L/\sqrt{S}$  for the longest flow path from the catchment characteristics is estimated as 1,426,460.89. Then value for constant C is determined from Eq. (4.3).

*Table 5.5 Details of Points located on the river and its tributaries and Time of Travels up to the gauging site*

Point	Summation of $\left( \frac{L}{\sqrt{S}} \right)$ VALUE	time of travel to the outlet $t=C \cdot \sum \left( \frac{L}{\sqrt{S}} \right)$ in hrs	Longitude (East)	Latitude (North)
A	1,132,345.68	14.29	80.265	7.19
B	1,317,418.31	16.62	80.374	7.174
C	1,336,209.16	16.86	80.374	7.139

D	1,023,160.01	12.91	80.382	7.098
E	853,874.28	10.77	80.427	7.074
F	1,128,944.54	14.25	80.417	7.012
G	1,037,349.75	13.09	80.11	7.03
H	840,759.93	10.61	80.178	6.94
I	1,170,618.49	14.77	80.382	6.93
J	1,208,009.93	15.24	80.436	6.891
K	1,209,753.94	15.27	80.426	6.87
L	1,057,064.47	13.34	80.319	6.879
M	1,318,760.50	16.64	80.607	6.871
N	250,405.30	3.16	80.174	6.856
O	1,381,513.04	17.43	80.611	6.792
P	1,426,460.89	18	80.703	6.784

*Inverse Distance Weighted (IDW) Interpolation Method (using ArcGIS):* These isochrones were drawn using inverse distance weighted (IDW) interpolation technique of ArcGIS which helps to interpolate a raster surface from points with its known time of travel as shown in Figure 5.7.

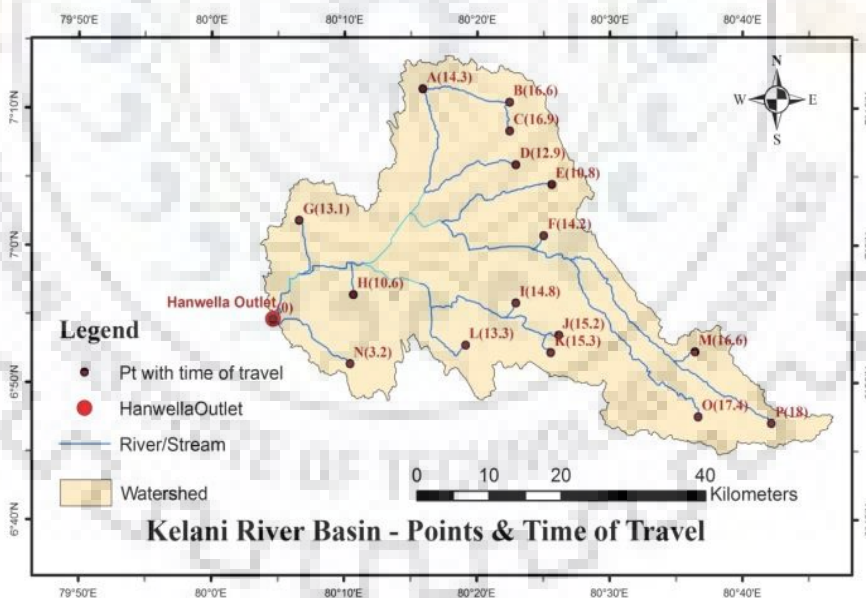


**Figure 5.7** Points located on the river and its tributaries and its Time of travel

The time of concentration ( $T_c$ ) is considered as 18 hrs during the computations. Kelani river basin is divided into 9 different subareas enclosed between the two consecutive isochrones having time of travels of 2 hours as shown in Figure 5.8. The time of travels associated with each isochrone and the area enclosed between the two consecutive isochrones were computed

as given in Table 5.6. The cumulative area and time of travels are computed as given in Table 5.6. Subsequently, the value of  $t/T_c$  and  $A_t/A$  are computed. These values are also given in Table 5.6.

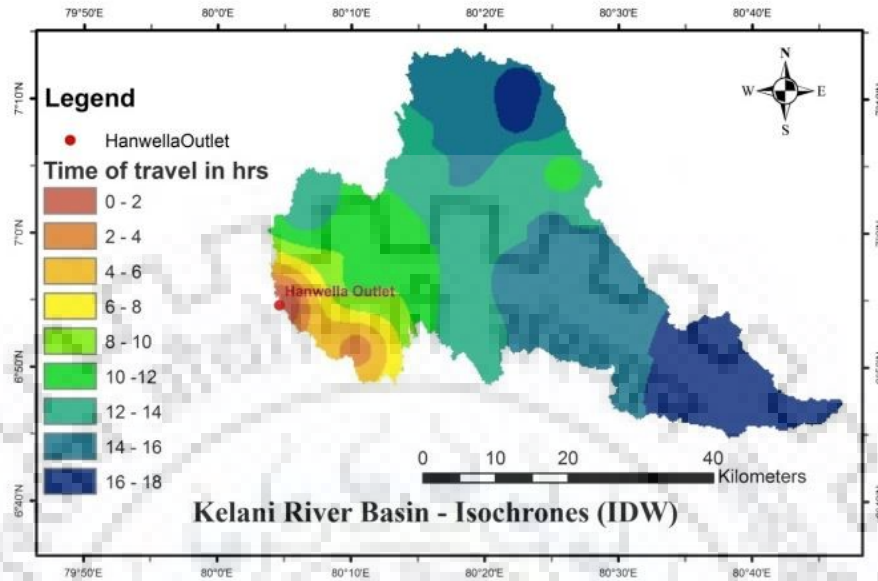


Figure 5.8 Isochrones of Kelani River Basin (IDW)

Table 5.6 Time - Area table of IDW interpolation method

Time of travel between two consecutive isochrones	Area( $A_t$ ) enclosed between two consecutive isochrones (sq.km)	Cumulative time of travel (hr)	Cumulative area ( $A_t$ )	$t/T_c$	$A_t/A$
0-2	10.45	2	10.45	0.11	0.01
2-4	28.01	4	38.46	0.22	0.02
4-6	60.28	6	98.74	0.33	0.05
6-8	48.73	8	147.47	0.44	0.08
8-10	67.67	10	215.14	0.56	0.12
10-12	234.7	12	449.84	0.67	0.25
12-14	481.78	14	931.62	0.78	0.51
14-16	609.0	16	1540.62	0.89	0.84
16-18	292.02	18	1832.64	1	1

Table 5.6 was used to develop the time-area diagram and the time-area percent curve of the river basin as shown in Figure 5.9. The time-area diagram or time-area percent curves as shown in Figure 5.9 represent that first half of the time of concentration is consumed by around 12 % of the basin area and the second half of time of concentration is consumed by the remaining



area of the basin from the outlet Hanwella. It means that upper terrain yields predominant contribution of flow compare to lower terrain.

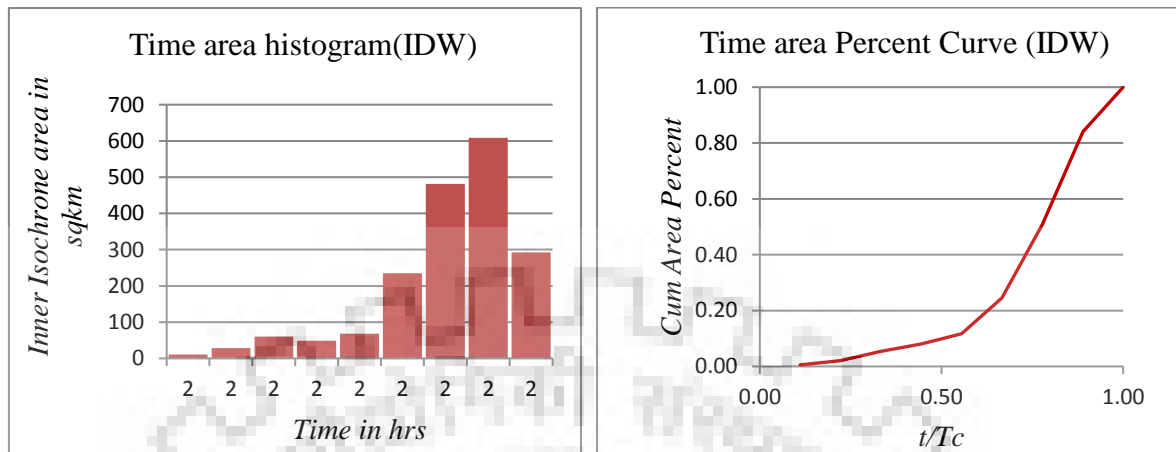


**Figure 5.9 Time-Area histogram & Cumulative Time-Area percent curves-IDW**

*Kriging Interpolation Method (using ArcGIS):* The Figure 5.10. shows the isochrones of Kelani river basin developed using the Kriging interpolation technique of ArcGIS. Kelani river basin is divided into 9 different subareas enclosed between the two consecutive isochrones having time of travels of 2 hours as shown in Figure 5.10. The time of travels associated with each isochrone and the area enclosed between the two consecutive isochrones were computed as given in Table 5.7. The cumulative area and time of travels are computed as given in Table 5.7. Subsequently, the value of  $t/T_c$  and  $At/A$  are computed. These values are also given in Table 5.7.

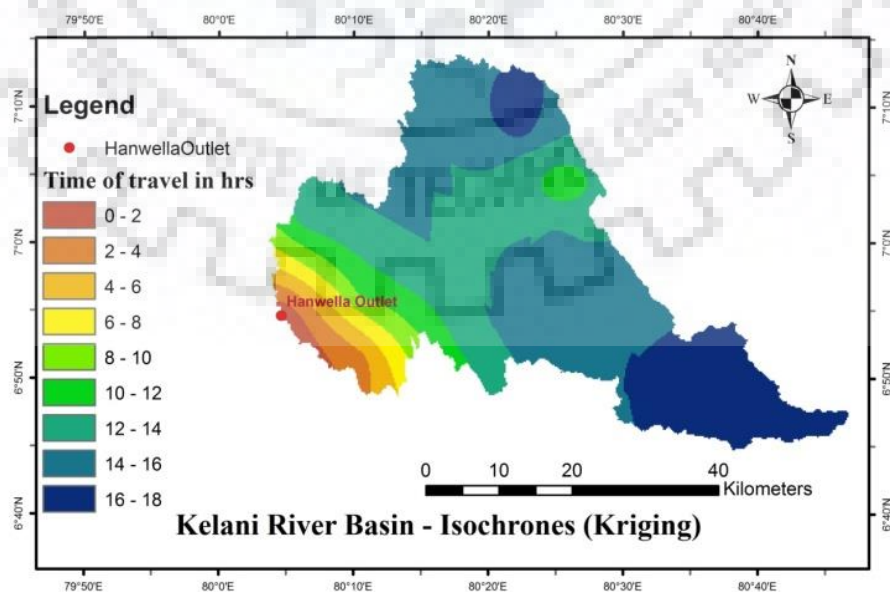


**Figure 5.10 Isochrones of Kelani river Basin (Kriging Method)**

**Table 5.7 Time - Area table of Kriging interpolation method**

Time of travel between two consecutive isochrones	Area( $A_t$ ) enclosed between two consecutive isochrones (sq.km)	Cumulative time of travel (hr)	Area( $A_t$ ) in sq.km	$t/T_c$	$A_t/A$
0-2	15.64	2	15.64	0.11	0.01
2-4	49.46	4	62.60	0.22	0.03
4-6	50.88	6	113.48	0.33	0.06
6-8	52.82	8	166.30	0.44	0.09
8-10	113.48	10	224.19	0.56	0.12
10-12	118.93	12	343.12	0.67	0.19
12-14	497.19	14	840.31	0.78	0.46
14-16	649.76	16	1,490.10	0.89	0.82
16-18	335.69	18	1,825.79	1.00	1.00

Table 5.7 was used to develop the time-area diagram and the time-area percent curve of the river basin as shown in Figure 5.11. The time-area diagram or time-area percent curves as shown in Figure 5.11 represent that first half of the time of concentration is consumed by around 12 % of the basin area and the second half of time of concentration is consumed by the remaining area of the basin from the outlet Hanwellla. It means that upper terrain yields predominant contribution of flow compare to lower terrain.

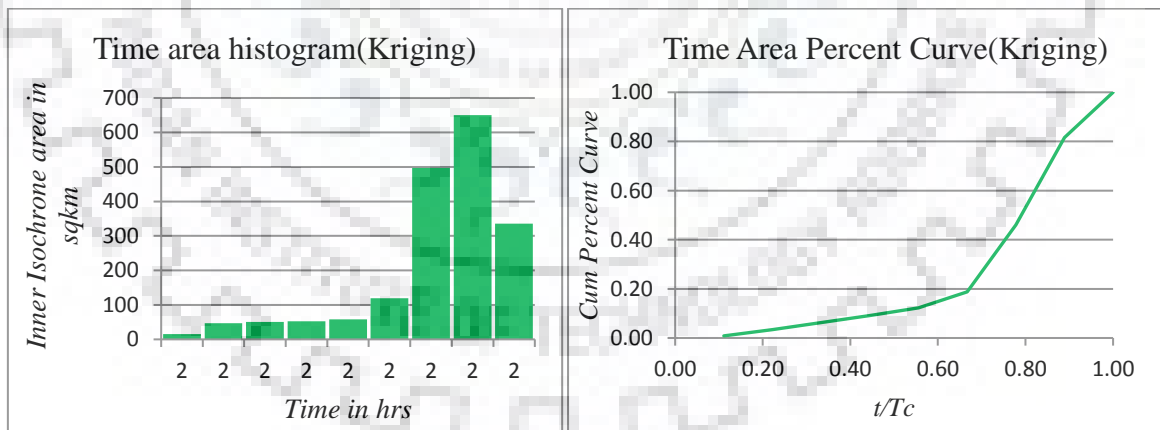


**Figure 5.11 Time-Area histogram & Time-Area percent curves-Kriging**

*Synthetic Method:* The HEC-HMS software has a predefined typical time-area relationship which has been built inside the programme as described in section 4.1.6. Table 5.8 was performed using the time area relationship shown in Eq (4.4) to develop time-area diagram and time area percent curve.

**Table 5.8 Time - area table of synthetic method**

<b>Time of travel between two consecutive isochrones</b>	<b>Area(<math>A_t</math>) enclosed between two consecutive isochrones (sq.km)</b>	<b>Cumulative time of travel (hr)</b>	<b>Cumulative area (<math>A_t</math>)</b>	<b><math>t/T_c</math></b>	<b><math>A_t/A</math></b>
0-2	95.8692	2	95.8692	0.1111	0.0524
2-4	175.2898	4	271.1590	0.2222	0.1481
4 -6	226.9919	6	498.1510	0.3333	0.2721
6-8	268.8026	8	766.9536	0.4444	0.4190
8-10	296.6928	10	1063.6464	0.5556	0.5810
10-12	268.8026	12	1332.4490	0.6667	0.7279
12-14	226.9919	14	1559.4410	0.7778	0.8519
14-16	175.2898	16	1734.7308	0.8889	0.9476
16-18	95.8692	18	1830.6000	1.0000	1.0000

Figure 5.12 reveals that the time of travel and the relevant isochrones area are well distributed in order to obtain the time - area percent curve considering the diamond shape catchment.

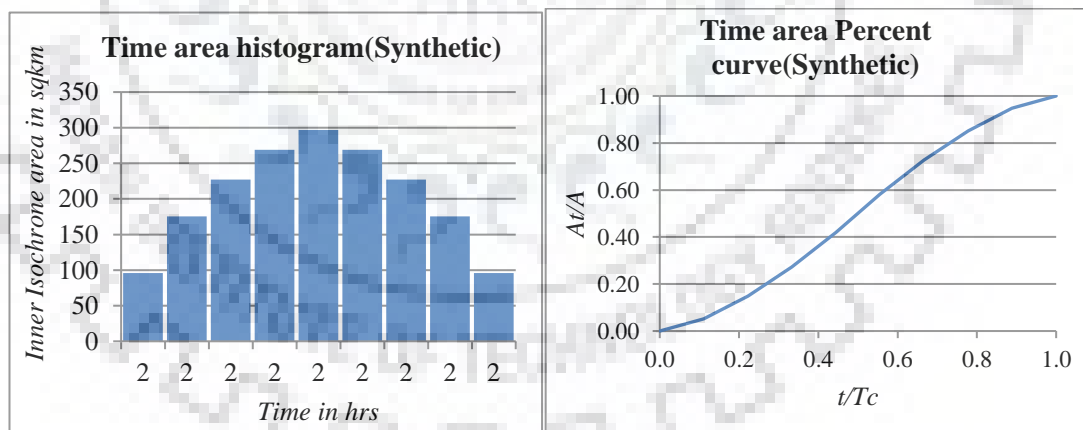


**Figure 5.12 Time-Area histogram & Time-Area percent curves-Synthetic**

Finally, the time-area percent curves obtained from three different methods were compared as shown in Figure 5.13. From this figure, it was observed that there is not much variation in the shape of the time-area percent curves developed by both the two interpolation methods. However, the time-area percent curve generated by the synthetic time-area relationship shows considerable deviation as compared to the time-area percent curves derived from the two

interpolation methods. The time-area relationship obtained from Kriging interpolation method was adopted in the Clark transform model of HEC-HMS.

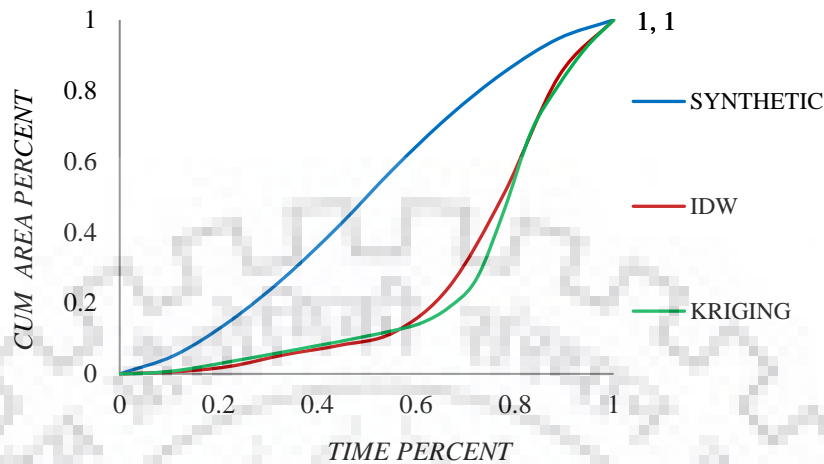


**Figure 5.13 Comparison of Time-Area percent curves**

## 5.2 Temporal Data Processing

### 5.2.1 RAINFALL DATA PROCESSING

The storm events given in Table 5.9 were considered for rainfall – runoff modelling using HEC-HMS. The hourly rainfall values were recorded at six rain gauge stations for all the storm events of the Kelani river basin. To compute the average hourly rainfall for each event, Thiessen polygon weight factors of those six rain gauge stations were used in HEC-HMS programme. The computations of those gauge weights were already discussed in section 5.1.3

**Table 5.9 Storm Events considered for Rainfall-Runoff Modelling**

Storm Events	Duration in days
May 2017	14
December 2014	8
June 2014	16
November 2012	9

### 5.2.2 STREAM FLOW DATA PROCESSING

**Graphical Method - Logarithmic plot:** In graphical method, the daily stage-discharge values, obtained from the Department of Irrigation, Sri Lanka, are plotted on log-log scale and a best fit line is drawn from the eye judgment to develop the linear stage – discharge relationship in

log domain at Hanwella gauging site as shown in Figure 5. 14.. Here  $y=\log(Q)$  and  $x=\log(H-H_0)$ . From the figure, it is observed that the points corresponding to lower stages and corresponding discharges are more scattered than those of higher stages and corresponding discharges.

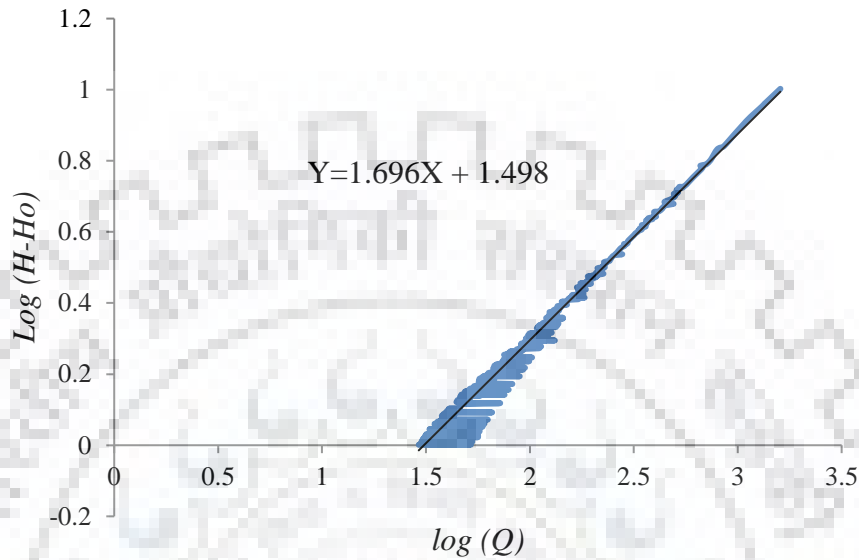


**Figure 5.14 Logarithmic Plot**

However, the stage –discharge relationship obtained in log domain under graphical method are represented as follows in the form of Eqn (4.5):

$$Q = 31.48 (H - 0.48)^{1.696} \quad (5.1)$$

*Analytical Method:* In analytical method, the linear form of stage-discharge curve is developed using method of least square, also known as simple linear regression method, as per the methodology described under section 4.2.2 considering  $Y=\log(Q)$  as dependent variable and  $X=\log(H-H_0)$  as independent variable. The computations of the slope (b) as well as intercept(c) of the fitted line are performed using Eqn.s(4.7) and (4.8) respectively. The correlation coefficient (r) is computed using Eqn.(4.9).

**Table 5.10 Calculations for Stage-Discharge Relationship-Analytical Method**

N	$\Sigma X$	$\Sigma Y$	$\Sigma XY$	$\Sigma X^2$	$\Sigma Y^2$	<b>b</b>	<b>Log(a)=c</b>	<b>r</b>
765	93.03	1,369.21	261.42	82.53	2,585.94	1.33	1.63	0.97

The computed values of slope (b), intercept(c) and coefficient of correlation (r) are given in Table 5.10. The stage –discharge relationship, expressed in the form of eq.4.5, may be represented as follows

$$Q = 21.38 (H - 0.48)^{1.63} \quad (5.2)$$

The stage-discharge curve, given by Eqn. (5.2), is used to compute hourly discharge values corresponding to the observed stages. Further, the stage-discharge curve may be used to get the discharge values corresponding to any observed stages.

### 5.3 Application of HEC-GeoHMS and HEC-HMS

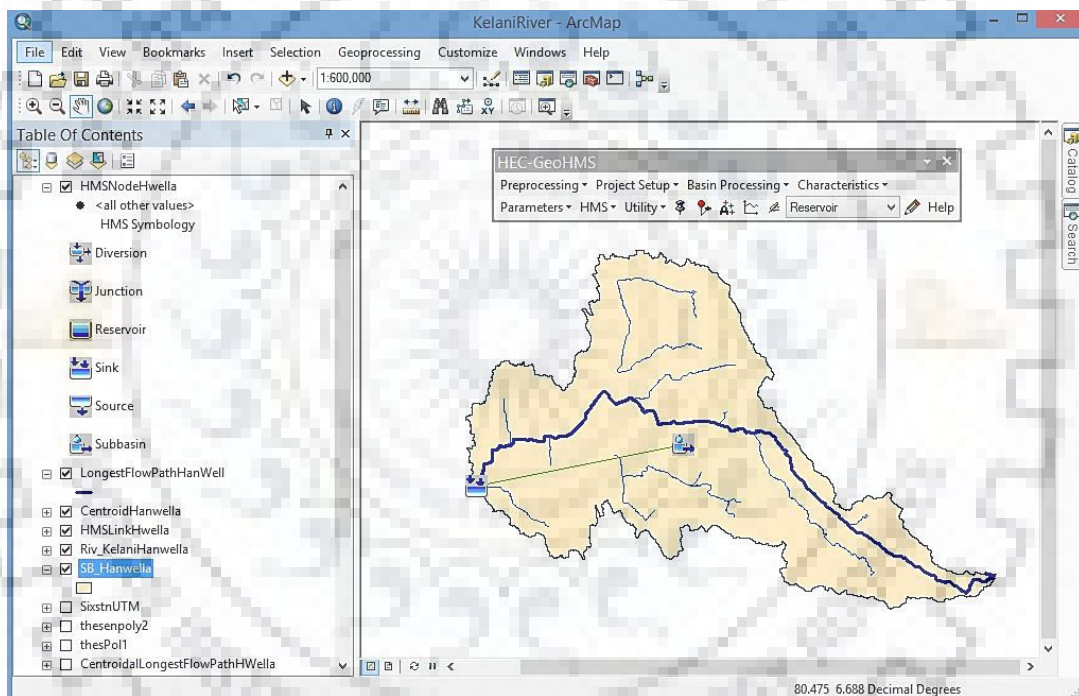


*Figure 5.15 Basin Model processed in HEC-GeoHMS*

The basin model of Kelani river basin including required physical characteristics of the basin was processed using the software HEC-GeoHMS as shown in Figure 5.15. Further, the element networks of the basin to be represented in the HEC-HMS desktop also was developed using the software HEC-GeoHMS as shown in Figure 5.15. For this processing, DEM of the study area was used as raw data in the software HEC-GeoHMS. Then, the processed Kelani river basin model with element networks was imported to the HEC-HMS desktop as shown in Figure 5.16. Further, the components of HEC-HMS and the description of the project used in HEC-

HMS programme are also displayed in watershed explorer and component editor respectively as shown in Figure 5.16.

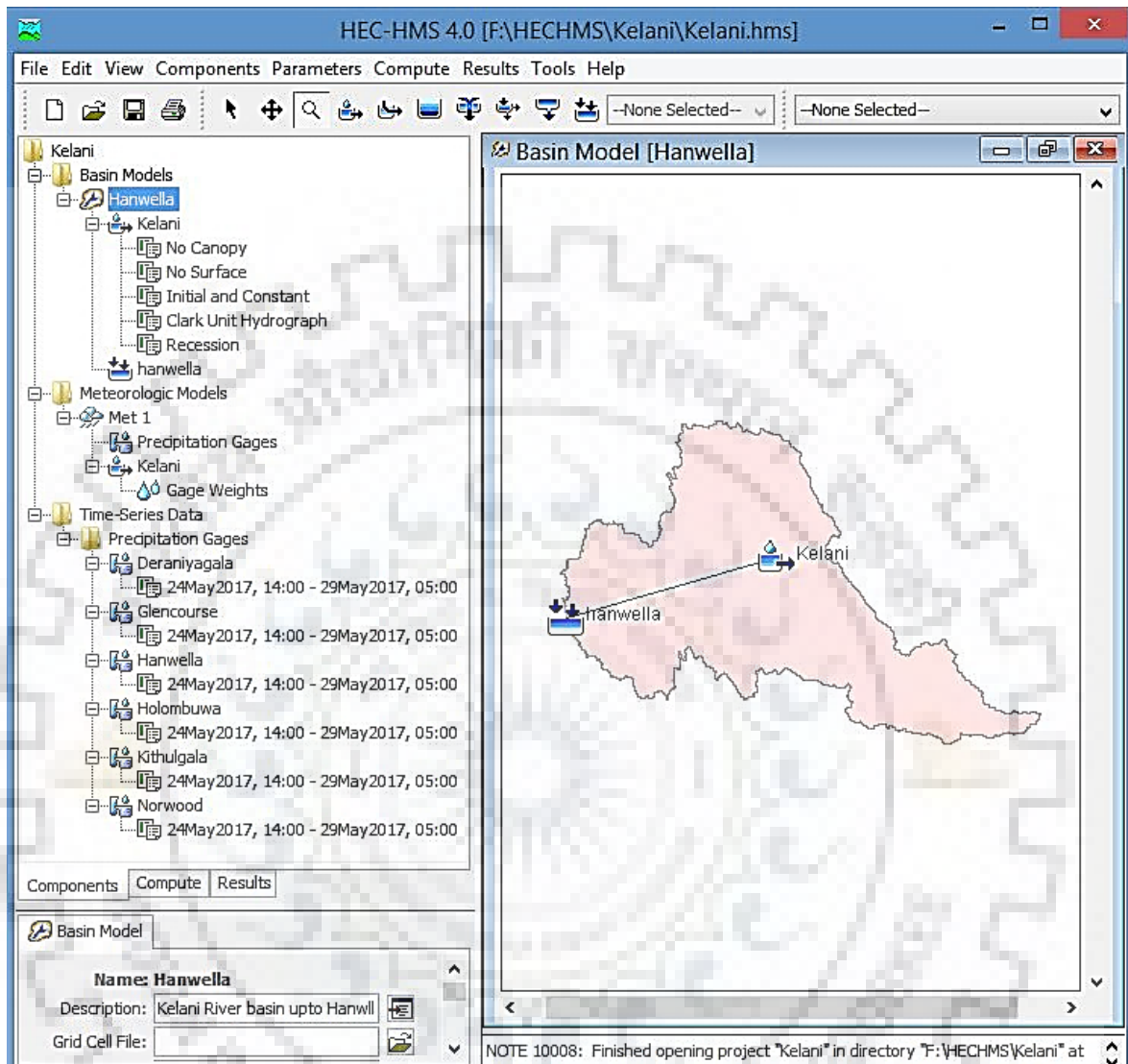


*Figure 5.16 Models used in HEC-HMS for Event May 2017*

### 5.3.1 METEOROLOGICAL MODEL

The Thiessen polygon weights already computed, were used under the meteorological model of HEC-HMS programme. The component editor displays the table containing those Thiessen polygon weights as shown in Figure 5.17. Thus, the average hourly rainfall computed for the Event May 2017 is displayed in the results preview as shown in Figure 5.18.

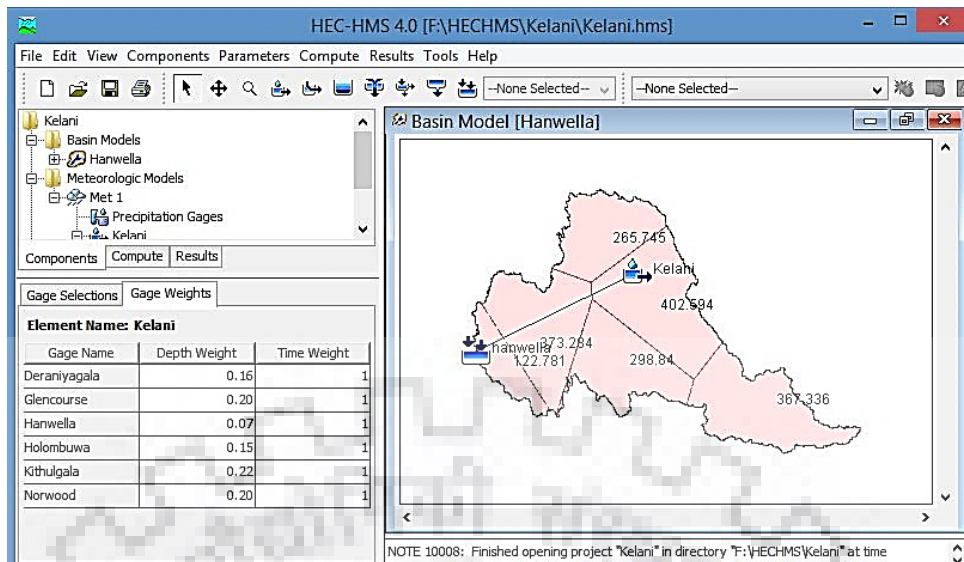


Figure 5.17 Meteorological Model used in HEC-HMS

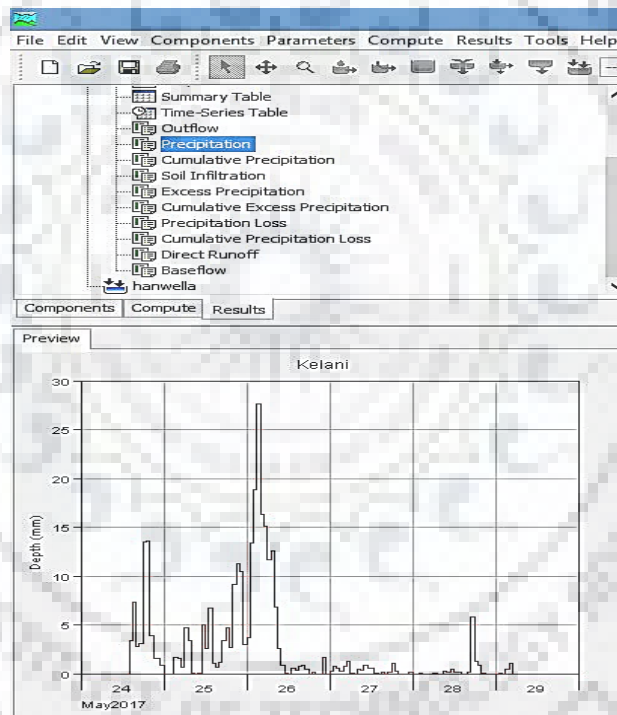


Figure 5.18 Output of Rainfall in HEC-HMS for the Event May 2017

### 5.3.2 BASE FLOW MODEL

The direct surface runoff hydrographs are computed separating the base flow from the observed flood hydrograph for each flood events using recession method. For this method of base flow separation, the initial value of the recession constant was derived as 0.9 whereas the initial discharge and threshold discharge are obtained as  $39 \text{ m}^3/\text{s}$  and  $214.8 \text{ m}^3/\text{s}$  respectively from the observed flood hydrograph as base flow model initial parameters during the optimisation as



shown in Figure 5.19. The variation in base flow with the time is shown in the results preview in Figure 5.20

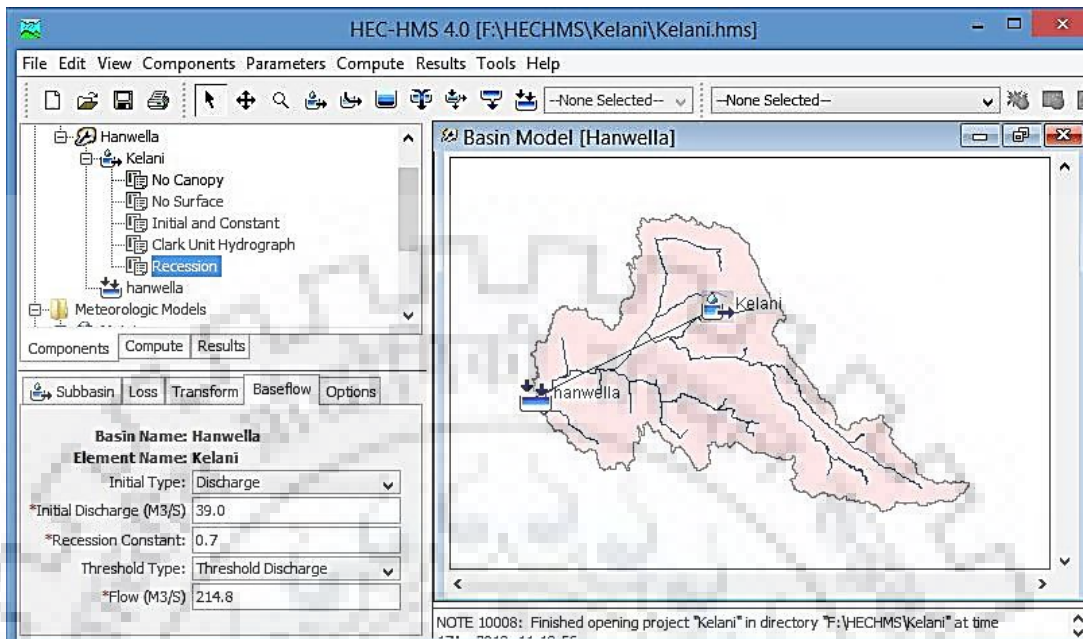


**Figure 5.19 Base flow Model used in HEC-HMS**

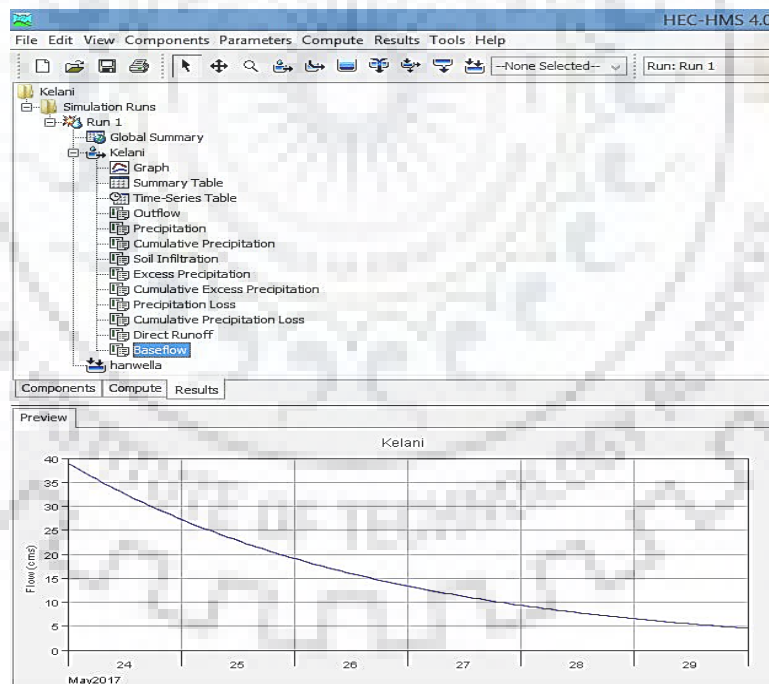


**Figure 5.20 Output as Base flow in HEC-HMS for the Event May 2017**

### 5.3.3 LOSS MODEL

Initial and Constant loss rate model was chosen as loss model and the corresponding values of that loss parameter are used in the HEC-HMS as shown in Figure 5.21. From these parameter values, the variation of soil infiltration with time was simulated in the HEC-HMS program as

shown in Figure 5.22. These soil infiltration values were subtracted from the average rainfall to compute the excess rainfall. The excess rainfall computed within the HEC-HMS programme is shown in Figure 5.23.

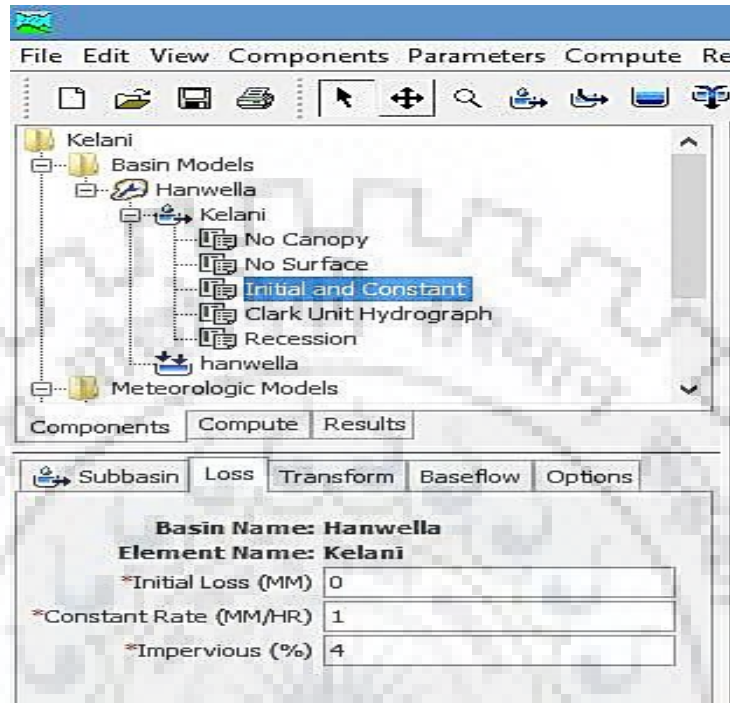


Figure 5.21 Loss Model used in HEC-HMS

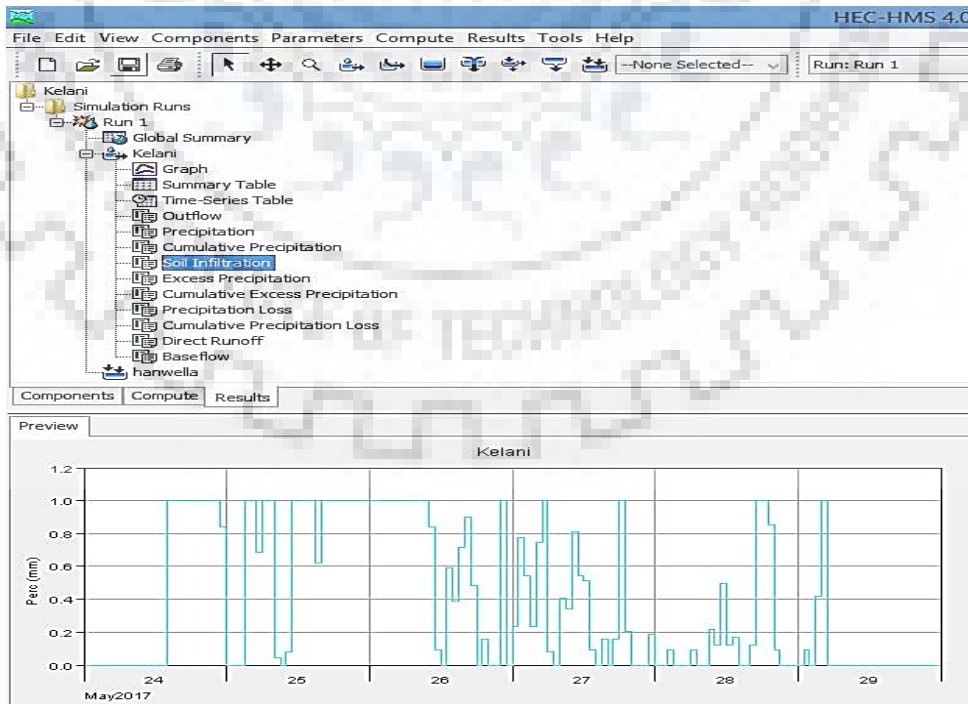
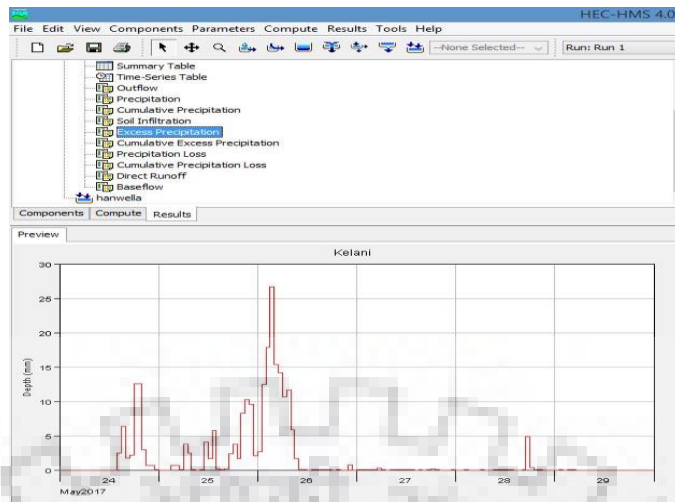


Figure 5.22 Output as Soil Infiltration in HEC-HMS for the Event May 2017



**Figure 5.23** Output of Excess Rainfall in HEC-HMS for the Event May 2017

### 5.3.4 TRANSFORM MODEL

#### 5.3.4.1 CLARK UH MODEL

Figure 5.24 shows the initial values of the parameters  $T_c$  and  $R$  for Clark UH model. Also, the time - area percent curve, considered as the input for Clark UH model, was used in the HEC-HMS programme as shown in Figure 5.25. Finally, the direct runoff hydrograph for the event May 2017, was computed under Clark UH model by running the HEC-HMS programme as shown Figure 5.26. Figure 5.27 shows the summary results yielded by Clark UH model after simulation of the event May 2017.

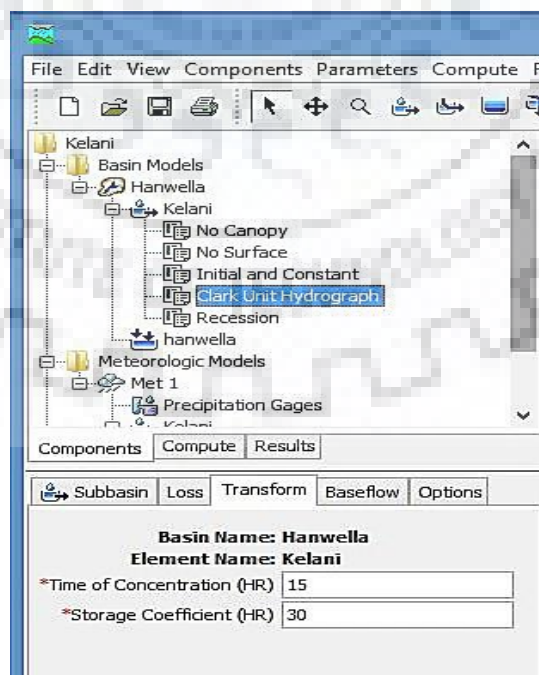


**Figure 5.24** Clark UH Model used in HEC-HMS

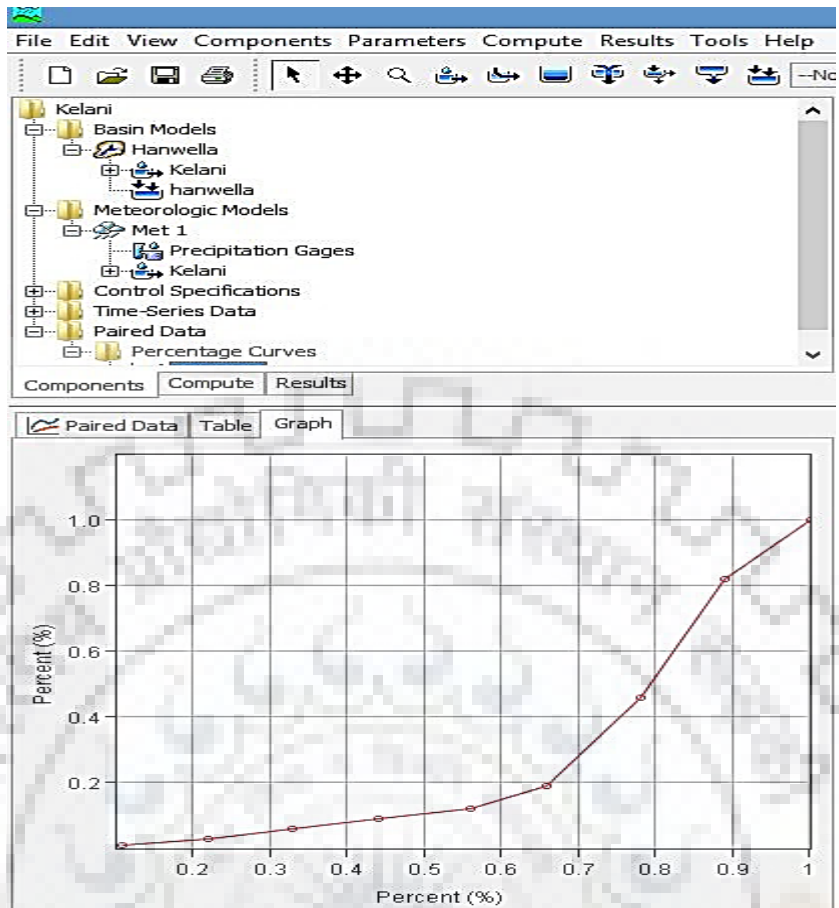


Figure 5.25 Time Area Percent Curve used in Clark UH Model of HEC-HMS

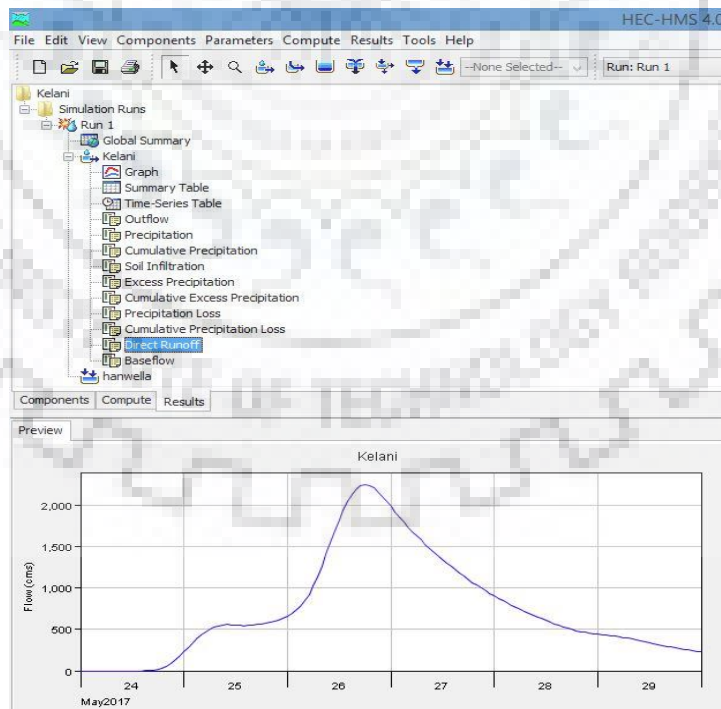


Figure 5.26 Output as Direct Runoff (Clark UH) in HEC-HMS for the Event May 2017

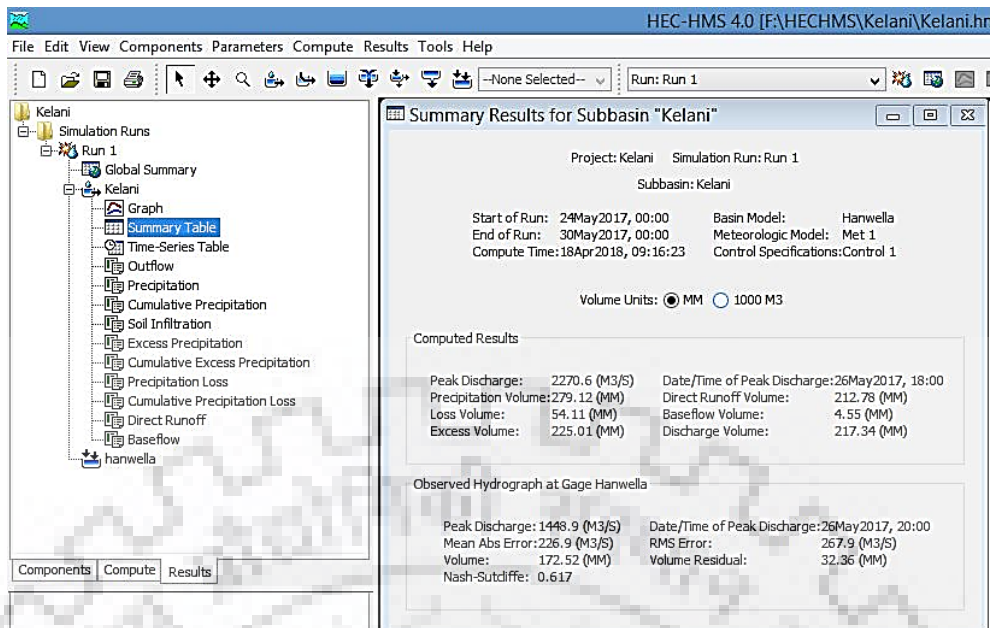


Figure 5.27 Summary Results of HEC-HMS for the Event May 2017

#### 5.3.4.2 SCS UH MODEL

Figure 5.28 shows the initial values of the parameter Lag Time under SCS UH model. Finally, the direct runoff hydrograph for the May 2017 event, was computed for SCS UH model by running the HEC-HMS programme for optimisation option as shown Figure 5.29.

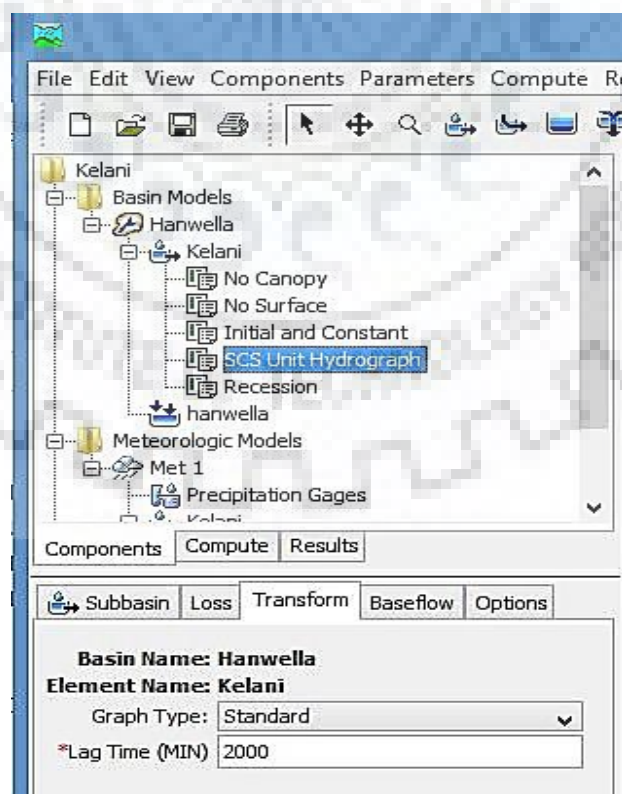
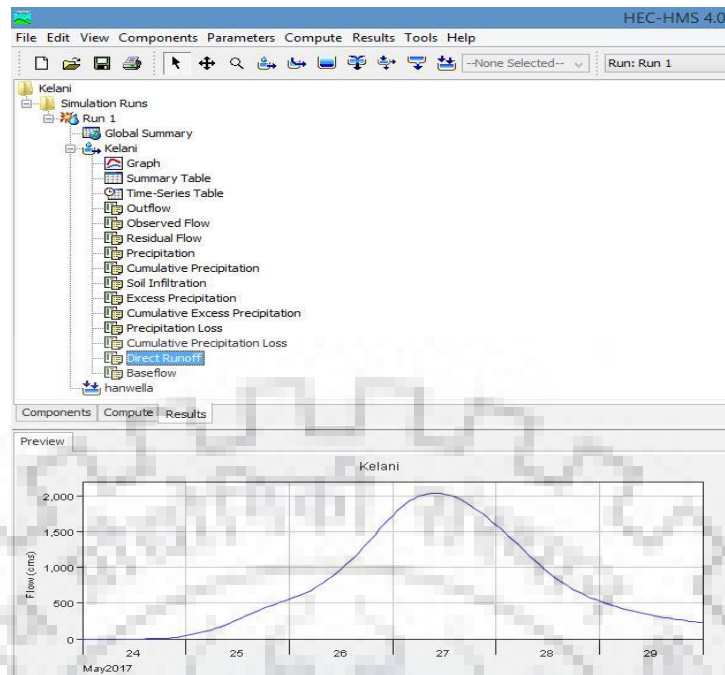


Figure 5.28 SCS UH Model used in HEC-HMS



**Figure 5.29 Output as Direct Runoff (SCS UH) in HEC-HMS for the Event May 2017**

#### 5.3.4.3 SNYDER UH MODEL

Figure 5.30 shows the initial values of the parameters Peaking coefficient ( $C_p$ ) and Standard lag ( $t_p$ ) under Snyder UH model. Finally, the direct runoff hydrograph for the event May 2017, was computed for Snyder UH model by running the HEC-HMS programme for optimisation option as shown in Figure 5.31.

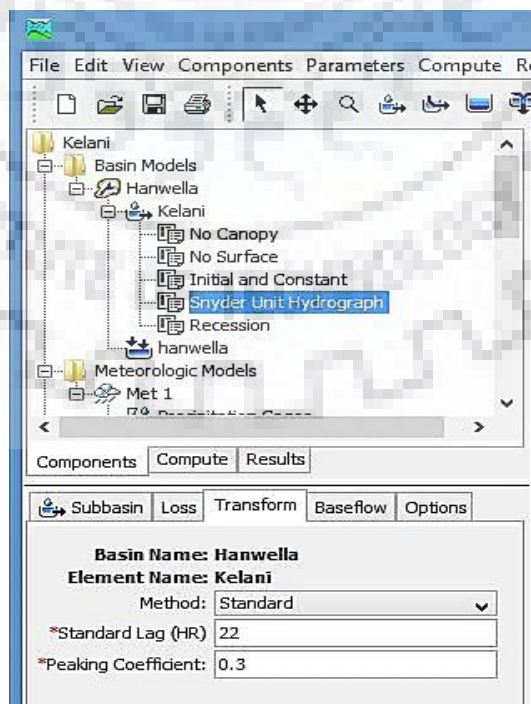


**Figure 5.30 Snyder UH Model used in HEC-HMS**

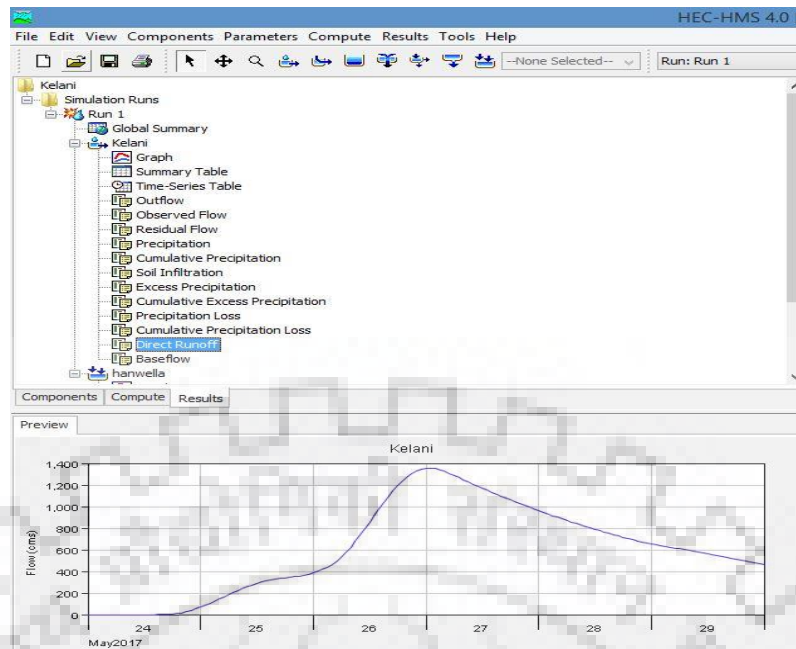


**Figure 5.31** Output as Direct Runoff (SCS UH) in HEC-HMS for the Event May 2017

### 5.4 Sensitivity Analysis

The sensitivity analysis for the three transform models such as Clark UH, SCS UH and Snyder UH was carried as described in section 4.8. The NSE values for the various sets of Tc and R parameters were found during simulation of the storm event May 2017 and those NSE values are given in Table 5.11. The computed NSE values, corresponding to a set of Tc and R values, were plotted and contours for NSE values were drawn. The NSE contours drawn are shown in Figure 5.32. The initial values of parameters Tc and R were identified from highest range of NSE contour. Thus, the initial values of Tc and R values, obtained from sensitivity analysis, were considered as 15hr and 30hr respectively for computing the optimum values of Tc and R using HEC-HMS.

**Table 5.11** Parameters Tc and R on sensitivity analysis

storage coef.R(hrs)=	6	24	42	66	84
Tc(hrs)	Nash-Sutcliffe Model Efficiency Coefficient				
6	-3.36	0.34	0.74	0.68	0.55
18	-1.31	0.68	0.72	0.66	0.5
30	-0.01	0.61	0.71	0.64	0.52
48	0.47	0.65	0.7	0.64	0.53
72	0.47	0.65	0.7	0.64	0.48
96	0.44	0.65	0.7	0.64	0.44
120	0.47	0.64	0.7	0.64	0.4

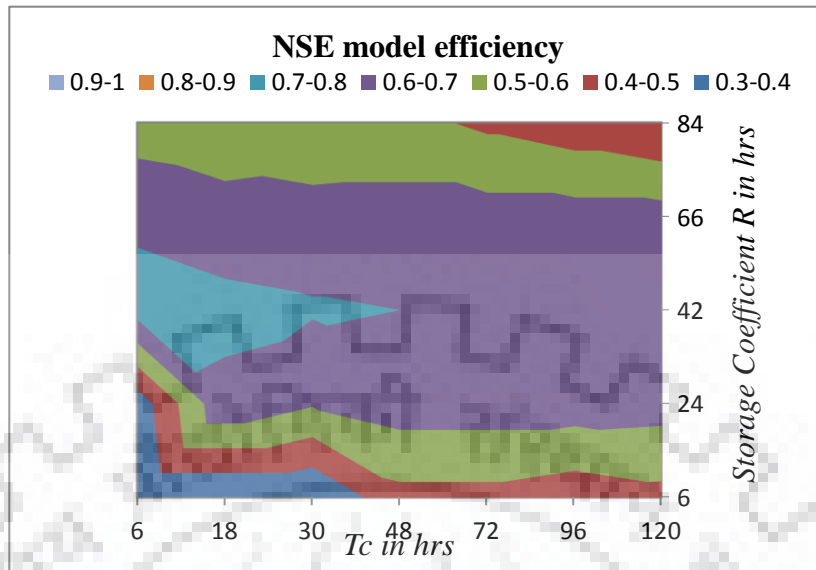


**Figure 5.32 Contour of NSE model efficiency with Sensitive Parameters  $T_c$  &  $R$**

There is only single parameter available under SCS UH transform model i.e. the lag time. The NSE values were computed for different set of the Lag Time during the simulation of storm event May 2017 as given in Table 5.12. From the table it is observed that the highest value of NSE is obtained corresponding to lag time equals to 2000. Thus, the initial value of the parameter, lag time was taken as 2000 minutes for optimization. Figure 5.33 shows the variation of NSE with the model parameter Lag Time to illustrate it graphically.

**Table 5.12 Parameter Lag time and NSE on sensitivity analysis**

Lag Time(Min)	NS model efficiency
1200	0.12
1400	0.24
1600	0.29
1800	0.42
2000	0.45
2200	0.41
2400	0.36

The NSE values, corresponding to the various sets of peaking coefficients ( $C_p$ ) and Standard lag ( $t_p$ ) parameters, were estimated during the simulation of the storm event May 2017 as given in Table 5.13. NSE values are plotted corresponding to the peaking coefficient ( $C_p$ ) and standard lag ( $t_p$ ) and contours of NSE values were drawn as shown in Figure 5.34. The initial values of parameters peaking coefficient ( $C_p$ ) and Standard lag ( $t_p$ ) were identified from highest



range of NSE contour. Thus, the initial values of peaking coefficient( $C_p$ ) and standard lag( $t_p$ ) were considered as 0.3 and 22hr respectively for optimising these parameters using HEC-HMS.

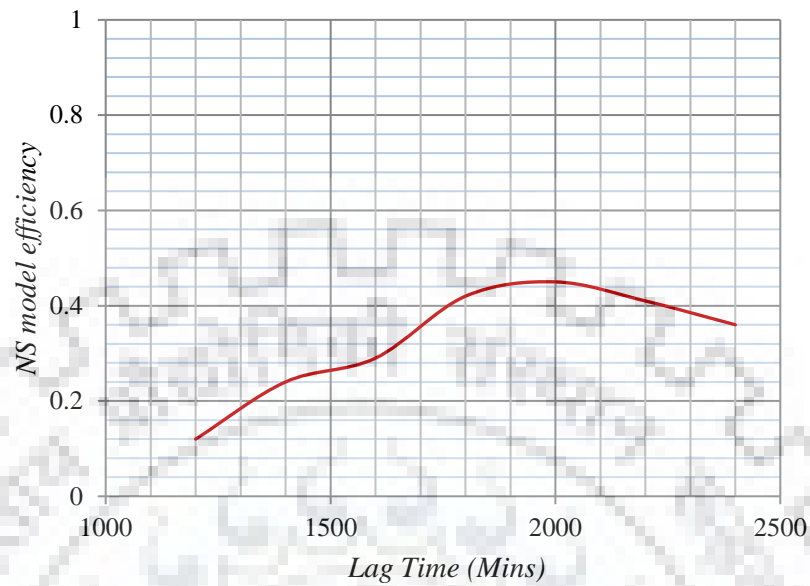
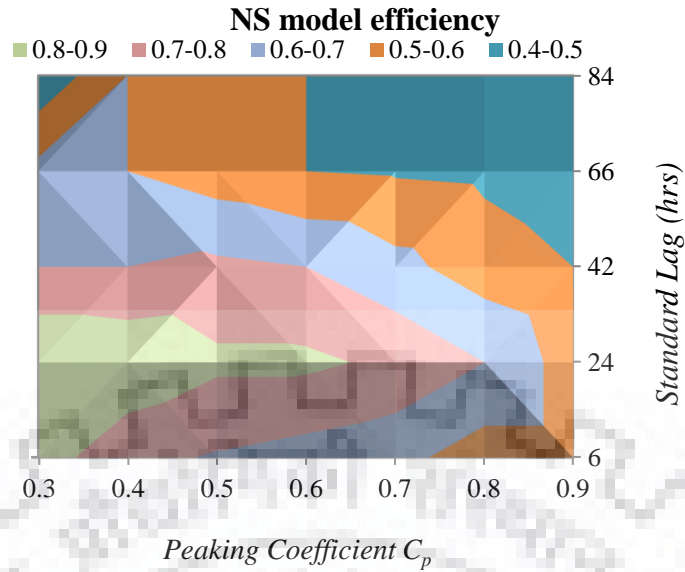


Figure 5.33 Variation of NSE with model Parameter Lag Time

Table 5.13 Parameters Standard Lag and  $C_p$  on sensitivity analysis

Standard Lag(hrs)=	6	24	42	66	84
<b>Peaking Coefficient <math>C_p</math></b>	<b>Nash-Sutcliffe Model Efficiency Coefficient</b>				
<b>0.3</b>	0.85	0.9	0.7	0.63	0.42
<b>0.4</b>	0.73	0.88	0.7	0.6	0.6
<b>0.5</b>	0.69	0.82	0.72	0.55	0.55
<b>0.6</b>	0.66	0.82	0.7	0.5	0.5
<b>0.7</b>	0.63	0.78	0.63	0.49	0.49
<b>0.8</b>	0.55	0.7	0.55	0.48	0.48
<b>0.9</b>	0.55	0.55	0.5	0.44	0.44



**Figure 5.34** Variation of NSE with Parameters  $C_p$  & Standard Lag ( $t_p$ )

### 5.5 Error Criteria for comparing the performance of Three Transform Models

The error-criteria for the performance of the transform models were considered as described under section 4.5. Out of those four criteria, NSE value was considered for evaluating the overall performance of the transform model during calibration and validation.

### 5.6 Calibration and Validation

For the calibration of the transform models, three extreme events data were considered whereas one extreme event data was used for their validation for Kelani river basin. The details about those four extreme flood events were given in Table 3.1. The initial values of hydrological parameters were obtained from the sensitivity analysis of the corresponding transform model whereas initial values of the other measured parameters were derived from the spatial data processing.

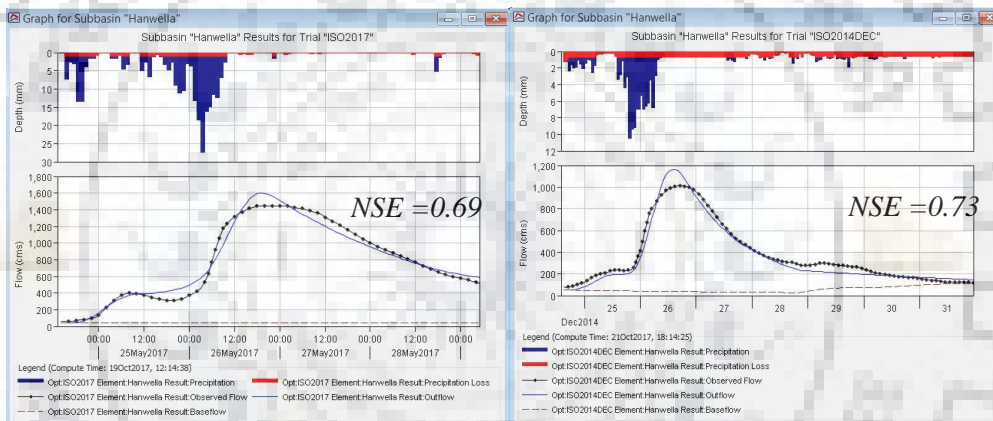
#### 5.6.1 CALIBRATION OF CLARK UH MODEL

The Clark UH transform model was calibrated from three events. During the calibration of the Clark Model Parameters, the optimization option available in the simulation manager of HEC-HMS was used for the individual events to optimize the Clark UH model parameters such as  $T_c$  and  $R$ . The initial values of  $T_c$  and  $R$ , which were obtained from the sensitivity analysis, were used as 15hr and 30hr respectively. The optimized values of those parameters of the individual events including average values of those parameters are given in Table 5.14. and the

representative parameters of Clark model for the basin were computed taking the average of the optimised parameters obtained from analysing the data of three events using HEC-HMS programme.

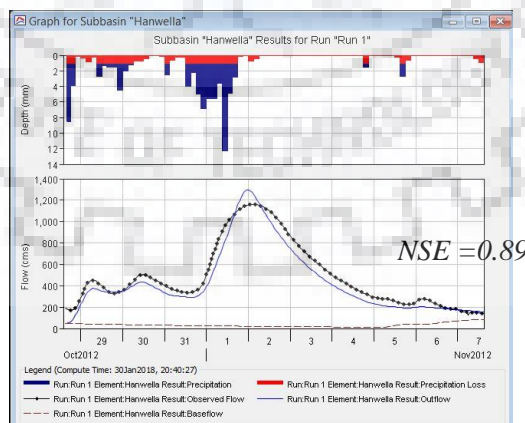
**Table 5.14 Average of optimized Parameters – Clark UH Transform Model**

Model	Parameters	Events considered for calibration			Representative Parameters (Average Parameters )
		May 2017	Dec 2014	Nov-12	
Transform	Clark Unit Hydrograph - Time of Concentration Tc in hrs	30.799	14.118	15.157	20.02
	Clark Unit Hydrograph - Storage Coefficient R in hrs	30.555	28.812	30.153	29.84



(a) May 2017

(b) Dec 2014

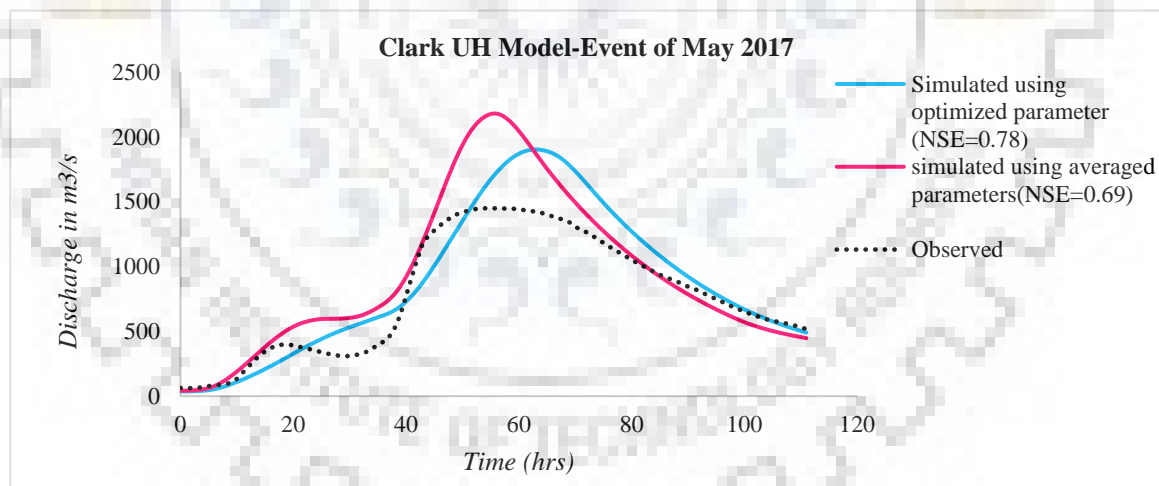


(c) Nov 2012

**Figure 5.35 Comparison of observed and Simulated Flood Hydrographs using optimised parameters of Clark Model for all the three events considered for Calibration**

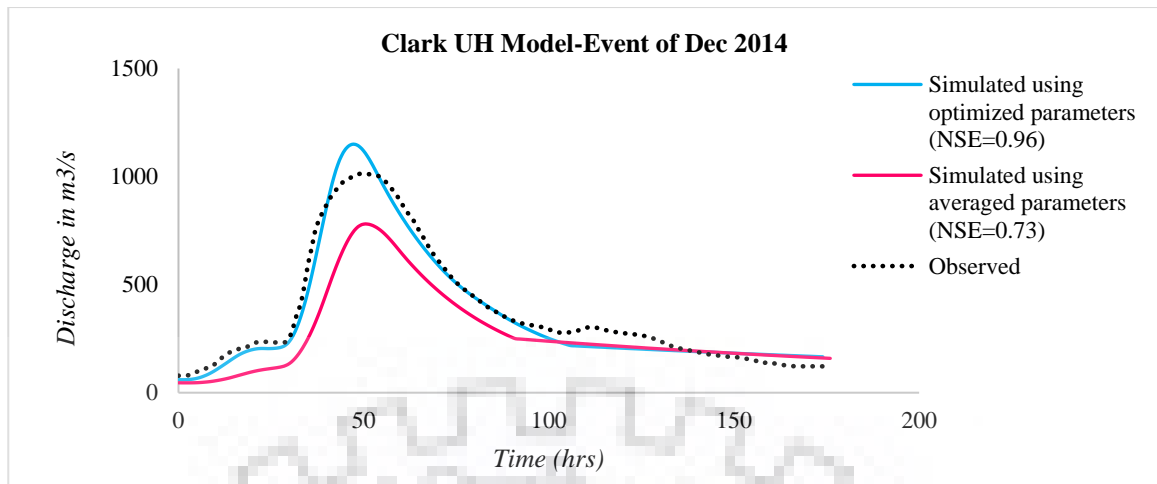
The simulated flood hydrographs using the optimised parameters of Clark Model are shown in the Figures 5.35. (a), (b) and (c) for the different three events. These figures illustrate the comparison observed flood hydrograph with the simulated flood hydrographs for the three events. During calibration of those three events, the optimization option available in the simulation manager of HEC-HMS was individually used for the events to optimize the Clark UH model parameters such as  $T_c$  and  $R$ . The initial values of  $T_c$  and  $R$ , which were obtained from the sensitivity analysis, were used as 15hr and 30hr respectively. The optimized values of those parameters of the individual events including average values of those parameters are given in Table 5.14. from this table, it is observed that the average value of optimized  $T_c$  (=20 hrs) differs from its optimised values obtained from the three events whereas the average value of optimized  $R$  (=30 hrs) is almost the same for all the events

Figure 5.36 shows the comparison of observed flood hydrograph with simulated flood hydrographs using optimized parameters and representative parameters of the Clark UH model for the event May 2017. From this figure, it is observed that NSE value (NSE=0.69) obtained from the representative parameters of the Clark Model is lower than the NSE value (NSE=0.78) obtained from the optimised parameters of the Clark Model. for the May 2017 flood event.



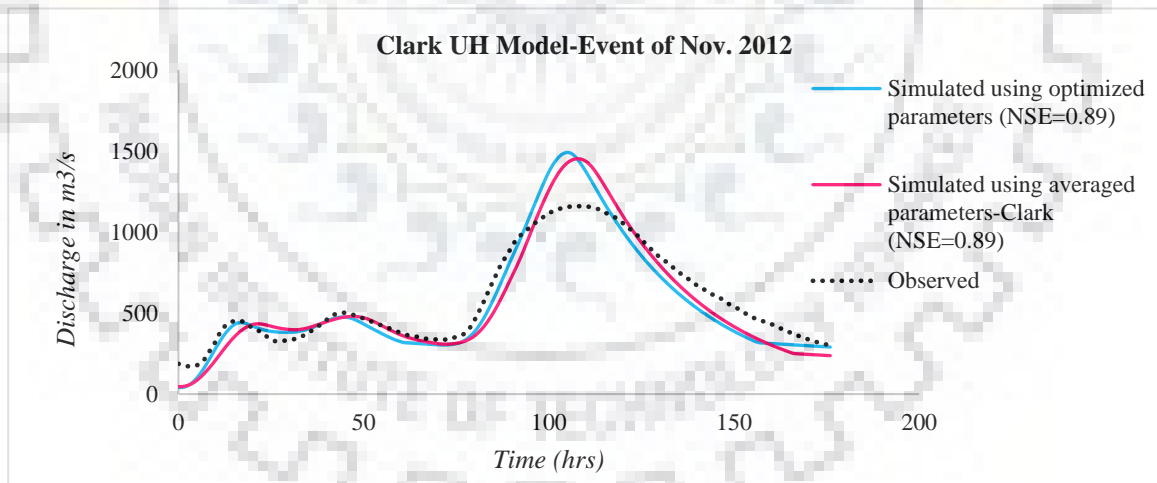
**Figure 5.36 Comparison of observed and Simulated Flood Hydrographs using optimised as well as representative parameters of Clark Model for May 2017 event**

Figure 5.37 shows the comparison of observed flood hydrograph with simulated flood hydrographs using optimized parameters and representative parameters of the Clark UH model for the event Dec 2014. From this figure, it is observed that NSE value (NSE=0.73) obtained from the representative parameters of the Clark Model is lower than the NSE value (NSE=0.96) obtained from the optimised parameters of the Clark Model for the Dec 2014 flood event.



**Figure 5.37 Comparison of observed and Simulated Flood Hydrographs using optimised as well as representative parameters of Clark Model for Dec 2014 event**

Figure 5.38 shows the comparison of observed flood hydrograph with simulated flood hydrographs using optimized parameters and representative parameters of the Clark UH model for the event Nov 2012. From this figure, it is observed that NSE value (NSE=0.89) obtained from the representative parameters of the Clark Model is same as the NSE value (NSE=0.89) obtained from the optimised parameters of the Clark Model for the Nov 2012 flood event.



**Figure 5.38 Comparison of observed and Simulated Flood Hydrographs using optimised as well as representative parameters of Clark Model for Nov 2012 event**

### 5.6.2 CALIBRATION OF SCS UH MODEL

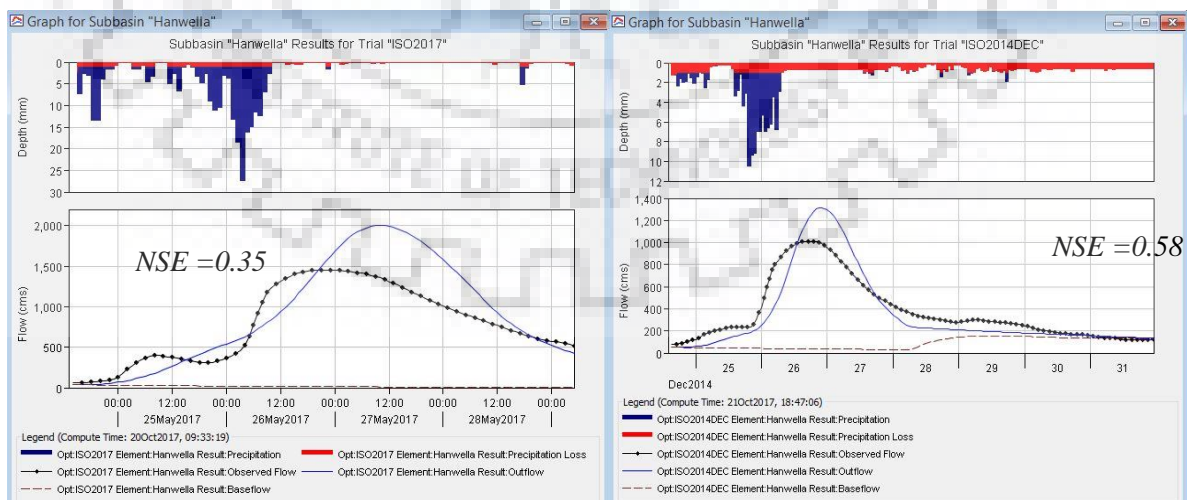
The SCS UH transform model was calibrated from three events. During the calibration of the Clark Model Parameters, the optimization option available in the simulation manager of HEC-HMS was used for the individual events to optimize the SCS UH model parameter such Lag time. The initial value of Lag time, which was obtained from the sensitivity analysis, were used

1742 minutes. The optimized values of those parameters of the individual events including average value of those parameters are given in Table 5.15. and the representative parameter of SCS model for the basin was computed taking the average of the optimised parameters obtained from analysing the data of three events using HEC-HMS programme.

**Table 5.15 Optimized Parameters and Representative Parameters – SCS UH Transform Model**

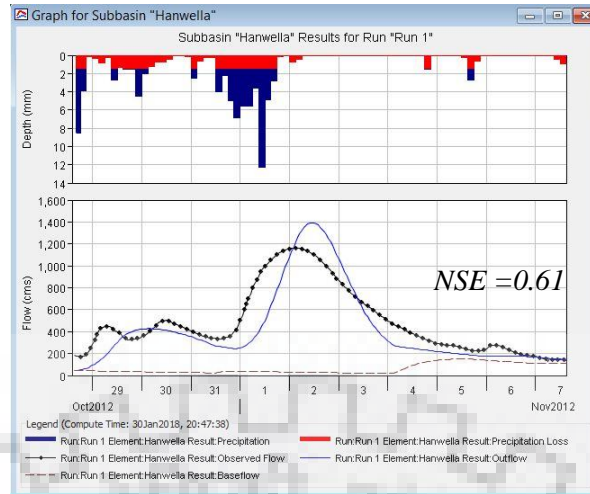
Model	Parameters	Events considered for calibration			Representative Parameters
		May 2017	Dec 2014	Nov-12	
Transform	SCS Unit Hydrograph - Lag Time in minutes	2017.4	1362.5	1844.7	1,741.53

The simulated flood hydrographs using the optimised parameters of SCS UH Model are shown in the Figures 5.39. (a), (b) and (c) for the different three events. These figures illustrate the comparison observed flood hydrograph with the simulated flood hydrographs for the three events. During calibration of those three events, the optimization option available in the simulation manager of HEC-HMS was individually used for the events to optimize the SCS UH model parameter Lag time. The initial value of Lag time, which was obtained from the sensitivity analysis, was used as 1742 minutes. The optimized values of those parameters of the individual events including average values of those parameters are given in Table 5.15. from this table, it is observed that the average value of optimized Lag time (=20 hrs) differs from its optimised values obtained from the three events



**(a) May 2017**

**(b) Dec 2014**



(c) Nov 2012

**Figure 5.39 Comparison of observed and Simulated Flood Hydrographs using optimised parameters of SCS Model for all the three events considered for Calibration**

Figure 5.40 shows the comparison of observed flood hydrograph with simulated flood hydrographs using optimized parameters and representative parameters of the SCS UH model for the event May 2017. From this figure, it is observed that NSE value (NSE=0.35) obtained from the representative parameters of the SCS Model is lower than the NSE value (NSE=0.47) obtained from the optimized parameters of the SCS Model. for the May 2017 flood event.

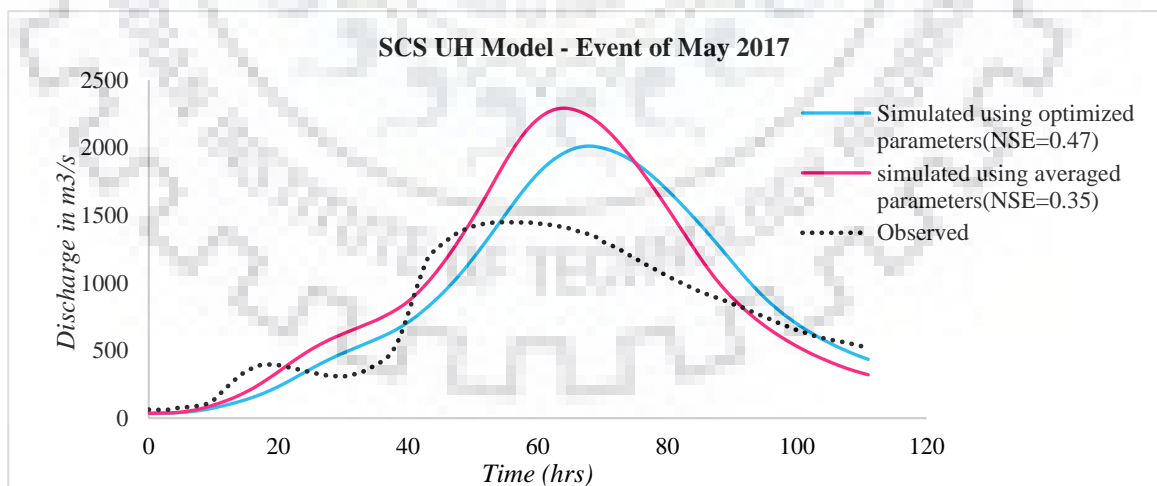


**Figure 5.40 Comparison of observed and Simulated Flood Hydrographs using optimised as well as representative parameters of SCS Model for May 2017 event**

Figure 5.41 shows the comparison of observed flood hydrograph with simulated flood hydrographs using optimized parameters and representative parameters of the SCS UH model for the event Dec 2014. From this figure, it is observed that NSE value (NSE=0.58) obtained

from the representative parameters of the SCS Model is lower than the NSE value (NSE=0.76) obtained from the optimised parameters of the SCS Model for the Dec 2014 flood event.

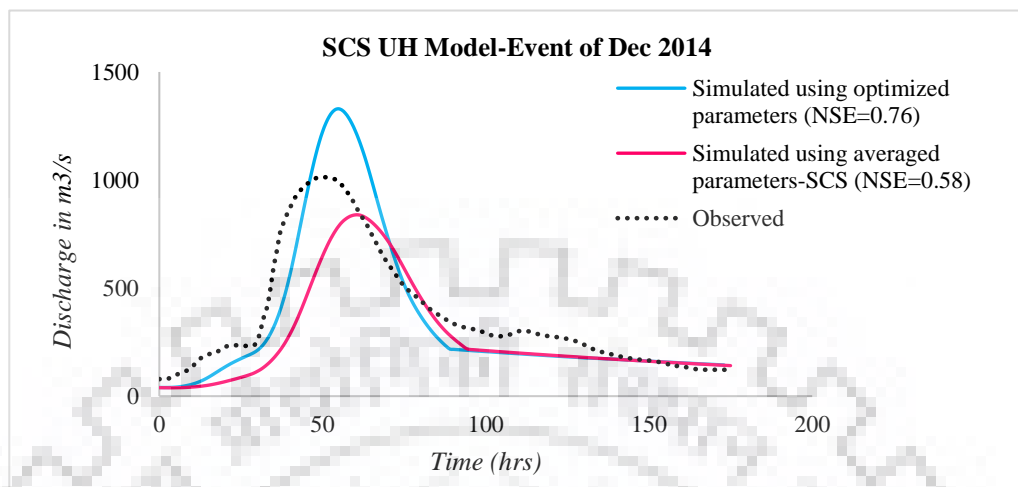


**Figure 5.41 Comparison of observed and Simulated Flood Hydrographs using optimised as well as representative parameters of SCS Model for Dec 2014 event**

Figure 5.42 shows the comparison of observed flood hydrograph with simulated flood hydrographs using optimized parameters and representative parameters of the SCS UH model for the event Nov 2012. From this figure, it is observed that NSE value (NSE=0.61) obtained from the representative parameters of the SCS Model is same as the NSE value (NSE=0.61) obtained from the optimised parameters of the SCS Model for the Nov 2012 flood event.

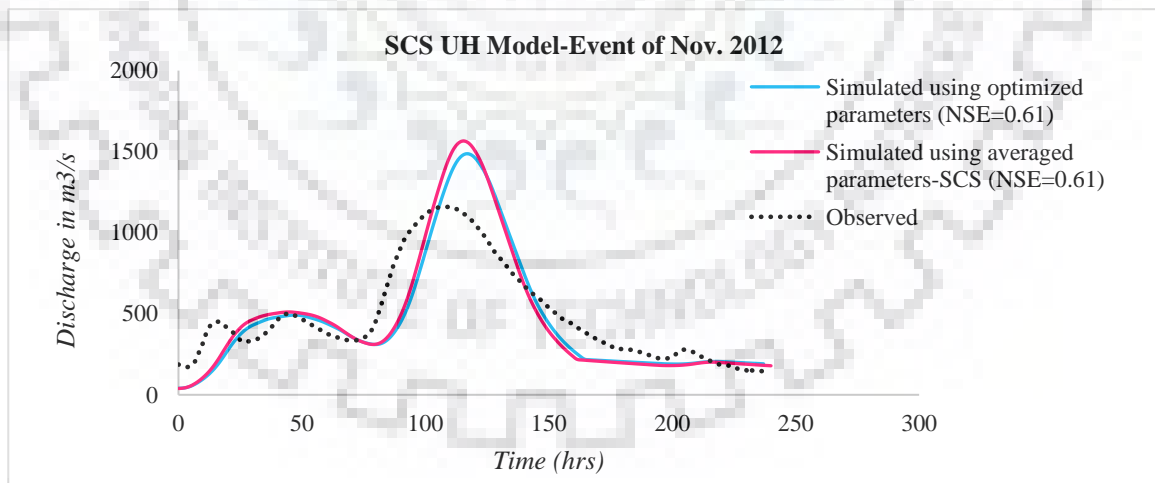


**Figure 5.42 Comparison of observed and Simulated Flood Hydrographs using optimised as well as representative parameters of SCS Model for Nov 2012 event**

### 5.6.3 CALIBRATION OF SNYDER UH MODEL

The Snyder UH transform model was calibrated from three events. During the calibration of the Snyder Model Parameters, the optimization option available in the simulation manager of



HEC-HMS was used for the individual events to optimize the Snyder UH model parameters such as  $C_p$  and  $t_p$ . The initial values of  $C_p$  and  $t_p$ , which were obtained from the sensitivity analysis, were used as 0.3 and 22 hr respectively. The optimized values of those parameters of the individual events including average values of those parameters are given in Table 5.16. and the representative parameters of Snyder model for the basin were computed taking the average of the optimised parameters obtained from analysing the data of three events using HEC-HMS programme.

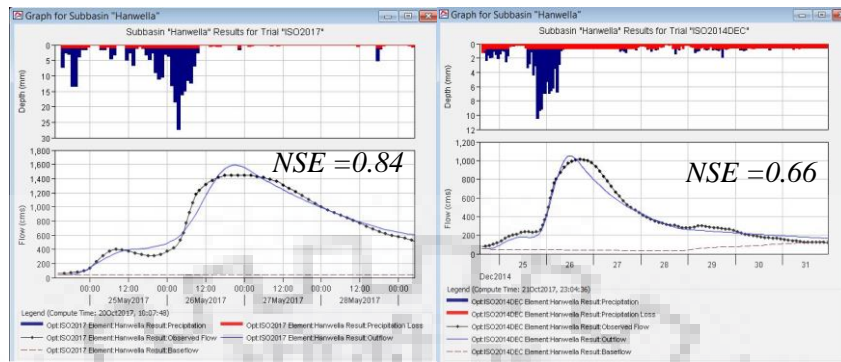
**Table 5.16 Optimized Parameters and Representative Parameters – Snyder UH Transform Model**

Model	Parameters	Events considered for calibration			Representative Parameters
		May 2017	Dec 2014	Nov-12	
Transform	Snyder Unit Hydrograph - Peaking Coefficient	0.3	0.3	0.3	0.30
	Snyder Unit Hydrograph - Standard lag in hrs	17.698	9.81	14.7	14.07

The simulated flood hydrographs using the optimised parameters of Snyder Model are shown in the Figures 5.43. (a), (b) and (c) for the different three events. These figures illustrate the comparison observed flood hydrograph with the simulated flood hydrographs for the three events. During calibration of those three events, the optimization option available in the simulation manager of HEC-HMS was individually used for the events to optimize the Clark UH model parameters such as  $C_p$  and  $t_p$ . The initial values of  $C_p$  and  $t_p$ , which were obtained from the sensitivity analysis, were used as 0.3 and 22hr respectively. The optimized values of those parameters of the individual events including average values of those parameters are given in Table 5.16. from this table, it is observed that the average value of optimized  $C_p$  (=0.3) is same as its optimised values obtained from the three events whereas the average value of optimized  $t_p$  (=14 hrs) differs from the optimized values for all the events.

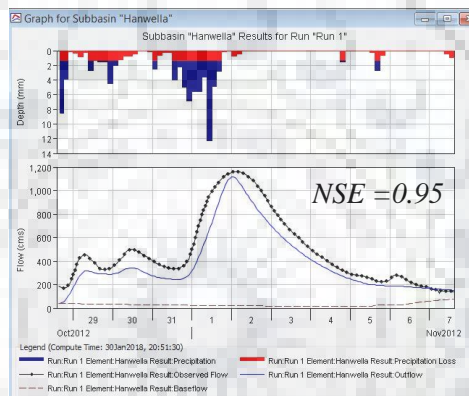
Figure 5.44 shows the comparison of observed flood hydrograph with simulated flood hydrographs using optimized parameters and representative parameters of the Snyder UH model for the event May 2017. From this figure, it is observed that NSE value (NSE=0.84) obtained from the representative parameters of the Snyder Model is lower than the NSE value

(NSE=0.97) obtained from the optimised parameters of the Snyder Model. for the May 2017 flood event.



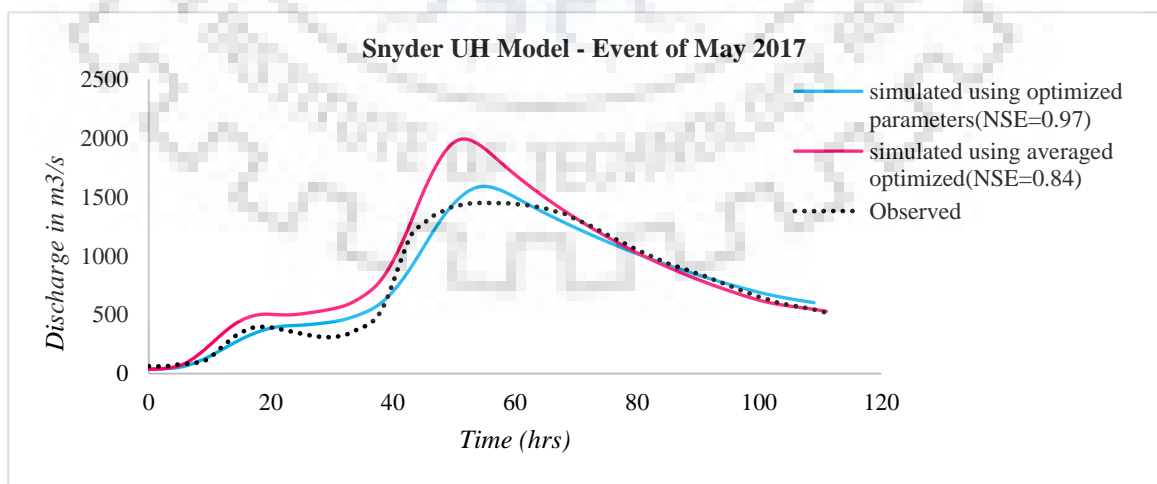
(a) May 2017

(b) Dec 2014



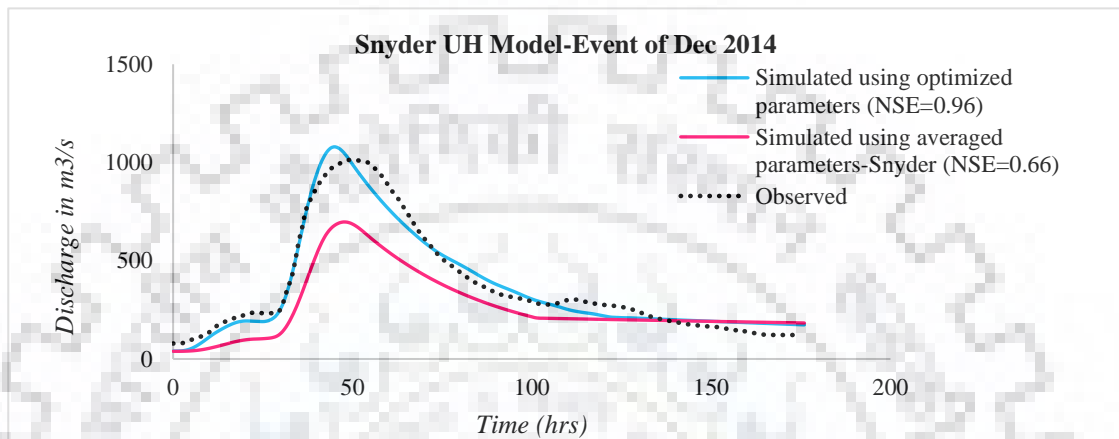
(c) Nov 2012

**Figure 5.43 Comparison of observed and Simulated Flood Hydrographs using optimised parameters of Snyder Model for all the three events considered for Calibration**



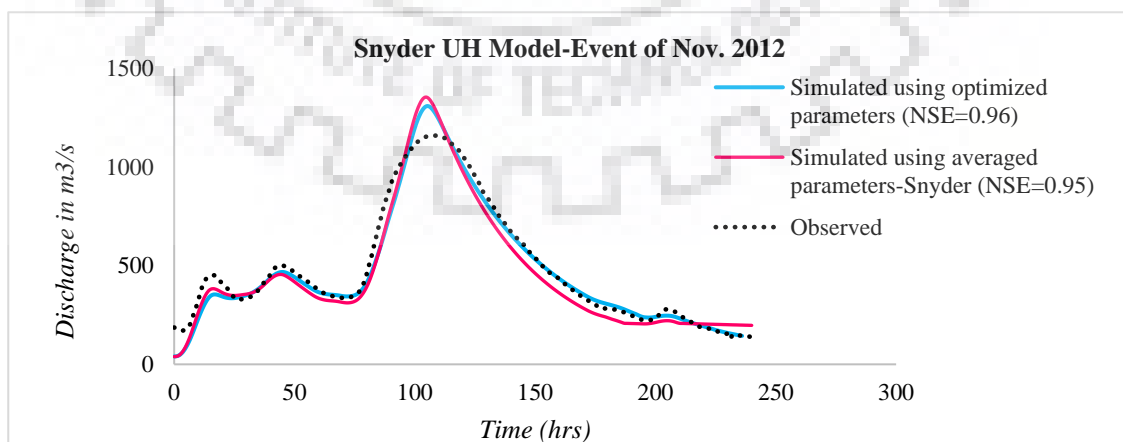
**Figure 5.44 Comparison of observed and Simulated Flood Hydrographs using optimised as well as representative parameters of Snyder Model for May 2017 event**

Figure 5.45 shows the comparison of observed flood hydrograph with simulated flood hydrographs using optimized parameters and representative parameters of the Snyder UH model for the event Dec 2014. From this figure, it is observed that NSE value (NSE=0.66) obtained from the representative parameters of the Snyder Model is lower than the NSE value (NSE=0.96) obtained from the optimised parameters of the Snyder Model. for the Dec 2014 flood event.



**Figure 5.45 Comparison of observed and Simulated Flood Hydrographs using optimised as well as representative parameters of Snyder Model for Dec 2014 event**

Figure 5.46 shows the comparison of observed flood hydrograph with simulated flood hydrographs using optimized parameters and representative parameters of the Snyder UH model for the event Nov 2012. From this figure, it is observed that NSE value (NSE=0.95) obtained from the representative parameters of the Snyder Model is same as the NSE value (NSE=0.96) obtained from the optimised parameters of the Snyder Model for the Nov 2012 flood event.



**Figure 5.46 Comparison of observed and Simulated Flood Hydrographs using optimised as well as representative parameters of Snyder Model for Nov 2012 event**

#### 5.6.4 COMPARISON OF THREE TRANSFORM MODELS DURING CALIBRATION

Figure 5.47 shows the comparison of simulated flood hydrographs using representative parameters of the three transform models with the observed flood hydrograph for the event of May 2017 during calibration. From this Figure 5.47, it is observed that the Snyder UH transform model gave best performance with the NSE value of 0.84. The SCS UH transform model performed poorest with the NSE value of 0.35 whereas the Clark UH transform model is the second best performing model with the NSE value of 0.69.

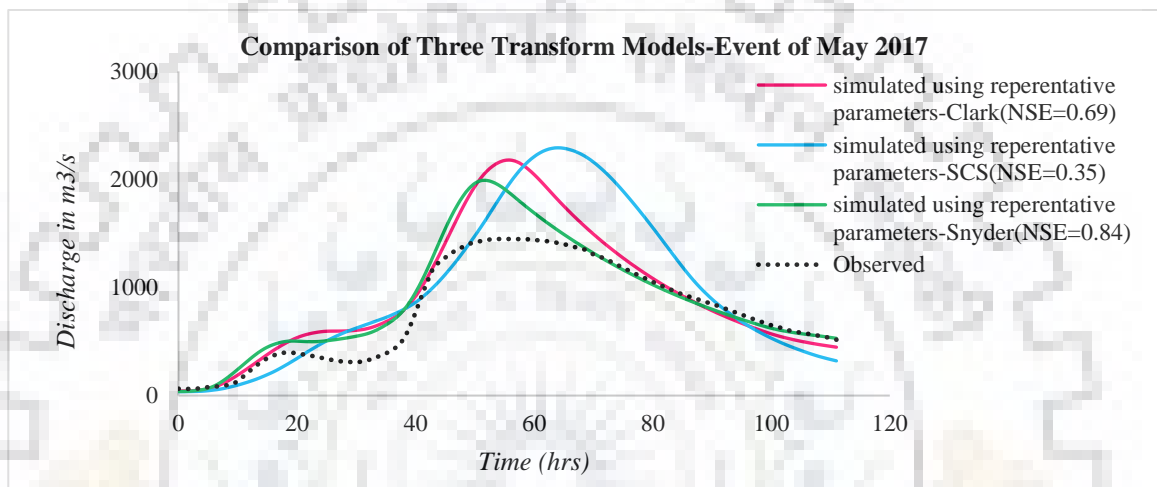


**Figure 5.47 Comparison of observed and Simulated Flood Hydrographs using Representative Parameters of three transform models for May 2017 event**

Figure 5.48 shows the percent errors of three performance criteria such as percent error in peak, percent error in time to peak and percent error in discharge volume along with NSE values, computed during the calibration from the event May 2017 using three transform models. All the percent errors, computed from three different performance criteria, for SCS UH transform model are more than that of the other two transform models. All the percent errors, computed from three different performance criteria, for Snyder UH transform model are lower than that of the other transform models. Furthermore, NSE value, which is an indicator of the overall performance of the transform model, is highest for Snyder model (NSE=0.84) whereas SCS model has lowest value of NSE (NSE=0.35). The NSE value for Clark model (NSE=0.69) is second best among the three transform models considered.

Figure 5.49 shows the comparison of simulated flood hydrographs using representative parameters of the three transform models with the observed flood hydrograph for the event of Dec 2014 during calibration. From this Figure 5.49, it is observed that the Clark UH transform model gave best performance with the NSE value of 0.73. The SCS UH transform model

performed poorest with the NSE value of 0.58 whereas the Snyder UH transform model is the second best performing model with the NSE value of 0.66.

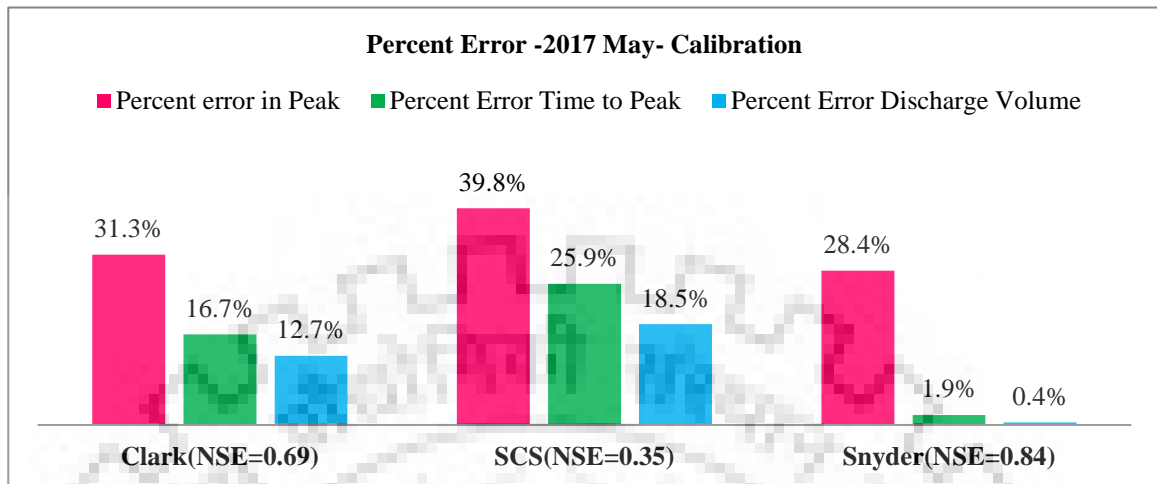


Figure 5.48 Comparison of Percent Errors of Three Transform Models during Calibration using Representative Parameters -May 2017

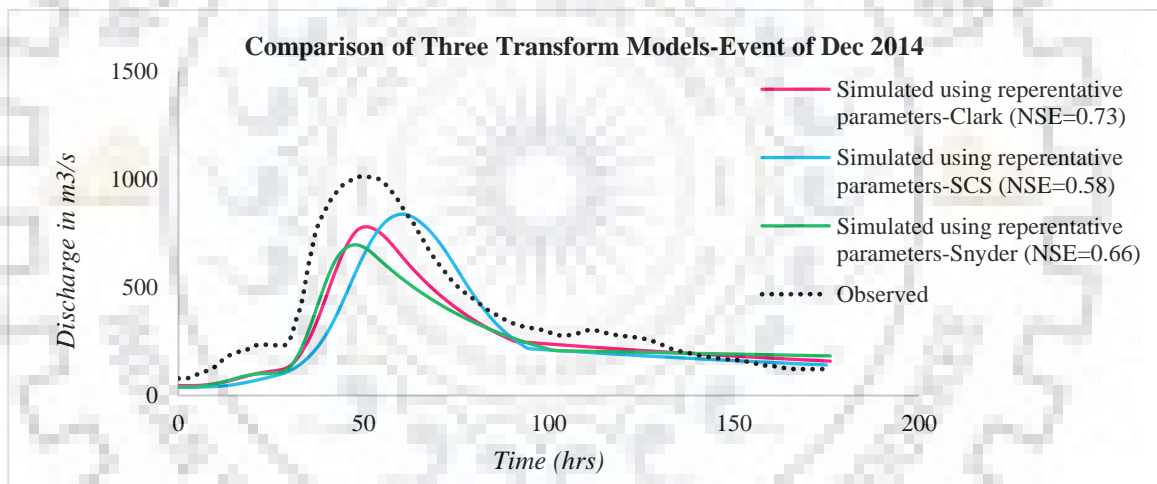


Figure 5.49 Comparison of Observed and Simulated Flood Hydrographs using Representative Parameters of three transform models for Dec 2014 event

Figure 5.50 shows the percent errors of three performance criteria such as percent error in peak, percent error in time to peak and percent error in discharge volume along with NSE values, computed during the calibration from the event Dec 2014 using three transform models. All the percent errors, computed from three different performance criteria, for SCS UH transform model are more than that of the other two transform models. All the percent errors, computed from three different performance criteria, for Clark UH transform model are lower than that of the other transform models. Furthermore, NSE value, which is an indicator of the overall performance of the transform model, is highest for Clark model (NSE=0.73) whereas SCS

model has lowest value of NSE (NSE=0.58). The NSE value for Snyder model (NSE=0.66) is second best among the three transform models considered.

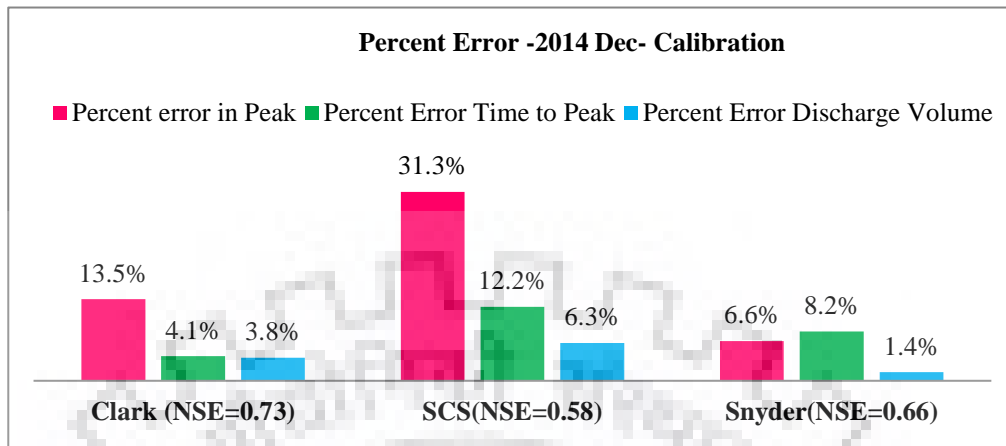


Figure 5.50 Comparison of Percent Errors of Three Transform Models during Calibration using Representative Parameters -Dec 2014

Figure 5.51 shows the comparison of simulated flood hydrographs using representative parameters of the three transform models with the observed flood hydrograph for the event of Nov 2012 during calibration. From this Figure 5.51, it is observed that the Snyder UH transform model gave best performance with the NSE value of 0.95. The SCS UH transform model performed poorest with the NSE value of 0.61 whereas the Clark UH transform model is the second best performing model with the NSE value of 0.89.

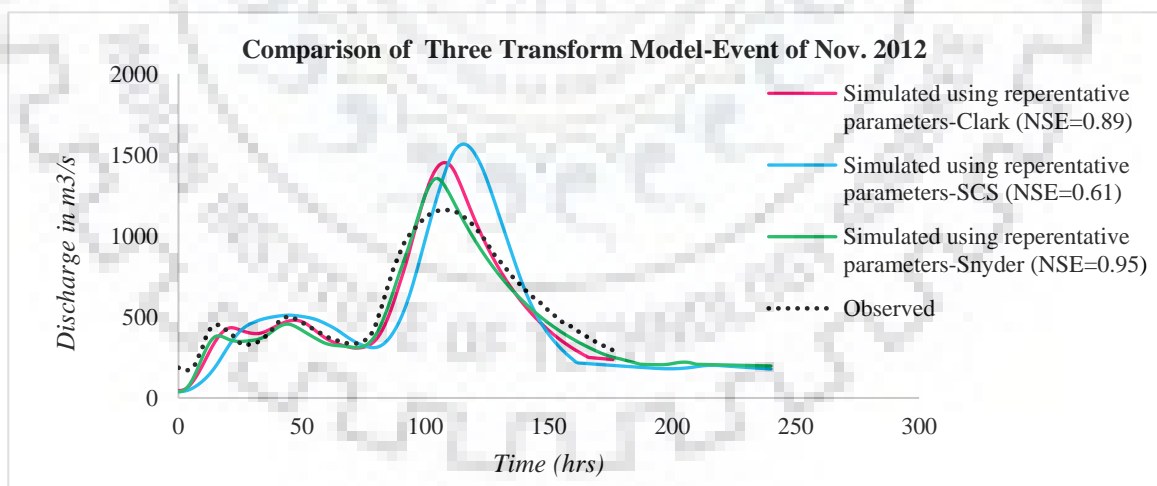


Figure 5.51 Comparison of Observed and Simulated Flood Hydrographs using Representative Parameters of three transform models for Nov 2012 event

Figure 5.52 shows the percent errors of three performance criteria such as percent error in peak, percent error in time to peak and percent error in discharge volume along with NSE values, computed during the calibration from the event Nov 2012 using three transform models. All the percent errors, computed from three different performance criteria, for SCS UH transform

model are more than that of the other two transform models. All the percent errors, computed from three different performance criteria, for Snyder UH transform model are lower than that of the other transform models. Furthermore, NSE value, which is an indicator of the overall performance of the transform model, is highest for Snyder model (NSE=0.95) whereas SCS model has lowest value of NSE (NSE=0.61). The NSE value for Clark model (NSE=0.89) is second best among the three transform models considered.

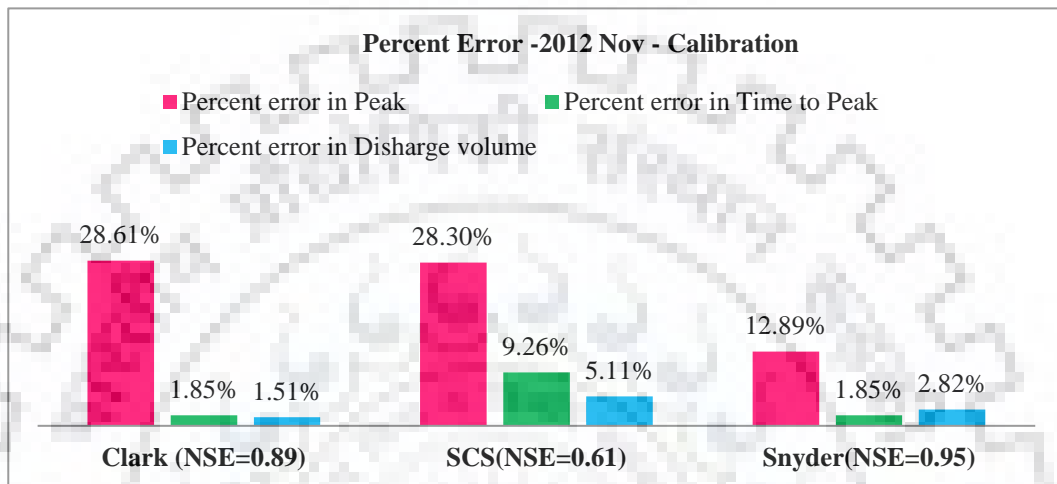


Figure 5.52 Percent Errors of Three Transform Models during Calibration using Representative Parameters -Nov 2012

### 5.6.5 VALIDATION OF CLARK UH MODEL - EVENT JUN. 2014

Figure 5.53 shows the comparison of observed and simulated flood hydrograph at Hanwella gauging site using representative parameters of Clark model for Jun.2014 event considered for validation. The NSE value, obtained during the validation of Clark Model, was 0.74.

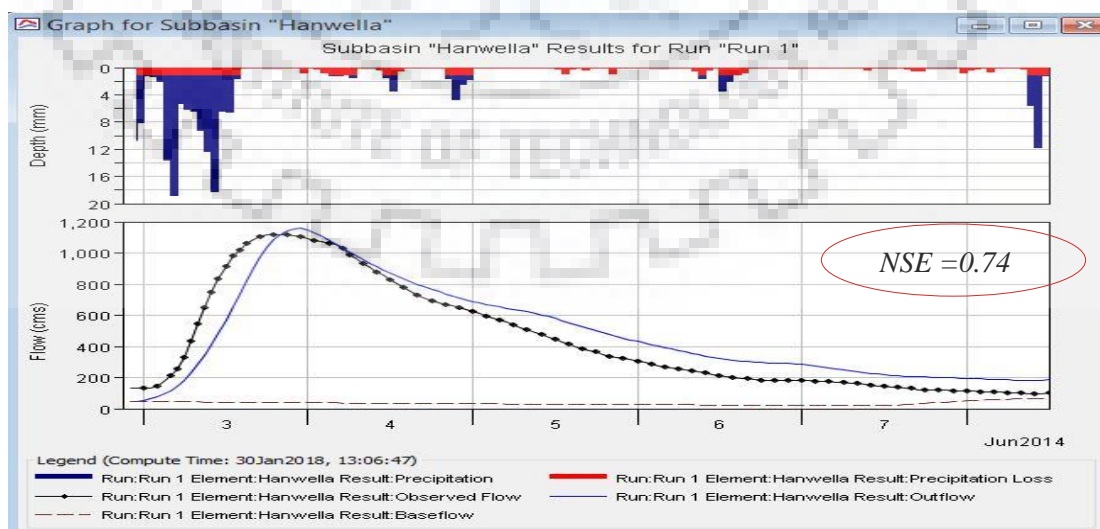
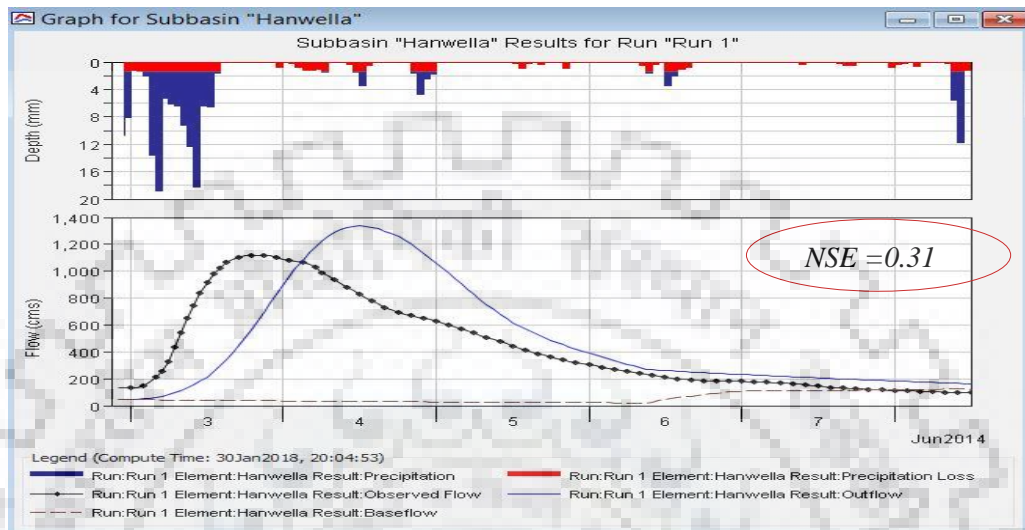


Figure 5.53 Comparison of observed and Simulated flood hydrograph at Hanwella gauging site using representative parameters of Clark model for Jun.2014 event considered for validation

### 5.6.6 VALIDATION OF SCS UH MODEL - EVENT JUN. 2014

Figure 5.54 shows the comparison of observed and Simulated hydrograph at Hanwella gauging site using representative parameters of SCS model for Jun.2014 event considered for validation. The NSE value, obtained during the validation of SCS Model, was 0.31.



*Figure 5.54 Comparison of Observed and Simulated Hydrograph at Hanwella gauging site using representative parameters of SCS model for Jun.2014 event considered for validation*

### 5.6.7 VALIDATION OF SNYDER UH MODEL - EVENT JUN. 2014

Figure 5.55 shows the comparison of observed and Simulated hydrograph at Hanwella gauging site using representative parameters of Snyder model for Jun.2014 event considered for validation. The NSE value, obtained during the validation of Snyder model, was 0.82.

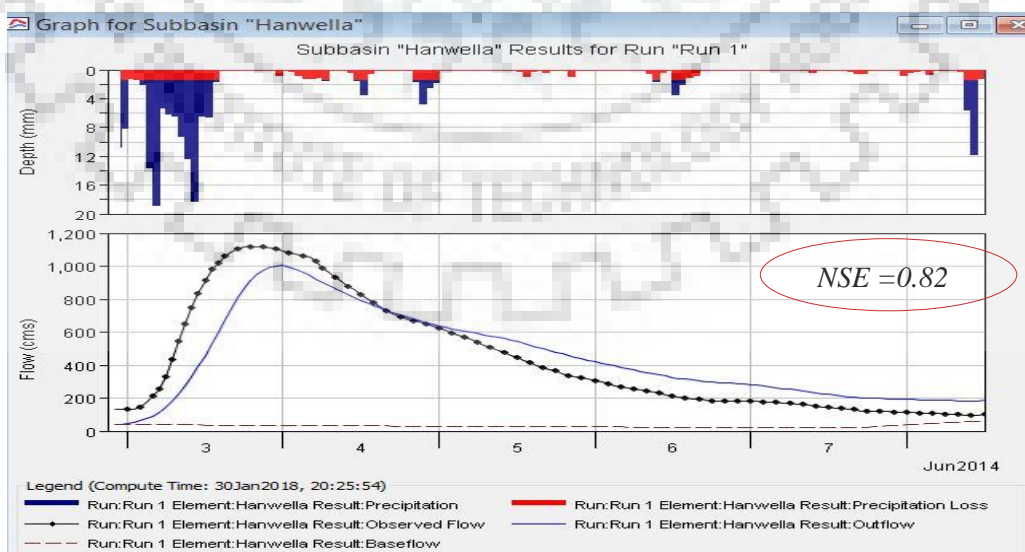


*Figure 5.55 Comparison of Observed and Simulated Hydrograph at Hanwella gauging site using representative parameters of Snyder model for Jun.2014 event considered for validation*



### 5.6.8 COMPARISON OF THREE TRANSFORM MODELS DURING VALAIDATION

Figure 5.56 shows the comparison of observed and simulated flood hydrographs by the three transform models for the event of Jun. 2014 during validation. The performance of the Snyder UH transform model was best as it had resulted in the highest NSE value of 0.82. The performance of SCS UH transform model was extremely poor but with the lowest NSE value of 0.31 whereas the performance of the Clark UH transform model was second best with the NSE of 0.74.

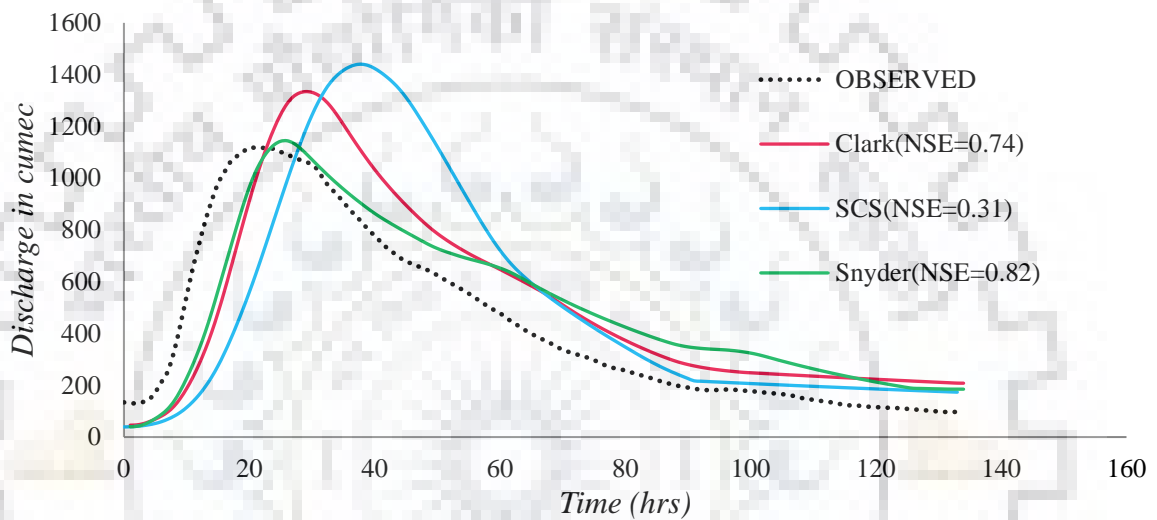


**Figure 5.56 Comparison of observed and Simulated Flood Hydrographs of Three Transform Models during Validation considering Jun.2014 event**

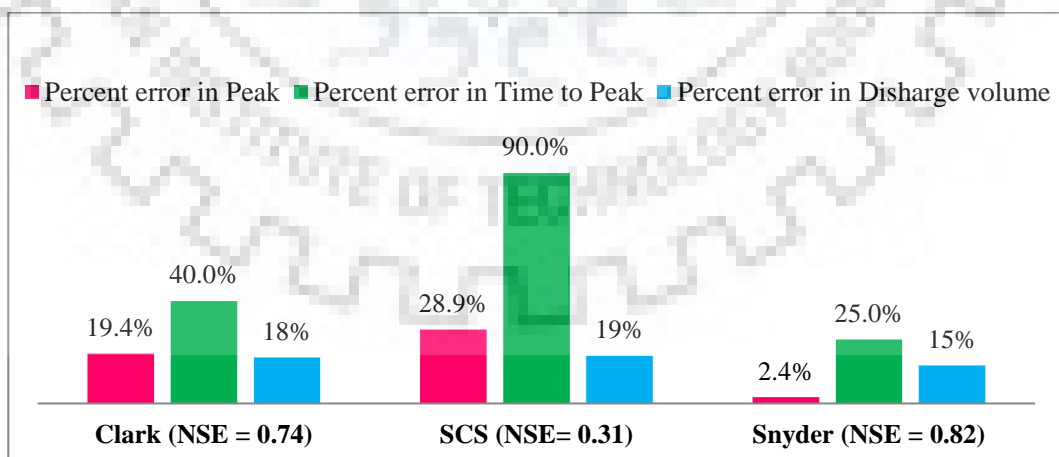


**Figure 5.57 Comparison of Percent Errors of Three Transform Models during Validation using Representative parameters considering Jun 2014 event.**

Figure 5.57 shows the percent errors of three performance criteria such as percent error in peak, percent error in time to peak and percent error in discharge volume along with NSE values computed during the validation from the event Jun 2014 using three transform models. All the percent errors, computed from three different performance criteria, for SCS UH transform model, are more than that of the other two transform models. All the percent errors, computed from three different performance criteria, for Snyder UH transform model are lower than that of the other transform models. Furthermore, NSE value, which is an indicator of the overall performance of the transform model, is highest for Snyder model (NSE=0.82) whereas SCS UH model has lowest value of NSE (NSE=0.31). The NSE value for Clark model (NSE=0.74) is second best among the three transform models considered.

From the calibration and validation results of three transform models, Snyder UH model is found to be best performing model whereas Clark model is the second best performing model. The performance of SCS-CN UH model is extremely poor as compared to the other two transform models. Thus, the unit hydrograph derived from Snyder UH model is considered for further applications.

## 5.7 Real Time Flood Forecasting

### 5.7.1 DEVELOPMENT OF UNIT HYDROGRAPH

The representative parameters of Snyder Unit hydrograph model,  $C_p$  and standard lag  $t_p$  were 0.3 and 14 hrs respectively. Normally, the Snyder UH is developed based on seven (7) sets of unit hydrograph characteristics derived from Snyder's synthetic equations applicable for the basin. However, the HEC-HMS programme considers the computed UH peak and time to peak derived from the equivalent UH with Clark model IUH approach rather than using seven synthetic relationships. The time area relationship is given in Table 5.17 to develop the Snyder UH based on this approach. However, the Snyder UH was developed as shown in Figure 5.58

*Table 5.17 Time-Area relations to develop Snyder UH from Clark IUH*

time of travel in hrs.	Area( $A_t$ ) in sqkm	$t/T_c$	$A_t/A$	Increment area
1	61.63	0.071	0.034	61.63
2	145.95	0.143	0.080	84.32
3	258.64	0.214	0.141	112.69
4	400.87	0.286	0.219	142.23
5	555.75	0.357	0.304	154.88

6	728.55	0.429	0.398	172.80
7	915.30	0.500	0.500	186.75
8	1,102.05	0.571	0.602	186.75
9	1,274.85	0.643	0.696	172.80
10	1,429.73	0.714	0.781	154.88
11	1,571.96	0.786	0.859	142.23
12	1,684.65	0.857	0.920	112.69
13	1,768.97	0.929	0.966	84.32
14	1,830.60	1.000	1.000	61.63

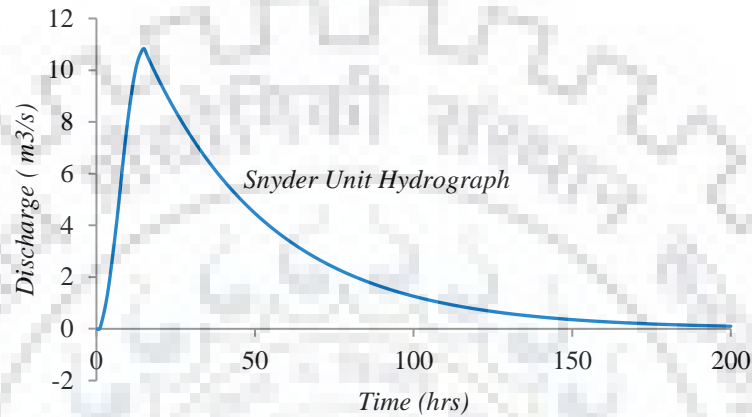


**Figure 5.58 Snyder Unit Hydrograph**

### 5.7.2 FORECASTING OF FLOOD HYDROGRAPH

Flood hydrographs were forecasted for the event of Jun. 2014 at each time step whenever a fresh observed rainfall values arrived at the forecasting station. For this purpose, excess rainfall computed for Jun 2014 event from HEC-HMS programme were convoluted with Snyder Unit Hydrograph using Equation  $[Q_j = \sum_{i=1}^j (R_i \cdot U_{j-i+1})]$ . Those forecasted flood hydrographs were developed for the successive 4 hrs duration rainfall blocks of that event. The forecasted flood hydrographs for different lead times were computed as shown in Figure 5.59.

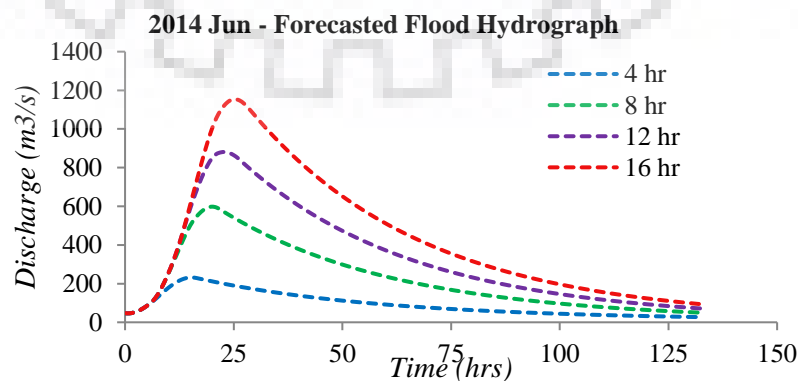


**Figure 5.59 Forecasted Flood Hydrograph in real time for different lead times for Jun.2014 event**

Department of Irrigation, Sri Lanka, follows the reference given in Table 5.18 to take the precautionary steps over flood mitigation measures according to the flood extent. The risk assessment was carried out for the event Jun.2014. The Maximum water levels corresponding to the peaks of forecasted flood hydrographs were computed using the developed rating curve. The peak of the forecasted flood hydrographs and corresponding water levels, time to peak of the forecasted flood hydrograph. The properties of forecasted flood hydrographs such as peak discharges, corresponding water levels, time to peaks and lead times along with the limits of risks are given in Table 5.19.

**Table 5.18 Risk Assessment at Hanwella maintained by Dept. of Irrigation, Sri Lanka**

Water Level in m MSL	Limit of Risk
Less than 18	No Risk
18 - 18.5	Low
18.5 - 19.0	Moderate
19.0 - 19.5	High
above 19.5	Very high

**Table 5.19 Forecasted flood hydrograph peak and corresponding water levels, time to peak and lead time along with limits of risks for Jun.2014 event**

Duration of Excess Rainfall (hr)	Peak Discharge ( $Q_p$ ) forecasted ( $m^3/s$ )	Water level forecasted (m MSL)	Time to peak (hrs)	Lead Time (hrs)	Limits of Risk
1	188.9	17.7	15	14	No Risk
2	291.3	17.9	15	13	No Risk
3	295.3	17.9	15	12	No Risk
4	300.2	17.9	15	11	No Risk
5	311.3	17.9	15	10	No Risk
6	476.5	18.2	18	12	Low
7	732.5	18.5	20	13	Low
8	790.2	18.6	20	12	Moderate
9	855.4	18.7	20	11	Moderate
10	912.8	18.7	21	11	Moderate
11	1005.7	18.8	21	10	Moderate
12	1140.2	19.0	23	11	High
13	1363.5	19.2	24	11	High
14	1431.2	19.3	25	11	High
15	1484.8	19.3	25	10	High
16	1491.1	19.3	25	9	High

Figure 5.60 shows the comparison of the forecasted flood hydrograph considering 16 hrs rainfall block and observed flood hydrographs for the event of Jun.2014. The forecasted flood hydrograph closely fits the observed flood hydrograph. From the figure, it is observed that the forecasted flood hydrograph considering all the rainfall blocks is in closed agreement with the observed flood hydrograph. Thus, the forecasted flood hydrograph peaks and corresponding water levels considering the excess rainfall of different durations would provide very useful information for evacuating the people likely to be submerged during flood for the various forecasted water levels.

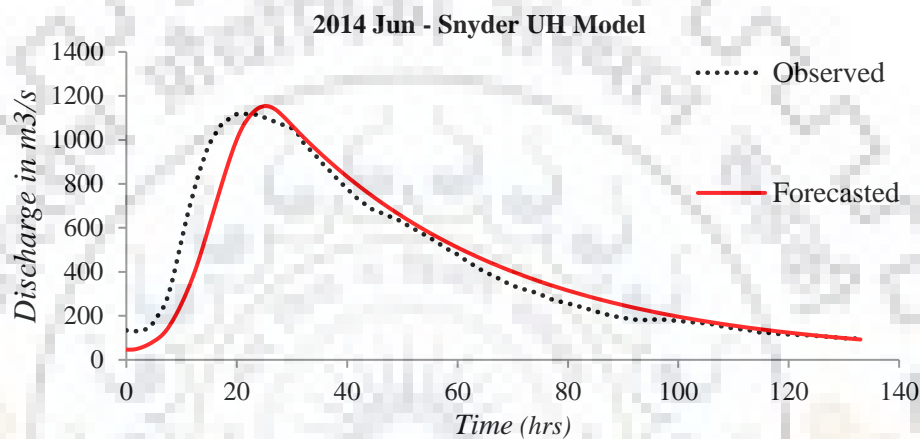


*Figure 5.60 Comparison of Observed & Forecasted Flood Hydrographs (considering 16 hrs of excess rainfall) using Snyder UH model for Jun 2014 event*

## 5.8 Estimation of Design Flood

### 5.8.1 ESTIMATION OF 100- YEAR RETURN PERIOD FLOOD

The maximum amount of rainfall depth for various desired durations and for various desired return periods were computed using the methodology described in section 4.8.1. Those computed rainfall depths are given in Table 5.20. Maximum rainfall depths for durations 1 day and 2 days were computed from the observed data available whereas the maximum rainfall depth for durations 1 hr, 2 hr, 3 hr, 6 hr and 12 hr were determined from the one-day rainfall depth by employing hourly distribution factors. These distribution factors were derived from the hourly rainfall data of the available flood events. Based on Table 5.20, DDF curves for specified return periods were developed considering the durations up to 6 hrs only on x-axis and rainfall depths (mm) on y-axis, as shown in Figure 5.61.

**Table 5.20 Max.Rainfall Depth for various Duration and various Frequency**

Duration (hrs)	Return Period (yrs.)				
	1000	500	100	50	25
1	68.33	62.40	48.64	42.71	36.78
2	116.90	106.76	83.21	73.07	62.93
3	147.51	134.71	105.00	92.21	79.41
6	245.70	224.39	174.90	153.58	132.27
12	382.19	349.03	272.06	238.90	205.75
24	472.24	431.27	336.16	295.19	254.23
48	568.19	518.90	404.45	355.16	305.87

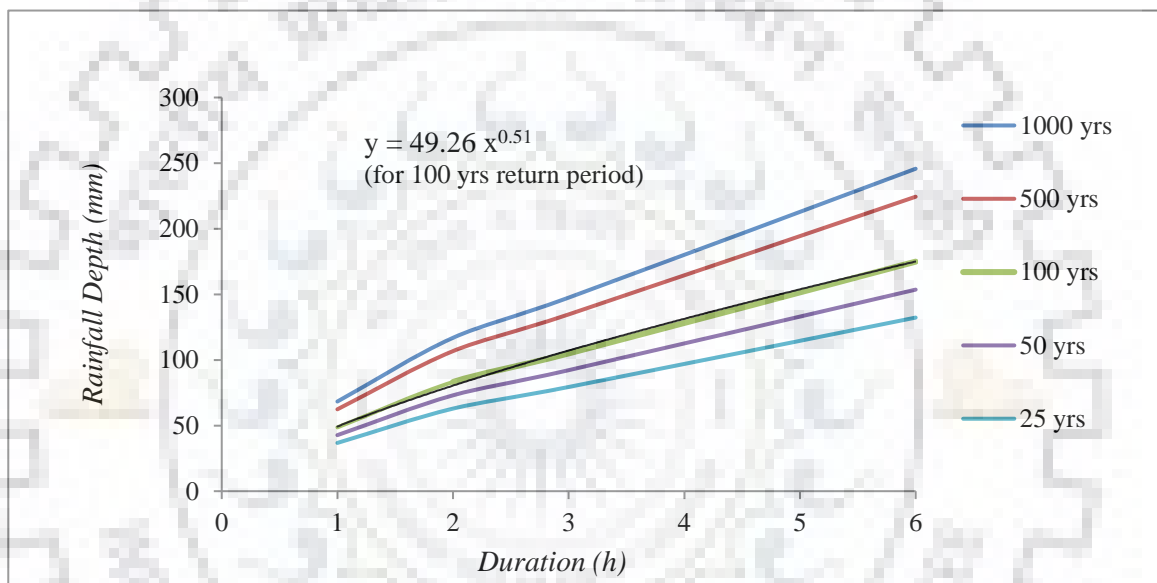


**Figure 5.61 Depth – Duration - Frequency Curve**

The duration of the design storm was obtained as 72 hrs as described in section 4.8.1. Based on the DDF curve developed, a common relationship of rainfall depth and duration for 100 yrs. return period was derived (Figure 5.61). Thus the 72-hour rainfall of 100-year return period is considered to be the design storm. The cumulative rainfall depth and hourly incremental rainfall depth for 72 hrs were computed as given in Table 5.21.

**Table 5.21 Design storm from DDF curve (100 yrs. Return Period)**

Duration in hrs	Cumulative RF in mm	Incremental RF in mm	Duration in hrs	Cumulative RF in mm	Incremental RF in mm
x	$y = 49.26 x^{0.51}$		x	$y = 49.26 x^{0.51}$	
1	49.3	49.3	37	310.7	4.3

2	70.1	20.9	38	314.9	4.3
3	86.3	16.1	39	319.1	4.2
4	99.9	13.6	40	323.3	4.1
5	111.9	12.0	41	327.4	4.1
6	122.8	10.9	42	331.4	4.0
7	132.9	10.0	43	335.4	4.0
8	142.3	9.4	44	339.4	4.0
9	151.1	8.8	45	343.3	3.9
10	159.4	8.3	46	347.1	3.9
11	167.3	7.9	47	351.0	3.8
12	174.9	7.6	48	354.8	3.8
13	182.2	7.3	49	358.5	3.8
14	189.2	7.0	50	362.2	3.7
15	196.0	6.8	51	365.9	3.7
16	202.6	6.6	52	369.5	3.6
17	208.9	6.4	53	373.1	3.6
18	215.1	6.2	54	376.7	3.6
19	221.1	6.0	55	380.3	3.5
20	227.0	5.9	56	383.8	3.5
21	232.7	5.7	57	387.2	3.5
22	238.3	5.6	58	390.7	3.5
23	243.8	5.5	59	394.1	3.4
24	249.1	5.3	60	397.5	3.4
25	254.4	5.2	61	400.9	3.4
26	259.5	5.1	62	404.2	3.3
27	264.5	5.0	63	407.5	3.3
28	269.5	5.0	64	410.8	3.3
29	274.4	4.9	65	414.1	3.3
30	279.1	4.8	66	417.3	3.2
31	283.8	4.7	67	420.5	3.2
32	288.5	4.6	68	423.7	3.2
33	293.0	4.6	69	426.9	3.2
34	297.5	4.5	70	430.0	3.1
35	302.0	4.4	71	433.1	3.1
36	306.3	4.4	72	436.2	3.1

The rainfall excess of design storm was computed as given in Table 5.22. For critical sequencing and design flood estimation, Snyder model UH ordinates were used. The design loss was considered as 1 mm/hr as per the reference given in section 5.8.1.

**Table 5.22 Rainfall excess of design storm from DDF curve**

<b>Duration in hrs</b>	<b>Cumul ative RF in mm</b>	<b>Increme ntal RF in mm</b>	<b>Ordinate of UH m<sup>3</sup>/s</b>	<b>First arrangeme nt of rainfall increment</b>	<b>Design sequence of rainfall increment</b>	<b>Design loss in mm</b>	<b>Rainfall excess of design storm in mm</b>
0	0		0		0		
1	49.3	49.3	0.43	3.00	3.10	1.00	2.1
2	70.1	20.9	1.00	3.00	3.10	1.00	2.1
3	86.3	16.1	1.76	3.20	3.10	1.00	2.1
4	99.9	13.6	2.71	3.50	3.20	1.00	2.2
5	111.9	12.0	3.71	3.60	3.20	1.00	2.2
6	122.8	10.9	4.82	4.10	3.20	1.00	2.2
7	132.9	10.0	6.00	4.80	3.20	1.00	2.2
8	142.3	9.4	7.15	5.60	3.30	1.00	2.3
9	151.1	8.8	8.17	6.60	3.30	1.00	2.3
10	159.4	8.3	9.04	7.60	3.30	1.00	2.3
11	167.3	7.9	9.81	8.80	3.30	1.00	2.3
12	174.9	7.6	10.34	13.60	3.40	1.00	2.4
13	182.2	7.3	10.67	20.90	3.40	1.00	2.4
14	189.2	7.0	10.83	49.30	3.40	1.00	2.4
15	196.0	6.8	10.56	16.10	3.50	1.00	2.5
16	202.6	6.6	10.30	12.00	3.50	1.00	2.5
17	208.9	6.4	10.04	10.90	3.60	1.00	2.6
18	215.1	6.2	9.79	10.00	3.60	1.00	2.6
19	221.1	6.0	9.54	9.40	3.70	1.00	2.7
20	227.0	5.9	9.31	8.30	3.70	1.00	2.7
21	232.7	5.7	9.07	7.90	3.80	1.00	2.8
22	238.3	5.6	8.85	7.60	3.80	1.00	2.8
23	243.8	5.5	8.62	7.30	3.80	1.00	2.8
24	249.1	5.3	8.41	7.00	3.90	1.00	2.9
25	254.4	5.2	8.20	6.80	3.90	1.00	2.9
26	259.5	5.1	7.99	6.40	4.00	1.00	3.0
27	264.5	5.0	7.79	6.20	4.10	1.00	3.1
28	269.5	5.0	7.60	6.00	4.20	1.00	3.2
29	274.4	4.9	7.41	5.90	4.30	1.00	3.3
30	279.1	4.8	7.22	5.70	4.30	1.00	3.3
31	283.8	4.7	7.04	5.50	4.40	1.00	3.4
32	288.5	4.6	6.87	5.30	4.40	1.00	3.4
33	293.0	4.6	6.70	5.20	4.50	1.00	3.5
34	297.5	4.5	6.53	5.10	4.60	1.00	3.6
35	302.0	4.4	6.37	5.00	4.70	1.00	3.7
36	306.3	4.4	6.21	5.00	4.90	1.00	3.9
37	310.7	4.3	6.05	4.90	5.00	1.00	4.0
38	314.9	4.3	5.90	4.70	5.00	1.00	4.0
39	319.1	4.2	5.75	4.60	5.10	1.00	4.1
40	323.3	4.1	5.61	4.50	5.20	1.00	4.2
41	327.4	4.1	5.47	4.40	5.30	1.00	4.3



42	331.4	4.0	5.33	4.40	5.50	1.00	4.5
43	335.4	4.0	5.20	4.30	5.70	1.00	4.7
44	339.4	4.0	5.07	4.30	5.90	1.00	4.9
45	343.3	3.9	4.94	4.20	6.00	1.00	5.0
46	347.1	3.9	4.82	4.10	6.20	1.00	5.2
47	351.0	3.8	4.70	4.00	6.40	1.00	5.4
48	354.8	3.8	4.58	3.90	6.80	1.00	5.8
49	358.5	3.8	4.47	3.90	7.00	1.00	6.0
50	362.2	3.7	4.35	3.80	7.30	1.00	6.3
51	365.9	3.7	4.25	3.80	7.60	1.00	6.6
52	369.5	3.6	4.14	3.80	7.90	1.00	6.9
53	373.1	3.6	4.04	3.70	8.30	1.00	7.3
54	376.7	3.6	3.93	3.70	9.40	1.00	8.4
55	380.3	3.5	3.84	3.60	10.00	1.00	9.0
56	383.8	3.5	3.74	3.60	10.90	1.00	9.9
57	387.2	3.5	3.65	3.50	12.00	1.00	11.0
58	390.7	3.5	3.56	3.50	16.10	1.00	15.1
59	394.1	3.4	3.47	3.40	49.30	1.00	48.3
60	397.5	3.4	3.38	3.40	20.90	1.00	19.9
61	400.9	3.4	3.30	3.40	13.60	1.00	12.6
62	404.2	3.3	3.21	3.30	8.80	1.00	7.8
63	407.5	3.3	3.13	3.30	7.60	1.00	6.6
64	410.8	3.3	3.05	3.30	6.60	1.00	5.6
65	414.1	3.3	2.98	3.30	5.60	1.00	4.6
66	417.3	3.2	2.90	3.20	4.80	1.00	3.8
67	420.5	3.2	2.83	3.20	4.10	1.00	3.1
68	423.7	3.2	2.76	3.20	3.60	1.00	2.6
69	426.9	3.2	2.69	3.20	3.50	1.00	2.5
70	430.0	3.1	2.62	3.10	3.20	1.00	2.2
71	433.1	3.1	2.56	3.10	3.00	1.00	2.0
72	436.2	3.1	2.49	3.10	3.00	1.00	2.0

The ordinates of direct surface runoff hydrograph were obtained convoluting the computed excess rainfall of design storm with the ordinates of the Snyder model UH. A constant design base flow of 201.41 cumec was adopted as per reference described in section 4.8.1. This design baseflow was added to each ordinates of the direct surface runoff to get the design flood hydrograph. The computed ordinates of the design flood hydrograph for 100 yrs. return period is given in Table 5.23. From the table it is observed that the peak flood and the time to peak are 5532.5  $m^3/s$  and 67 hrs respectively. Using the design flood hydrograph ordinates given in Table 5.23, the design flood hydrograph was developed and shown in Figure 5.62.

**Table 5.23 Ordinates of 100- years Return Period Design flood hydrograph**

Duration in hrs	Ordinates of Des.flood hydrograph m <sup>3</sup> /s	Duration in hrs	Ordinates of Des.flood hydrograph m <sup>3</sup> /s	Duration in hrs	Ordinates of Des.flood hydrograph m <sup>3</sup> /s	Duration in hrs	Ordinates of Des.flood hydrograph m <sup>3</sup> /s
0	202.57						
1	205.28	51	2,255.10	101	321.65	151	235.32
2	210.03	52	2,312.75	102	318.65	152	234.47
3	217.34	53	2,377.12	103	315.72	153	233.64
4	227.37	54	2,449.71	104	312.86	154	232.84
5	240.44	55	2,537.04	105	310.07	155	232.05
6	256.78	56	2,646.09	106	307.36	156	231.29
7	276.36	57	2,779.01	107	304.71	157	230.54
8	298.86	58	3,132.75	108	302.13	158	229.81
9	323.96	59	3,330.93	109	299.61	159	229.10
10	351.39	60	3,515.60	110	297.15	160	228.41
11	380.58	61	3,680.07	111	294.76	161	227.73
12	411.02	62	3,841.82	112	292.43	162	227.08
13	442.27	63	4,015.04	113	290.15	163	226.43
14	473.16	64	4,288.54	114	287.93	164	225.81
15	503.76	65	4,549.53	115	285.77	165	225.20
16	534.12	66	4,945.08	116	283.66	166	224.60
17	564.22	<b>67</b>	<b>5,532.50</b>	117	281.60	167	224.02
18	594.18	68	5,301.28	118	279.60	168	223.46
19	623.98	69	4,402.70	119	277.64	169	222.91
20	653.62	70	3,592.50	120	275.74	170	222.37
21	683.18	71	2,915.61	121	273.88	171	221.85
22	712.67	72	2,213.82	122	272.07	172	221.33
23	742.12	73	1,824.05	123	270.30	173	220.84
24	796.16	74	1,513.82	124	268.58	174	220.35
25	850.32	75	1,230.71	125	266.90	175	219.88
26	907.59	76	1,087.00	126	265.26	176	219.42
27	965.76	77	1,030.95	127	263.67	177	218.97
28	1,024.79	78	954.05	128	262.11	178	218.53
29	1,085.69	79	871.17	129	260.59	179	218.10
30	1,160.33	80	790.67	130	259.11	180	217.68
31	1,245.90	81	645.90	131	257.67	181	217.27
32	1,367.15	82	521.08	132	256.26	182	216.88
33	1,553.85	83	450.09	133	254.89	183	216.49
34	1,719.69	84	407.65	134	253.56	184	216.11
35	1,817.43	85	381.71	135	252.25	185	215.75

36	1,843.80	86	377.20	136	250.98	186	215.39
37	1,842.22	87	372.81	137	249.74	187	215.04
38	1,839.54	88	368.52	138	248.53	188	214.70
39	1,837.99	89	364.34	139	247.36	189	214.37
40	1,839.70	90	360.27	140	246.21	190	214.04
41	1,840.93	91	356.30	141	245.09	191	213.73
42	1,828.56	92	352.43	142	243.99	192	213.42
43	1,806.37	93	348.65	143	242.93	193	213.12
44	1,760.57	94	344.97	144	241.89	194	212.83
45	1,647.05	95	341.38	145	240.88	195	212.54
46	1,608.38	96	337.88	146	239.89	196	212.26
47	1,753.69	97	334.47	147	238.93	197	211.99
48	1,928.62	98	331.14	148	237.99	198	211.73
49	2,048.16	99	327.90	149	237.08	199	211.50
50	2,162.91	100	324.74	150	236.19	200	211.30

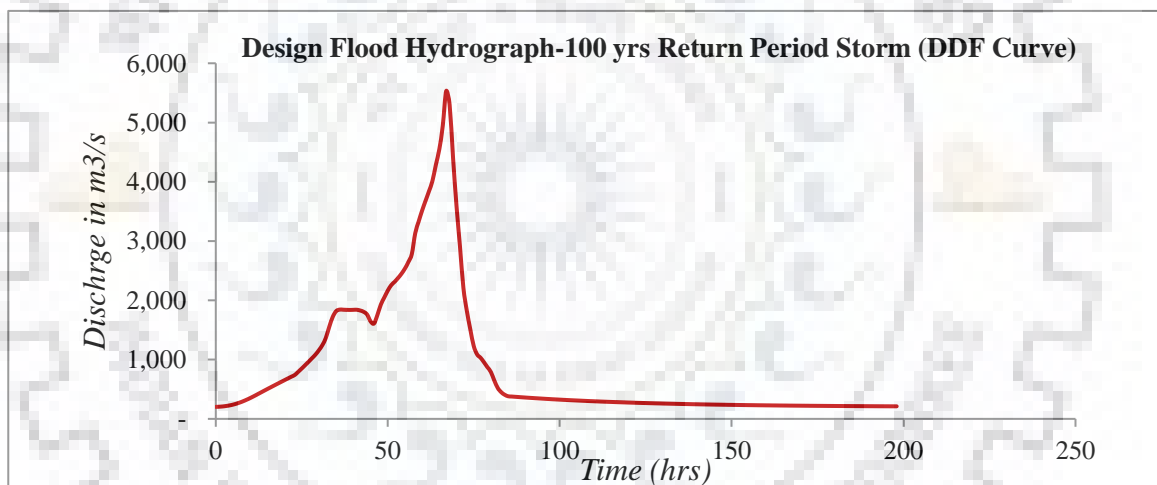


*Figure 5.62 Design Flood Hydrograph corresponding to 100 yrs. Return Period Storm (DDF Curve)*

### 5.8.2 COMPUTATION OF STANDARD PROJECT FLOOD (SPF)

Depth – area relation reflects the areal distribution characteristics of precipitation of a desired duration. Maximum rainfall depth of various durations 1 hr, 2 hr, 3 hr, 1 day, 2 days and 3 days for six rain-gauge stations over the river basin were computed as given in Table 5.24. Maximum rainfall depths for durations 1 day, 2 days and 3 days were computed from the observed data available. Whereas the maximum rainfall depth for durations 1 hr, 2 hr and 3 hr were determined from the one-day rainfall depth by employing hourly distribution factors.

These distribution factors were derived from the hourly rainfall data of the flood events available.

**Table 5.24 Max. Rainfall Depth (mm) of six (6) Stations for different Durations**

Serial No.	Station Name	Duration					
		1 hr	2 hr	3 hr	1 day	2 days	3 days
1	Norwood	31.80	66.16	74.78	312.00	323.60	327.00
2	Kithulgala	58.56	92.75	129.65	382.70	486.60	567.60
3	Holombuwa	36.06	57.05	72.54	248.40	264.20	296.10
4	Deraniyagala	50.77	63.66	107.17	355.60	453.50	535.69
5	Glencourse	42.41	60.36	104.46	346.60	381.80	383.50
6	Hanwella	36.76	55.11	87.20	289.60	340.90	391.80

Figure 5.63 represents the isohyet map of 1 hr duration of rainfall. This map was developed in ArcGIS using ‘kriging’ interpolation technique. The coordinates of the rain-gauge locations and 1 hr maximum rainfall depths were used for this interpolation.

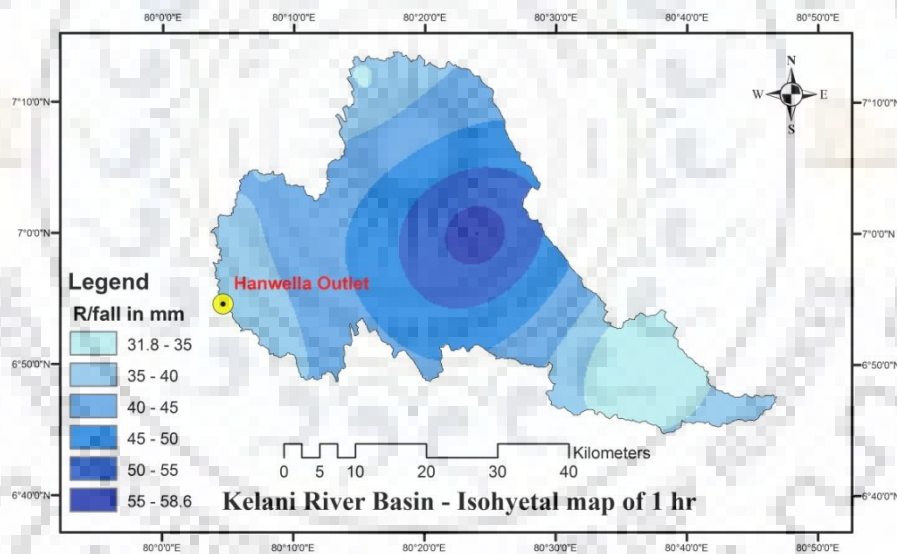


**Figure 5.63 Isohyet Map of 1 hr Duration**

The areal distribution of 1 hr-rainfall over the river basin was performed as shown in Table 5.25. The maximum average depth of 1 hr-rainfall over the river basin was found as 43.38 mm.

**Table 5.25 Computation of Max.average Rainfall Depth, from Isohyet Map of 1 hr. duration**

isohyets (mm)	Cum.isohyets area SQKM	Area SQKM	Mean isohyets	Total incremental Vol (1000 m3)	Total volume of rain (1000 m3)	Max.ave.D epth of Rainfall (mm)
55.00	53.88	53.88	58.60	3,157.37	3,157.37	58.60
50.00	302.06	248.18	52.50	13,029.45	16,186.82	53.59

45.00	710.59	408.53	47.50	19,405.18	35,591.99	50.09
40.00	1,247.64	537.05	42.50	22,824.63	58,416.62	46.82
35.00	1,625.35	377.71	37.50	14,164.13	72,580.74	44.66
31.80	1,833.12	207.77	33.40	6,939.52	79,520.26	43.38

Figure 5.64 represents the isohyet map of 2 hr duration of rainfall. This map was developed in ArcGIS using ‘kriging’ interpolation technique. The coordinates of the rain-gauge stations and 2 hr maximum rainfall depths were used for this interpolation.

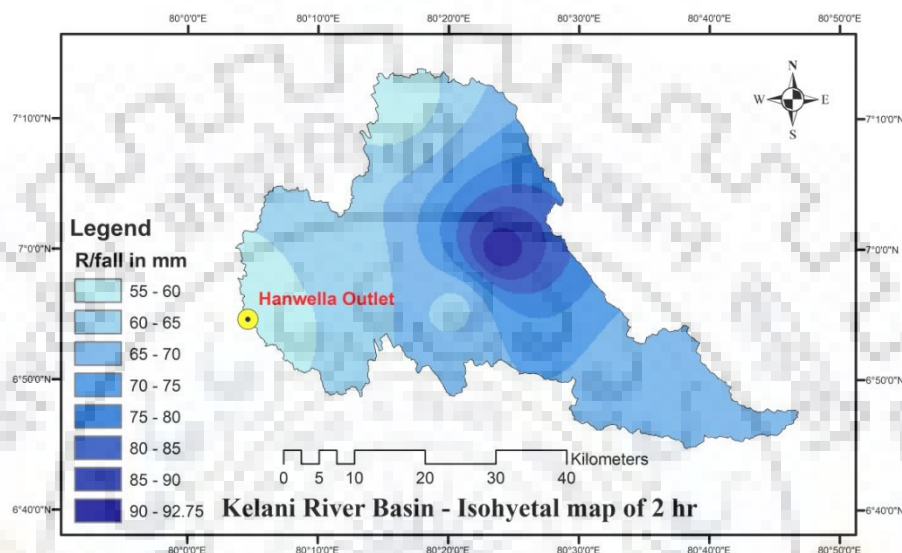


Figure 5.64 Isohyet Map of 2 hr Duration

The areal distribution of 2 hr-rainfall over the river basin was performed as shown in Table 5.26. The maximum average depth of 2 hr-rainfall over the river basin was found as 68.14 mm.

Table 5.26 Computation of Max.average Rainfall Depth, from Isohyet Map of 2 hr. duration

isohyet (mm)	Cum.isohyet area SQKM	Area SQKM	Mean isohyet	Total incremental Vol (1000 m3)	Total volume of rain (1000 m3)	Max.ave. Depth of Rainfall (mm)
90.00	23.20	23.20	92.75	2,151.80	2,151.80	92.75
85.00	86.26	63.06	87.50	5,517.75	7,669.55	88.91
80.00	182.03	95.77	82.50	7,901.03	15,570.58	85.54
75.00	308.38	126.35	77.50	9,792.13	25,362.70	82.24
70.00	530.87	222.49	72.50	16,130.53	41,493.23	78.16
65.00	1,148.28	617.41	67.50	41,675.18	83,168.40	72.43
60.00	1,620.56	472.28	62.50	29,517.50	112,685.90	69.54
55.00	1,833.31	212.75	57.50	12,233.13	124,919.03	68.14

Figure 5.65 represents the isohyet map of 3 hr duration of rainfall. This map was developed in ArcGIS using ‘kriging’ interpolation technique. The coordinates of the rain-gauge locations and 3 hr maximum rainfall depths were used for this interpolation.

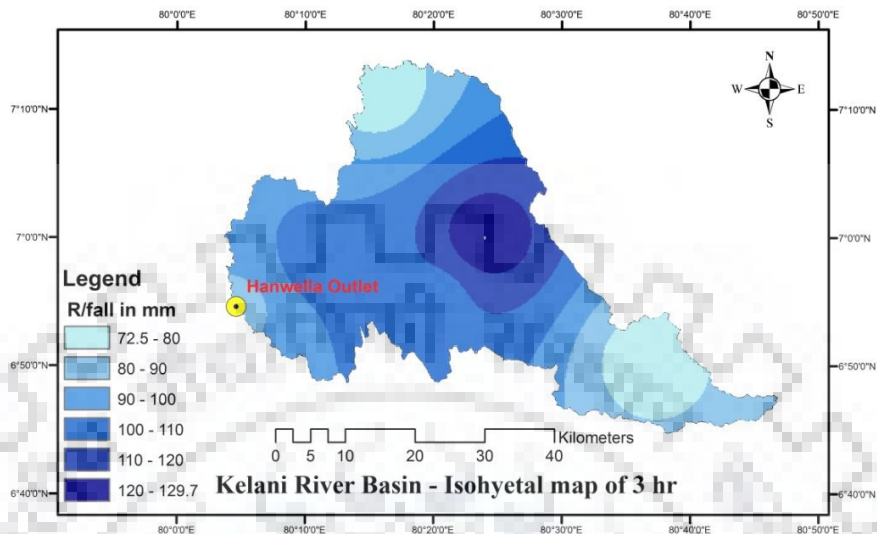


*Figure 5.65 Isohyet Map of 3 hr Duration*

*Table 5.27 Computation of Max.average Rainfall Depth, from Isohyet Map of 3 hr. duration*

isohyet (mm)	Cum.isohyet area SQKM	Area SQKM	Mean isohyet	Total incremental Vol (1000 m3)	Total volume of rain (1000 m3)	Max.ave.Depth of Rainfall (mm)
120.00	106.70	106.70	129.65	13,833.66	13,833.66	129.65
110.00	318.10	211.40	115.00	24,311.00	38,144.66	119.91
100.00	978.60	660.50	105.00	69,352.50	107,497.16	109.85
90.00	1,352.70	374.10	95.00	35,539.50	143,036.66	105.74
80.00	1,597.70	245.00	85.00	20,825.00	163,861.66	102.56
72.50	1,840.10	242.40	76.25	18,483.00	182,344.66	99.09

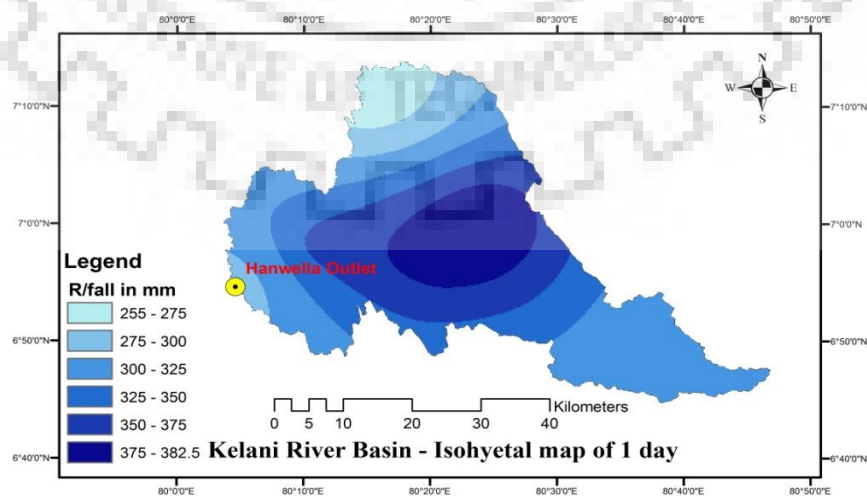


*Figure 5.66 Isohyet Map of 1-day Duration*

The areal distribution of 3 hr-rainfall over the river basin was performed as shown in Table 5.27. The maximum average depth of 3 hr-rainfall over the river basin was found as 99.09 mm.

Figure 5.66 represents the isohyet map of 1-day duration of rainfall. This map was developed in ArcGIS using ‘kriging’ interpolation technique. The coordinates of the rain-gauge stations and 1-day maximum rainfall depths were used for this interpolation.

The areal distribution of 1 day-rainfall over the river basin was performed as shown in Table 5.28. The maximum average depth of 1 day-rainfall over the river basin was found as 326.06 mm.

**Table 5.28 Computation of Max.average Rainfall Depth, from Isohyet Map of 1-day duration**

isohyet (mm)	Cum.isohyet area SQKM	Area SQKM	Mean isohyet	Total incremental Vol (1000 m3)	Total volume of rain (1000 m3)	Max.ave.Depth of Rainfall (mm)
375.00	0.46	0.46	382.50	176.45	176.45	382.50
350.00	287.39	286.93	362.50	104,012.20	104,188.65	362.53
325.00	940.64	653.25	337.50	220,472.04	324,660.69	345.15
300.00	1,656.91	716.26	312.50	223,832.63	548,493.31	331.03
275.00	1,775.51	118.60	287.50	34,097.76	582,591.07	328.13
250.00	1,833.31	57.80	262.50	15,172.82	597,763.89	326.06

Figure 5.67 represents the isohyet map of 2-day duration of rainfall. This map was developed in ArcGIS using ‘kriging’ interpolation technique. The coordinates of the rain-gauge stations and 2-day maximum rainfall depths were used for this interpolation.

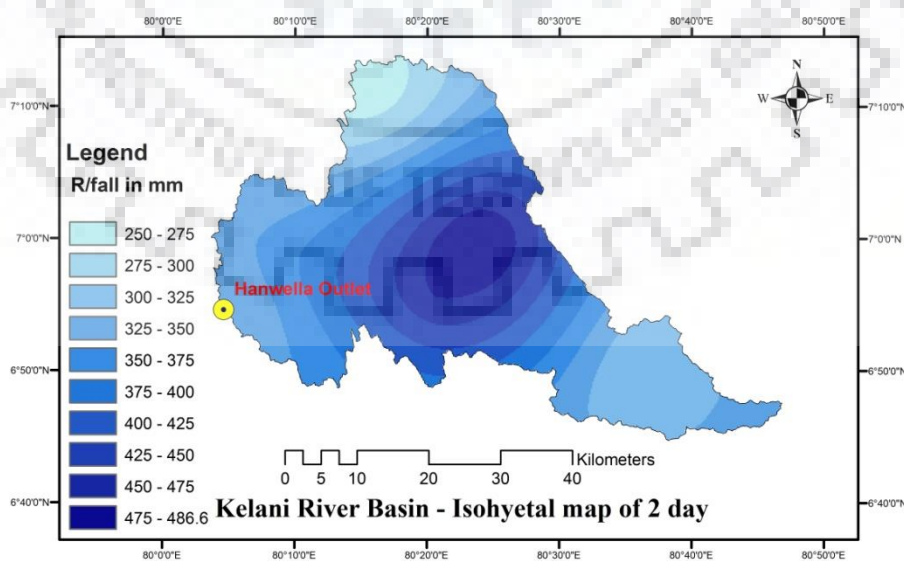


**Figure 5.67 Isohyet Map of 2-day Duration**

The areal distribution of 2 day-rainfall over the river basin was performed as shown in Table 5.29. The maximum average depth of 2 day-rainfall over the river basin was found as 380.69 mm.

**Table 5.29 Computation of Max.average Rainfall Depth, from Isohyet Map of 2-day duration**

isohyet (mm)	Cum.isohyet area SQKM	Area SQKM	Mean isohyet	Total incremental Vol (1000 m3)	Total volume of rain (1000 m3)	Max.ave.Depth of Rainfall (mm)
475.00	16.98	16.98	486.60	8,260.49	8,260.49	486.60
450.00	149.37	132.39	462.50	61,232.13	69,492.62	465.24
425.00	359.63	210.26	437.50	91,989.49	161,482.11	449.02
400.00	629.45	269.82	412.50	111,299.06	272,781.17	433.37
375.00	895.62	266.17	387.50	103,141.50	375,922.67	419.74
350.00	1,331.00	435.38	362.50	157,824.27	533,746.94	401.01
325.00	1,701.93	370.93	337.50	125,189.99	658,936.93	387.17
300.00	1,766.74	64.81	312.50	20,254.06	679,190.99	384.43
275.00	1,817.16	50.42	287.50	14,495.85	693,686.84	381.74
250.00	1,833.31	16.15	262.50	4,238.22	697,925.06	380.69

Figure 5.68 represents the isohyet map of 3-day duration of rainfall. This map was developed in ArcGIS using ‘kriging’ interpolation technique. The coordinates of the rain-gauge stations and 3-day maximum rainfall depths were used for this interpolation.

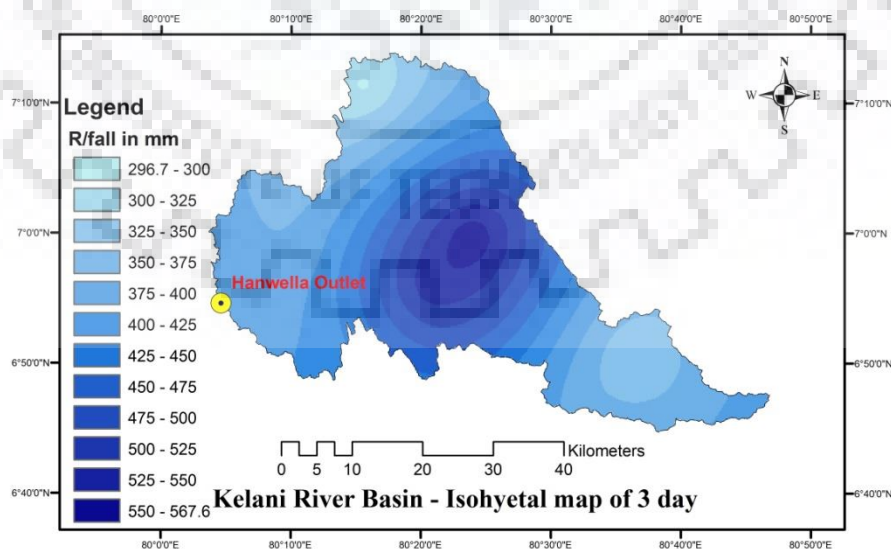


**Figure 5.68 Isohyet Map of 3-day Duration**



The areal distribution of 3 day-rainfall over the river basin was performed as shown in Table 5.30. The maximum average depth of 3 day-rainfall over the river basin was found as 421.02 mm.

**Table 5.30 Computation of Max.average Rainfall Depth, from Isohyet Map of 3-day duration**

isohyet (mm)	Cum.isohyet area SQKM	Area SQKM	Mean isohyet	Total incremental Vol (1000 m3)	Total volume of rain (1000 m3)	Max.ave.Depth of Rainfall (mm)
550.00	29.89	29.89	567.60	16,966.93	16,966.93	567.60
525.00	136.31	106.42	537.50	57,202.09	74,169.02	544.10
500.00	270.69	134.38	512.50	68,868.42	143,037.44	528.41
475.00	433.39	162.70	487.50	79,316.93	222,354.37	513.05
450.00	604.81	171.42	462.50	79,281.75	301,636.12	498.73
425.00	751.74	146.92	437.50	64,279.64	365,915.76	486.76
400.00	959.19	207.45	412.50	85,572.18	451,487.94	470.70
375.00	1,359.55	400.36	387.50	155,141.24	606,629.18	446.20
350.00	1,622.68	263.13	362.50	95,383.54	702,012.72	432.63
325.00	1,784.96	162.29	337.50	54,771.59	756,784.31	423.98
300.00	1,831.46	46.50	312.50	14,531.03	771,315.34	421.15
296.70	1,833.31	1.85	298.35	550.52	771,865.86	421.02

Based on the areal distribution of rainfall over the river basin for 1hr, 2 hr, 1 day, 2 days and 3-day durations, DAD curves were developed as represented in Figure 5.69.

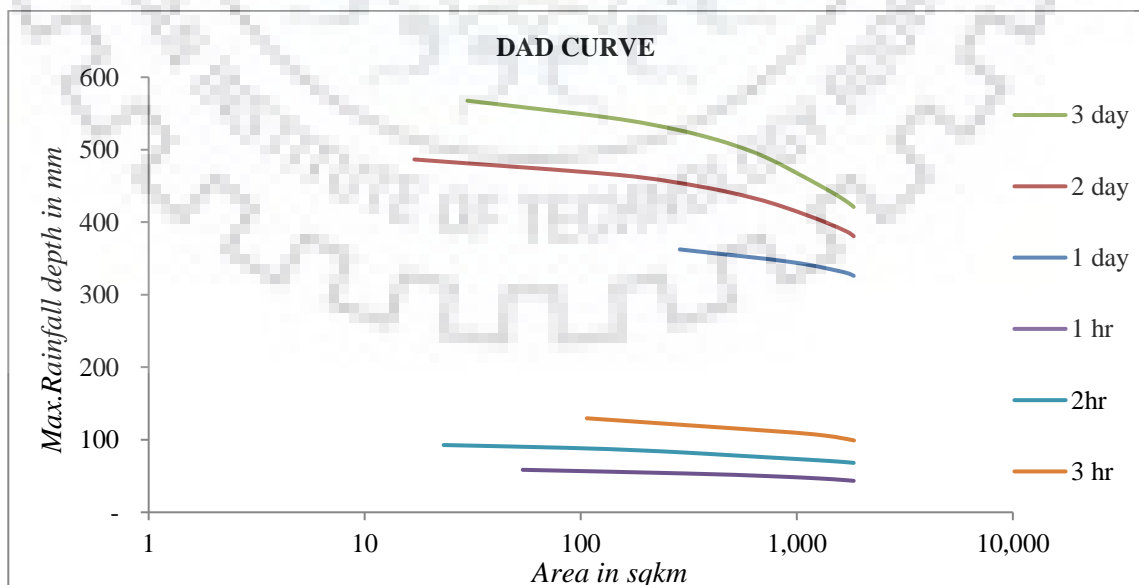


**Figure 5.69 Depth – Area – Duration Curve**

The duration of the design storm was obtained as 72 hrs as per the description in section 4.8.2. Based on the DAD curve developed, a common relationship of rainfall depth and duration for the river basin area 1812 sq.km was derived (Figure 5.70). The incremental rainfall depth up to 72 hrs were computed as represented in Table 5.31.

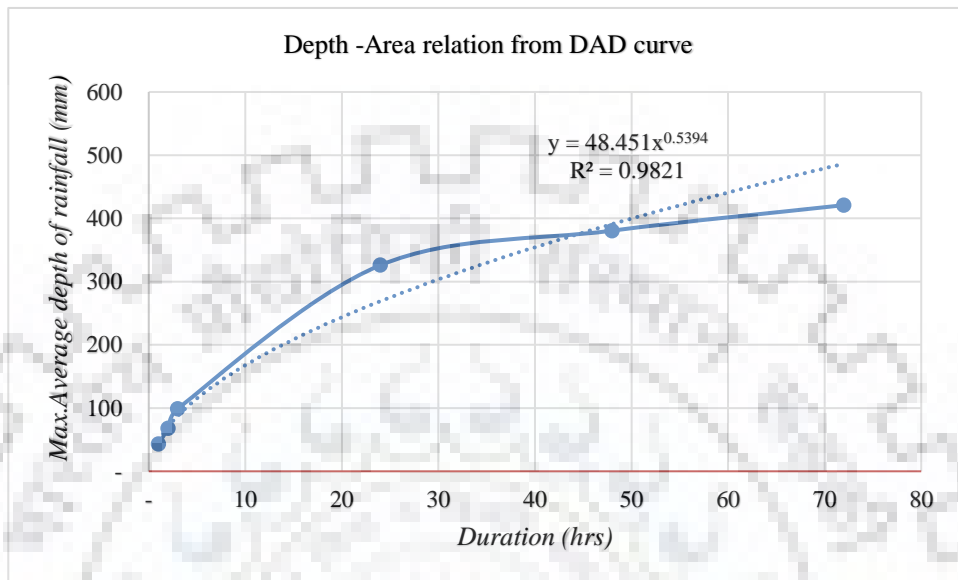


Figure 5.70 Depth – Area Relation plot for the basin for 72-hour duration

Table 5.31 Design storm from DAD curve(SPS)

Duration in hrs	Cumulative RF in mm	Incremental RF in mm	Duration in hrs	Cumulative RF in mm	Incremental RF in mm
$X$	$Y = 48.451X^{0.5394}$		$X$	$Y = 48.451X^{0.5394}$	
1	48.5	48.5	37	339.8	5.0
2	70.4	22.0	38	344.7	4.9
3	87.6	17.2	39	349.6	4.9
4	102.3	14.7	40	354.4	4.8
5	115.4	13.1	41	359.1	4.8
6	127.4	11.9	42	363.8	4.7
7	138.4	11.0	43	368.5	4.6
8	148.7	10.3	44	373.1	4.6
9	158.5	9.8	45	377.6	4.5
10	167.8	9.3	46	382.1	4.5
11	176.6	8.9	47	386.6	4.5
12	185.1	8.5	48	391.0	4.4
13	193.3	8.2	49	395.4	4.4
14	201.2	7.9	50	399.7	4.3
15	208.8	7.6	51	404.0	4.3
16	216.2	7.4	52	408.2	4.3

17	223.4	7.2	53	412.5	4.2
18	230.4	7.0	54	416.6	4.2
19	237.2	6.8	55	420.8	4.1
20	243.8	6.7	56	424.9	4.1
21	250.3	6.5	57	429.0	4.1
22	256.7	6.4	58	433.0	4.0
23	262.9	6.2	59	437.0	4.0
24	269.0	6.1	60	441.0	4.0
25	275.0	6.0	61	444.9	3.9
26	280.9	5.9	62	448.9	3.9
27	286.7	5.8	63	452.8	3.9
28	292.3	5.7	64	456.6	3.9
29	297.9	5.6	65	460.5	3.8
30	303.4	5.5	66	464.3	3.8
31	308.8	5.4	67	468.0	3.8
32	314.2	5.3	68	471.8	3.8
33	319.4	5.3	69	475.5	3.7
34	324.6	5.2	70	479.2	3.7
35	329.7	5.1	71	482.9	3.7
36	334.8	5.0	72	486.6	3.7

The rainfall excess of design storm was computed as given Table 5.32. For this computation, Snyder model UH ordinates were used for the design sequencing the incremental rainfall. The design loss was considered as 1 mm/hr as per the reference given in section 4.8.2.

*Table 5.32 Rainfall excess of design storm from DAD curve*

Duration in hrs	Cumulative RF in mm	Incremental RF in mm	Ordinate of UH m <sup>3</sup> /s	First arrangement of rainfall increment	Design sequence of rainfall increment	Design loss in mm	Rainfall excess of design storm in mm
			-				
1	48.5	48.5	0.43	3.6	3.7	1.00	2.7
2	70.4	22.0	1.00	3.6	3.7	1.00	2.7
3	87.6	17.2	1.76	3.8	3.7	1.00	2.7
4	102.3	14.7	2.71	4.3	3.7	1.00	2.7
5	115.4	13.1	3.71	4.4	3.7	1.00	2.7
6	127.4	11.9	4.82	4.9	3.8	1.00	2.8
7	138.4	11.0	6.00	5.7	3.9	1.00	2.9
8	148.7	10.3	7.15	6.7	3.9	1.00	2.9
9	158.5	9.8	8.17	7.9	3.9	1.00	2.9
10	167.8	9.3	9.04	9.3	4.0	1.00	3.0
11	176.6	8.9	9.81	11.9	4.0	1.00	3.0
12	185.1	8.5	10.34	14.7	4.0	1.00	3.0

13	193.3	8.2	10.67	22.0	4.1	1.00	3.1
14	201.2	7.9	10.83	48.5	4.1	1.00	3.1
15	208.8	7.6	10.56	17.2	4.1	1.00	3.1
16	216.2	7.4	10.30	14.7	4.2	1.00	3.2
17	223.4	7.2	10.04	13.1	4.3	1.00	3.3
18	230.4	7.0	9.79	11.9	4.3	1.00	3.3
19	237.2	6.8	9.54	11	4.5	1.00	3.5
20	243.8	6.7	9.31	10.3	4.5	1.00	3.5
21	250.3	6.5	9.07	9.8	4.5	1.00	3.5
22	256.7	6.4	8.85	9.3	4.6	1.00	3.6
23	262.9	6.2	8.62	8.9	4.6	1.00	3.6
24	269.0	6.1	8.41	8.5	4.7	1.00	3.7
25	275.0	6.0	8.20	8.2	4.8	1.00	3.8
26	280.9	5.9	7.99	7.6	4.8	1.00	3.8
27	286.7	5.8	7.79	7.4	4.9	1.00	3.9
28	292.3	5.7	7.60	7.2	5	1.00	4.0
29	297.9	5.6	7.41	7	5	1.00	4.0
30	303.4	5.5	7.22	6.8	5.1	1.00	4.1
31	308.8	5.4	7.04	6.5	5.2	1.00	4.2
32	314.2	5.3	6.87	6.4	5.3	1.00	4.3
33	319.4	5.3	6.70	6.2	5.4	1.00	4.4
34	324.6	5.2	6.53	6.1	5.5	1.00	4.5
35	329.7	5.1	6.37	6	5.6	1.00	4.6
36	334.8	5.0	6.21	5.9	5.8	1.00	4.8
37	339.8	5.0	6.05	5.8	5.9	1.00	4.9
38	344.7	4.9	5.90	5.6	6	1.00	5.0
39	349.6	4.9	5.75	5.5	6.1	1.00	5.1
40	354.4	4.8	5.61	5.4	6.2	1.00	5.2
41	359.1	4.8	5.47	5.3	6.4	1.00	5.4
42	363.8	4.7	5.33	5.2	6.5	1.00	5.5
43	368.5	4.6	5.20	5.1	6.8	1.00	5.8
44	373.1	4.6	5.07	5	7	1.00	6.0
45	377.6	4.5	4.94	5	7.2	1.00	6.2
46	382.1	4.5	4.82	4.9	7.4	1.00	6.4
47	386.6	4.5	4.70	4.8	7.6	1.00	6.6
48	391.0	4.4	4.58	4.8	8.2	1.00	7.2
49	395.4	4.4	4.47	4.7	8.5	1.00	7.5
50	399.7	4.3	4.35	4.6	8.9	1.00	7.9
51	404.0	4.3	4.25	4.6	9.3	1.00	8.3
52	408.2	4.3	4.14	4.5	9.8	1.00	8.8
53	412.5	4.2	4.04	4.5	10.3	1.00	9.3
54	416.6	4.2	3.93	4.5	11	1.00	10.0
55	420.8	4.1	3.84	4.3	11.9	1.00	10.9
56	424.9	4.1	3.74	4.3	13.1	1.00	12.1
57	429.0	4.1	3.65	4.2	14.7	1.00	13.7
58	433.0	4.0	3.56	4.1	17.2	1.00	16.2
59	437.0	4.0	3.47	4.1	48.5	1.00	47.5
60	441.0	4.0	3.38	4.1	22	1.00	21.0

61	444.9	3.9	3.30	4	14.7	1.00	13.7
62	448.9	3.9	3.21	4	11.9	1.00	10.9
63	452.8	3.9	3.13	4	9.3	1.00	8.3
64	456.6	3.9	3.05	3.9	7.9	1.00	6.9
65	460.5	3.8	2.98	3.9	6.7	1.00	5.7
66	464.3	3.8	2.90	3.9	5.7	1.00	4.7
67	468.0	3.8	2.83	3.8	4.9	1.00	3.9
68	471.8	3.8	2.76	3.7	4.4	1.00	3.4
69	475.5	3.7	2.69	3.7	4.3	1.00	3.3
70	479.2	3.7	2.62	3.7	3.8	1.00	2.8
71	482.9	3.7	2.56	3.7	3.6	1.00	2.6
72	486.6	3.7	2.49	3.7	3.6	1.00	2.6

The ordinates of flood hydrograph were computed using the computed excess rainfall of design storm and the ordinates of the Snyder model UH. Thus, the computed ordinates of the design flood hydrograph are given in Table 5.33. From the table it is observed that the peak flood and the time to peak are 7599.81  $m^3/s$  and 67 hrs respectively. Using the design flood hydrograph ordinates given in Table 5.33, the design flood hydrograph was developed and shown in Figure 5.71.

*Table 5.33 Ordinates of Design Flood Hydrograph(SPF)*

Duration in hrs	Ordinates of Des.flood hydrograph $m^3/s$	Duration in hrs	Ordinates of Des.flood hydrograph $m^3/s$	Duration in hrs	Ordinates of Des.flood hydrograph $m^3/s$	Duration in hrs	Ordinates of Des.flood hydrograph $m^3/s$
0	201.41						
1	205.31	51	4,785.23	101	562.28	151	303.17
2	214.44	52	4,819.10	102	553.25	152	300.63
3	230.47	53	4,861.02	103	544.46	153	298.15
4	255.14	54	4,909.60	104	535.88	154	295.73
5	289.05	55	4,967.56	105	527.52	155	293.37
6	333.16	56	5,041.96	106	519.37	156	291.07
7	388.13	57	5,132.01	107	511.42	157	288.83
8	453.77	58	5,253.54	108	503.67	158	286.64
9	528.98	59	5,458.93	109	496.11	159	284.51
10	612.46	60	5,754.97	110	488.74	160	282.43
11	703.25	61	6,010.53	111	481.56	161	280.41
12	799.38	62	6,246.09	112	474.56	162	278.43
13	899.00	63	6,470.79	113	467.73	163	276.51
14	1,000.66	64	6,738.55	114	461.07	164	274.63
15	1,100.50	65	6,923.19	115	454.58	165	272.80
16	1,198.58	66	7,151.65	116	448.25	166	271.02
17	1,295.07	<b>67</b>	<b>7,599.81</b>	117	442.08	167	269.28
18	1,390.04	68	7,025.09	118	436.06	168	267.58
19	1,483.56	69	6,461.77	119	430.20	169	265.92

20	1,575.73	70	5,775.91	120	424.48	170	264.31
21	1,666.61	71	4,941.49	121	418.90	171	262.74
22	1,756.26	72	4,262.67	122	413.46	172	261.21
23	1,844.74	73	3,804.11	123	408.16	173	259.71
24	1,930.70	74	3,382.06	124	402.99	174	258.25
25	2,035.95	75	2,820.10	125	397.95	175	256.83
26	2,184.21	76	2,748.44	126	393.04	176	255.45
27	2,348.73	77	2,527.37	127	388.25	177	254.10
28	2,528.18	78	2,331.96	128	383.58	178	252.78
29	2,722.25	79	2,202.05	129	379.02	179	251.49
30	2,955.62	80	1,972.64	130	374.58	180	250.24
31	3,203.79	81	1,499.61	131	370.25	181	249.02
32	3,493.96	82	1,214.50	132	366.03	182	247.83
33	4,015.60	83	975.81	133	361.92	183	246.67
34	4,319.67	84	803.18	134	357.90	184	245.54
35	4,568.85	85	742.50	135	353.99	185	244.44
36	4,732.34	86	728.98	136	350.18	186	243.36
37	4,730.68	87	715.79	137	346.46	187	242.31
38	4,621.98	88	702.93	138	342.83	188	241.29
39	4,514.44	89	690.39	139	339.30	189	240.29
40	4,439.71	90	678.17	140	335.85	190	239.32
41	4,369.07	91	666.25	141	332.49	191	238.37
42	4,273.33	92	654.63	142	329.21	192	237.45
43	4,178.62	93	643.30	143	326.02	193	236.55
44	4,089.65	94	632.25	144	322.90	194	235.67
45	3,759.98	95	621.48	145	319.86	195	234.81
46	3,730.52	96	610.98	146	316.90	196	233.98
47	4,041.80	97	600.74	147	314.02	197	233.16
48	4,202.39	98	590.75	148	311.20	198	232.37
49	4,455.10	99	581.02	149	308.46	199	231.60
50	4,690.53	100	571.53	150	305.78	200	230.00

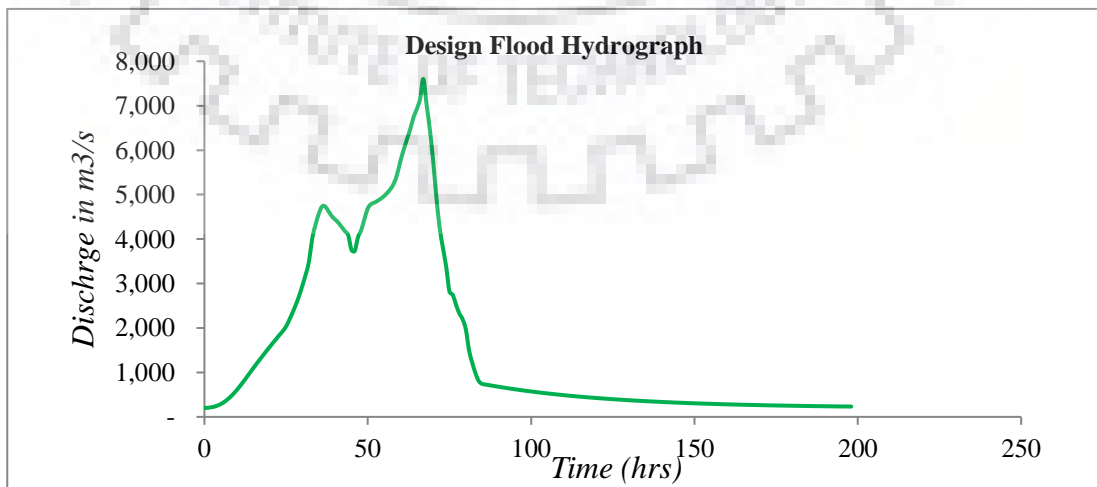


Figure 5.71 Design Flood Hydrograph (SPF)

## 5.9 Flood Frequency Analysis

### 5.9.1 GUMBEL'S METHOD

The statistical parameters were derived from the 42 years annual maximum peak flood series data. Those are given in Table 5.34. The frequency factors and flood estimates corresponding to different periods were estimated following the methodology described under section 4.9.1. The flood estimate for various return periods were computed at Hanwella gauging site using Gumbel distribution based on frequency factor approach. The such estimates are given in Table 5.35. From Table 5.35, it is observed that the flood estimates for 100 years return period is found to be 2751.7 m<sup>3</sup>/s fitting Gumbel Distribution.

*Table 5.34 Statistical Parameters derived from Annual maximum peak flood series*

Parameter	Value	Unit
Sample Size N	42	yrs.
Mean $\bar{\chi}$	1055.13	cumec
Standard Deviation $S_x$	479.35	cumec

*Table 5.35 Flood Estimates for different return periods using Gumble distribution*

Return Period (years)	Gumbel Reduced variate	Frequency Factor	Flood Estimates (cumec)
T	$Y_T$	K	$X_T$
5	1.50	0.83	1454.72
10	2.25	1.49	1768.66
20	2.97	2.12	2069.80
25	3.20	2.32	2165.33
50	3.90	2.93	2459.60
100	4.60	3.54	2751.70
150	5.01	3.89	2922.03
200	5.30	4.15	3042.73
500	6.21	4.95	3426.69
1000	6.91	5.55	3716.88

### 5.9.2 LOG. PEARSON TYPE III METHOD

The statistical parameters derived from 42 years of Annual Maximum peak flood series, transformed in log domain are given in Table 5.36. The frequency factors and flood estimates

for different return periods were determined at Hanwella gauging site following the methodology described under section 4.9 2. The floods for different return period using Log – Pearson Type III method based on frequency factor approach were computed which are given in Table 5.37. From this table, the flood for 100 yrs. return period was found to be 2746.6. m<sup>3</sup>/s.

**Table 5.36 Statistical Parameters of Log-Pearson Type III distribution**

Parameter	Value	Unit
Sample size N	42	yrs.
$\bar{Z}$	2.98( data in log base to 10 domain)	cumec
$\sigma_z$	0.19( data in log base to 10 domain)	cumec
$C_s$	0.0769(data in log base to 10 domain)	

**Table 5.37 Floods estimated using Log Pearson Type 3 Distribution for different return periods**

T(years)	Kz for Cs (=0.0769)	Kz .6z	Z <sub>T</sub>	X <sub>T</sub> =antilog Z <sub>T</sub>
2	-0.0131	-0.0025	2.98	956.96
10	1.2897	0.24	3.23	1680.81
25	1.7772	0.33	3.32	2,075.15
50	2.0948	0.39	3.38	2,380.62
100	2.3829	0.45	3.43	2,746.6
200	2.6483	0.50	3.48	3,024.33
1000	3.2016	0.60	3.58	3,841.59

**Table 5.38 Comparison of Floods of different Return Periods using Gumbel and Log Pearson Type 3 Distribution**

T(years)	Flood Frequency Analysis	
	Gumbel	LOG-PEARSON TYPE III
5	1,454.72	1,473.09
10	1,768.66	1,680.81
20	2,069.80	2,062.42
25	2,165.33	2,075.15
50	2,459.60	2,380.62



<b>100</b>	<b>2,751.70</b>	<b>2,746.60</b>
150	2,922.03	2,918.97
200	3,042.73	3,041.27
500	3,426.69	3,430.79
1000	3,716.88	3841.59

The peak floods for various return periods on different two methods were given in Table 5.38. However, the comparison of Floods of different Return Periods using Gumbel and Log Pearson Type 3 Distribution are represented in Figure 5.72.

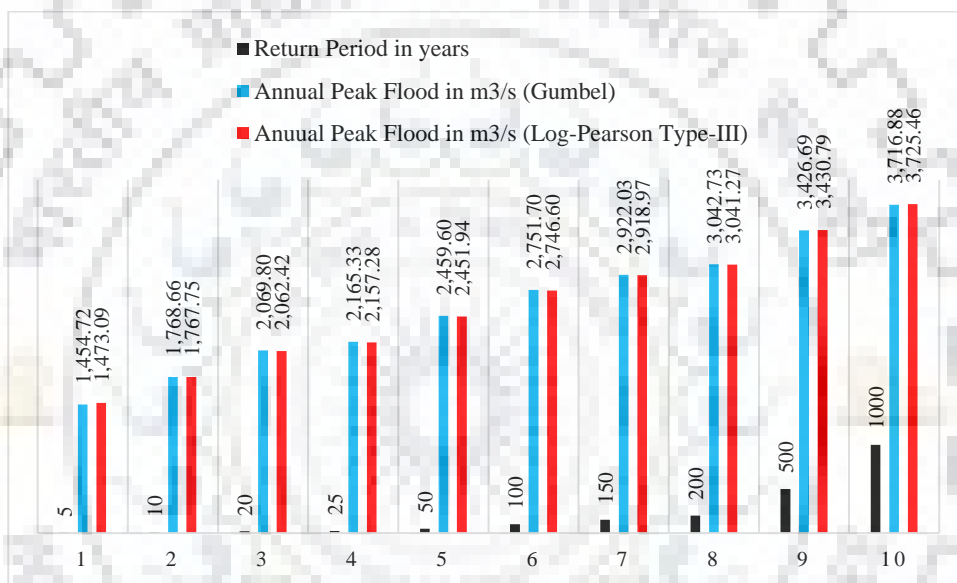


*Figure 5.72 Comparison of Floods of different Return Periods using Gumbel and Log Pearson Type III Distribution*

## CHAPTER 6 CONCLUSIONS

The following conclusions are drawn from the study:

- (i) ArcGIS software was used for preparing the watershed delineation, elevation map, Thiessen polygon, land use and land cover map, soil data map, isohyet maps and isochrone maps. For this purpose, the satellites data from the USGS web site was downloaded on the 30-metre resolution. However, better maps may be generated if the high-resolution satellite data were used.
- (ii) HEC-GeoHMS software was used to setup basin model development. The software was capable to prepare basin maps and provide the physiographic & some important geomorphological characteristic of the basin. The basin maps were the input for HEC-HMS programme during the simulation.
- (iii) A stage-discharge relationship (rating curve) at Hanwella gauging site, was developed using graphical and analytical approaches utilising daily gauge-discharge data of 42 years. The rating curve developed from the analytical approach was adopted for computing the hourly discharge values corresponding to the hourly gauge values for four flood events. Also, the adopted rating curve was used to compute annual maximum peak flood series corresponding to the annual maximum gauge values for 42 years for carrying out flood frequency analysis.
- (iv) The sensitivity analysis was carried out to identify the initial parameters values of three transform models considered.
- (v) Three flood events were considered for calibration whereas one event was considered for validation of the three transform models. The performance of the three transform models during calibration and validation, were compared base on the overall performance criteria NSE along with the error functions such as percent error in peak, percent error in time to peak and percent error in discharge volume. Based on this comparison, it was found that the Snyder UH model is best performing model whereas the SCS UH model performed poor. The Clark UH model is the second best performing model.
- (vi) HEC-HMS software has the capability of flood simulations using various transform models which include Clark UH Model, Snyder UH Model & SCS UH Model. The HEC-

HMS software has been successfully applied for simulating the four flood events observed in Kelani river basin (up to Hanwella Gauging Site). From the results, Snyder model is recommended for the simulation of flood events for this basin.

- (vii) The Snyder UH model was applied for the development of UH of the Kelani river basin up to Hanwella gauging site to forecast the flood of Jun. 2014 event, considering hourly rainfall blocks in real time. The limits of risk assessments were identified based on the criteria given by Irrigation Department Sri Lanka. Accordingly, the peak flood corresponding to each forecasted flood hydrographs were assigned qualitative associated risks. Such advance information would be very much useful for the flood management for planning & implementation of the evacuation of people from the flood affected areas to the safer places minimising the losses of lives & properties.
- (viii) To judge the performance of the Snyder transform model, The flood hydrographs of the June 2014 events were forecasted using this model considering different blocks of rainfall. The forecasted flood hydrographs were compared with the observed flood hydrograph of that event. During the comparison, it was observed that both the flood hydrographs are in closer agreement when all the blocks of the rainfall were considered for forecasting. However, criteria of limits of risk were already started to provide the signals for high & very high floods during the lead times of the different forecasted hydrographs which may be considered for taking advance actions by the concerned authorities as per the limits of the risk.
- (ix) Snyder model was used for estimating the floods of 100-year return period and standard project flood. Such estimates are required to design various structural measures such as diversion dams, flood embankments, levees etc. Such structural measures may be provided to protect the important cities and installations. For estimating 100-year return period flood, it was presumed that 100-year rainfall would produce the 100-year flood. However, this assumption is affected due to antecedent moisture conditions in the basin. However, for all practical purposes, this hypothesis was considered for converting 100-year rainfall to the 100-year flood.
- (x) For the estimation of floods of various return periods, the frequency analysis was carried out using Gumbel and Log-Pearson Type III distributions based on frequency factor approach.

- (xi) While developing the DDF curve, the available data of daily rainfall were utilised. The distribution factors used for distributing the daily values to hourly values, some synthetic relationship developed between depth and duration was used. However, if the hourly rainfall values for most severe rain storm experienced in the basin or region were available, then more accurate design storm for 100-year return period could have been estimated.
- (xii) While developing DAD curve, the daily rainfall data available at different rain gauge stations located within or nearby the basin were used. No data of the daily rainfall data located in the region were available. Thus, the storm transposition was not carried out and the DAD curve developed for the basin was used to estimate the Standard Project storm.



## REFERENCES

- i. Ahmad. M. M., Ghumman. A. R., Ahmad. S. (2009). “Estimation of Clark’s Instantaneous Unit Hydrograph parameters and Development of Direct Surface Runoff Hydrograph “. *Water Resour Manage*; 23:2417-2435
- ii. Clark. C. O.,(1945). “ Storage and the Unit Hydrograph. “ , *Transactions, ASCE*, 110; 1419-1446
- iii. De Silva M. M. G. T.: Weerakoon S. B and Srikantha Herath (2014) “ Modeling of Event and Continuous Flow Hydrographs with HEC–HMS: Case Study in the Kelani River Basin, Sri Lanka.” *J. of Hydrol. Eng.,ASCE*; 19(4); 800-806.
- iv. FAO website (<http://www.fao.org/soils-portal/soil-survey/soil-maps-and-databases/en/>)
- v. Iresh. A. D. S. Arya. S. (2017). *Flood Zone Mapping for Kelani River Basin, Sri Lanka*” Dissertation of M.Tech (Hydrology), Department of Hydrology, Indian Institute of Technology, Roorkee.
- vi. Jain. S. K., Singh. R. D., Seth. S. M., (2000). “Design Flood Estimation Using GIS Supported GIUH Approach.”, *J. of Water Resources Management*, 14:369-376.
- vii. Jaya Ram Prajapati, Goel. N. K. (2017). *Flood Estimation in River Basin Downstream of a Major Reservoir in Coastal Region*” Dissertation of M.Tech (Hydrology), Department of Hydrology, Indian Institute of Technology, Roorkee.
- viii. *Manual on Design flood Estimation.*(2001) Hydrology Studies Organization, Central Water Commission, New Delhi.
- ix. McCuen. R. H.,Knight. Z., Cutter. A. G.(2006). “Evaluation of Nash – Sutcliffe Efficiency Index.”, *J. of Hydrol. Eng.*, 11(6); 597-602.
- x. NandalalH. K. and RatnayakeU. R. (2010) “Event Based Modeling of a Watershed Using HEC-HMS.” *J.of Institution of Engineers, Sri Lanka*, Vol .xxxxiii, No.2, pp 28-37.
- xi. *Publication on Rationalization of Design Storm Parameters for Design flood Estimation.*(Dec.1993) Hydrology Studies Organization, Central Water Commission, New Delhi.
- xii. Rakesh Kumar. C., Chatterjee. C., Singh. R. D., Lohani. L. K., Sanjay Kumar. (2004). “ GIUH based Clark and Nash models for runoff estimation for ungauged basin and their uncertainty analysis. ”. *Intl. J. of River Basin Management*; Vol.2; No.4; 281-290.
- xiii. Rakesh Kumar. C., Chatterjee. C., Singh. R. D., Lohani. L. K., Sanjay Kumar. (2007). “ Runoff estimation for an ungauged catchment using geomorphological instantaneous unit hydrograph (GIUH) models ”. *Hydrol. Process*; .21; 1829-1840.

- xiv. Razi. M. A. M., Ariffin. J., Tahir. W., Arish. N. A. M. (2010). “Flood Estimation Studies using Hydrologic Modeling System (HEC-HMS) for Johor River, Malaysia”. J. Applied Sci., 10(11):930-939.
- xv. Sampath. D. S., Weerakoon. S. B., Herath. S. (2015). “ HEC-HMS Model for Runoff Simulation in a Tropical Catchment with Intra-Basin Diversions – Case Study of the Deduru Oya River Basin, Sri Lanka “..” J.of Institution of Engineers, Sri Lanka, Vol .XLVIII, No.1,pp 1-9.
- xvi. Singh. P. K., Mishra. S. K., Jain. M. K.(2014), “ A review of the synthetic unit hydrograph: from the empirical UH to advanced geomorphological methods “. Hydrological Sciences Journal; 59(2); 239-261.
- xvii. Subramanya.K, (2015),“ Engineering hydrology.” Fourth Edition. Tata McGraw. Hill Publications
- xviii. USACE-HEC, (2000), “Hydrologic Modelling System HEC-HMS , Technical Reference Manual.” USACE, Hydrologic Engineering Center, Davis, California,USA
- xix. USACE-HEC, (2015),“ Hydrologic Modelling System HEC-HMS , Application Guide.” USACE, Hydrologic Engineering Center, Davis, California,USA
- xx. USACE-HEC, (2016), “Hydrologic Modelling System HEC-HMS ,Version 4.2, User’s Manual.” USACE, Hydrologic Engineering Center, Davis, California,USA
- xxi. USACE-HEC, (2013), “ Geospatial Hydrologic Modelling Extension HEC-GeoHMS ,Version 10.1, User’s Manual “, USACE, Hydrologic Engineering Center, Davis, California,USA